Impact of magnesium based degradable alloys on a coculture model of osteoblast and osteoclast

Dissertation with the aim of achieving a doctoral degree
at the Faculty of Mathematics, Informatics and Natural Sciences
Department of Chemistry
University of Hamburg

submitted by
Steven Behr

Hamburg
2020

The following evaluators recommend the admission of the dissertation:

Prof. Dr. Regine Willumeit-Römer

Prof. Dr. Ulrich Hahn

Disputation: 29.04.2020

Print permission: 26.05.2020

Abstract

The currently available non-degradable implant materials may cause side effects like a stress shielding effect or an allergic reaction of patients to foreign implant materials. Finally, some of the non-degradable materials cannot remain in the body and must be removed *via* a second surgery. In order to counteract these undesired side effects, the degradable implant materials have already proven their effectiveness in the past. However, before new alloy materials can be tested and applied *in vivo*, a thorough *in vitro* investigation of these alloys is necessary. In order to create physiological osseous *in vitro* conditions as close as possible to *in vivo* (bone), a coculture of primary cells was established and applied in this study. The coculture consisted of peripheral blood mononuclear cells (PBMC) and human umbilical cord perivascular cells (HUCPV). The investigation of different experimental conditions has shown that at a ratio of 1:100 (HUCPV:PBMC), was optimal to obtain a differentiated coculture of osteoblasts and osteoclasts within 28 days. Based on this coculture, the aim of the study was to investigate the effects of different magnesium-based alloys. The reaction of the coculture to these alloys was investigated by different cellular, enzymatic and molecular assays. In addition, the function of osteoblasts was monitored by the formation of hydroxyapatite and the function of osteoclasts was demonstrated by a resorption assay. For a more comprehensive investigation, the alloys were examined in 3 different ways. Firstly (i), the reaction of the coculture to the corresponding ions (magnesium chloride, silver nitrate and gadolinium chloride) was investigated. Thus, it could be shown that the gadolinium ions increase the formation of hydroxyapatite. In addition, (ii) the different alloys were degraded in cell culture medium to prepare extract and the behaviour of the coculture was monitored in the presence of these extracts. The investigation of the Mg-8Ag alloy has shown that silver in high concentrations had a toxic effect on the coculture. Finally (iii), the coculture was applied directly to the materials (Mg-Pure, Mg-2Ag and Mg-10Gd) and incubated to determine, whether the cells could settle on these alloys despite degradation stress, grow, and whether direct contact with the material influenced the behaviour of the cells. The enhancing effect of gadolinium, both as a salt and as an extract, on mineralisation, is assumed to be mediated *via* the calcium sensing receptor found on both osteoblasts and osteoclasts. Calcium sensing receptor provides an affinity to positively charged ions and is an important component of bone homeostasis. By using a phospholipase C inhibitor, an important component of the calcium sensing receptor dependent pathway was inhibited and the influence of gadolinium on the formation of the calcium sensing receptor dependent pathways demonstrated by reducing hydroxyapatite formation.

In addition, Mg-Pure and magnesium-silver alloys have also been shown to interact with the calcium sensing receptor. This interaction led to an inhibition of the receptor signal. Nevertheless, a positive effect on bone formation of both magnesium and silver ions remained, indicating other implicated pathways. Indeed, magnesium positively influenced bone growth *via* the transient receptor potential cation channel 7 / phosphoinositide 3-kinase pathway. Furthermore, silver *via* the increased formation of reactive oxygen species supported alkaline phosphatase expression. Finally, a combination of the three materials magnesium, silver and gadolinium could be useful to combine their positive properties.

Zusammenfassung

Die derzeit verfügbaren, nicht abbaubaren Implantationsmaterialien können Nebenwirkungen wie einen Spannungsabschirmungseffekt (Stressshielding) oder eine allergische Reaktion der Patienten auf die körperfremden Implantatmaterialien hervorrufen. Schlussendlich können die nichtabbaubaren Materialien teilweise nicht im Körper verbleiben und müssen in einer zweiten Operation wieder entommen werden. Um diesen unerwünschten Nebeneffekten entgegenzuwirken, haben sich die abbaubaren Implantatmaterialien bereits in der Vergangenheit bewährt. Bevor jedoch neue Legierungsmaterialien in *vivo* getestet und angewendet werden können, ist eine gründliche *in vitro* Untersuchung dieser Legierungen notwendig. Um dabei physiologische knöcherne *in vitro* Bedingungen zu schaffen, die möglichst nahe an den *in vivo* Bedingungen (Knochen) sind, wurde in dieser Studie eine Kokultur von Primärzellen etabliert und angewendet. Die Kokultur bestand aus den Mononukleären Zellen des Blutes (Peripheral blood mononuclear cells; PBMC) und den mesenchymalen Stammzellen der menschlichen Nabelschnur (Human umbilical cord perivascular cells; HUCPV). Die Untersuchung verschiedener experimenteller Bedingungen hat gezeigt, dass ein Verhältnis von 1:100 (HUCPV:PBMC) optimal ist, damit die Zellen sich innerhalb von 28 Tagen zu einer Kokultur aus Osteoblasten und Osteoklasten entwickeln.

Ausgehend von dieser Kokultur war es das Ziel der Studie, die Auswirkungen verschiedener auf Magnesium basierender Legierungen zu untersuchen. Die Reaktion der Kokultur auf diese Legierungen wurde durch verschiedene zelluläre, enzymatische und molekulare Assays untersucht. Darüber hinaus wurde die Funktion der Osteoblasten durch die Bildung von Hydroxylapatit verfolgt und die Funktion der Osteoklasten durch einen Resorptionstest nachgewiesen.

Für eine umfassendere Untersuchung wurden die Legierungen auf 3 verschiedene Arten untersucht. Zunächst (i) wurde die Reaktion der Kokultur auf die entsprechenden Ionen (Magnesiumchlorid, Silbernitrat und Gadoliniumchlorid) untersucht. Dabei konnte bereits gezeigt werden, dass die Gadoliniumionen die Bildung von Hydroxylapatit erhöhen. Zusätzlich wurden (ii) die verschiedenen Legierungen in Zellkulturmedium zur Herstellung der Magnesiumextrakte inkubiert und das Verhalten der Kokultur in Gegenwart dieser Extrakte überwacht. Die Untersuchung der Mg-8Ag Legierung hat gezeigt, dass Silber in hohen Konzentrationen eine toxische Wirkung auf die Kokultur hat. Schließlich (iii) wurde die Kokultur direkt auf die Materialien (Mg-Pure, Mg-2Ag Mg-10Gd) aufgebracht und inkubiert, um festzustellen, ob die Zellen sich trotz Abbaustress auf diesen Legierungen absetzen und wachsen können sowie ob der direkte Kontakt mit dem Material das Verhalten der Zellen beeinflusst.

Es wird angenommen, dass die verstärkende Wirkung von Gadolinium, sowohl als Salz als auch als Extrakt, auf die Mineralisierung über den Calcium Sensing Receptor vermittelt wird, der sowohl auf Osteoblasten als auch auf Osteoklasten zu finden ist. Der Calcium Sensing Receptor besitzt eine Affinität zu positiv geladenen Ionen und ist ein wichtiger Bestandteil der Knochenhomöostase. Durch die Verwendung eines Phospholipase C Inhibitors wurde eine wichtige Komponente des Calcium Sensing Receptor abhängigen Signalwegs gehemmt und der Einfluss von Gadolinium auf die Bildung der Calcium Sensing Receptor abhängigen Signalwege durch die Reduzierung der Hydroxylapatitbildung nachgewiesen.

Darüber hinaus wurde auch gezeigt, dass Mg-Pure und Magnesium-Silber Legierungen mit dem Calcium Sensing Receptor interagieren. Diese Interaktion führt zu einer Hemmung des Rezeptorsignals. Dennoch blieb ein positiver Effekt auf die Knochenbildung sowohl von Magnesium- als auch von Silberionen erhalten, was auf andere implizierte Wege hinweist. Tatsächlich beeinflusste Magnesium das Knochenwachstum über den Transient Receptor Potential Cation Channel 7 / Phosphoinositide 3-kinase positiv. Darüber hinaus unterstützte Silber über die vermehrte Bildung reaktiver Sauerstoffspezies die Expression der alkalischen Phosphatase. Schließlich könnte eine Kombination der drei Materialien Magnesium, Silber und Gadolinium sinnvoll sein, um deren positive Eigenschaften zu kombinieren.

Content

List of abbreviations

3D	Three-dimensional
Ag	Silver
AKT	Protein kinase B
Al	Aluminium
ALP	Alkaline phosphatase
B-Actin	Actin beta
BGLAP	Osteoclacin
BMP	Bone morphogenetic proteins
BSP	Bone sialoprotein
Ca	Calcium
CaM	Calcium binding protein calmodolin
CaMKII	Calcium/calmodulin-dependent protein kinase II
CASR	Calcium sensing receptor
cDNA	Complimentary DNA
c-Fms	Colony-stimulating factor-1 receptor
CD^{+14}/CD^{+34}	Glykoprotein 14 and 34
Ch	Chapter
Cl	Chlorine
CTR1	Copper transporter 1
CTSK	Cathepsin K
DAPI	4′,6-Diamidin-2-phenylindol
DGE	Deutsche Gesellschaft für Ernährung
DNA	Deoxyribonucleic acid
DKK2	Dickkopf 2
DMT1	Divalent metal transporter
DMSO	Dimethyl sulfoxide
EMC7	ER membrane protein complex subunit 7
eNOS	Endothelial nitric oxide synthase
ER	Endoplasmic reticulum
FBS	Fetal Bovine Serum
FDA	Food and Drug Administration
Fe	Iron
GAPDH	Glyceraldehyde-3-phosphate dehydrogenase

Gd	Gadolinium
Gd-BOPTA	Gadobenate
H	Hydrogen
HA	Hydroxyapatite
hMSCs	Human mesenchymal stem cells
Ho	Holmium
HUCPV	Human umbilical cord perivascular cells
ICAM-1	Intercellular adhesion molecule-1
ICP-MS	Inductively coupled plasma mass spectrometry
IL	Interleukins
IL 1	Interleukin 1
IP3	Inositol trisphosphate
La	Lanthanum
Lu	Lutetium
K	Potassium
MagIC	Magnesium Innovation Center
MAPK	Mitogen-activated protein kinase
M-CSF	Macrophage colony-stimulating factor
Mg	Magnesium
Mg-xAg	Magnesium silver alloy (x = wt% silver)
Mg-xGd	Magnesium gadolinium alloy (x = wt% gadolinium)
MPO	Myeloperoxidase
MRI	Magnetic resonance imaging
mRNA	Messenger RNA
N	Nitrogen
NADH	Nicotinamide adenine dinucleotide
NADPH	Nicotinamidadenindinukleotidphosphat
NFAT	Nuclear factor of activated T cells
NFATC1	Nuclear factor of activated T-cells cytoplasmic 1
NF-κB	Nuclear factor 'kappa-light-chain-enhancer' of activated B-cells
NOX4	NADPH oxidase 4
O	Oxygen
OB	Osteoblast
OC	Osteoclast
OPG	Osteoprotegerin

OPN	Osteopontin
OSCAR	Osteoclast-associated immunoglobulin-like receptor
P	Phosphorous
PBMC	Peripheral blood mononuclear cell
PCR	Polymerase chain reaction
Pen	Penicillin
Pi	Inorganic phosphate
PI3K	Phosphoinositid-3-Kinasen
PKC	Protein kinase C
PLCG2	Phospholipase C gamma 2
PPP3CA	Protein phosphatase 3 catalytic subunit alpha
PPP3CB	Protein phosphatase 3 catalytic subunit beta
PPP3CC	Protein phosphatase 3 catalytic subunit gamma
PTH	Parathyroid hormone
RANK	Receptor activator of nuclear factor κ B
RANKL	Receptor activator of nuclear factor of kappa ligand
RNA	Ribonucleic acid
ROS	Reactive oxygen species
RUNX2	Runt related transcription factor 2
S	Sulfur
SD	Standard deviation
SEM	Scanning electron microscope
SEMA4D	Semaphorin 4D
SF6	Sulphur hexafluoride
sfrp2	Secreted frizzled-related protein 2
Sm	Samarium
Sn	Tin
Strep	Streptomycin
Taq	*Thermus aquaticus*
TGF-β	Transforming growth factor-beta
TNF	Tumour necrosis factor
TRAF	TNF receptor associated factor
TRAP	Tartrate-resistant acid phosphatase
TRPM	Transient receptor potential ion channel
UKE	University Hospital Eppendorf

Vitamin D3	1.25-dihydroxyvitamin D3
Wnt	Acronym from "Wingless" and "Int-1"
WST-1	Water soluble tetrazolium 1
Y	Yttrium
Yb	Ytterbium
Zn	Zinc
ZOL	Zoledronic acid
α-MEM	α-Minimum essential medium

1 Introduction

In our society, the population is getting older and is therefore accompanied by an increase bone fractures and bone tumours incidence. Thus, the replacement or restoration of the lost bone material with suitable materials is gaining importance in orthopaedics. This suitability also rely on the interaction of the biomaterials and the bone cells & their excretomes/secretomes [1,2]. Since all materials in the body are exposed to mechanical stress and to rather corrosive physiological environment, biomaterials can be prone to abrasion and thus release particles into the surrounding tissue. Therefore it is essential that the materials have no toxic side effects or do not cause any risk to the body [3]. Up to now, non-degradable metallic materials made of *e.g.* titanium or stainless steel are usually used in human medicine [4]. In addition to higher strength and the resulting stress shielding effect [5], discolorations and allergies could also be detected in some patients [6].

Therefore, degradable materials such as biopolymers and degradable metallic materials have emerged in the last two decades. When the function of the implant is fulfilled (*e.g*. providing mechanical stability to allow organ regeneration), the body can resorb these materials, avoiding an additional surgery [7]. Due to their mechanical properties, degradable metallic materials present a promising approach in the field of resorbable implants. Several studies have already investigated degradable implant materials made of zinc, iron, and magnesium (Mg) alloys [8,9]. Compared to ceramics and polymers, especially Mg demonstrates a good combination of mechanical strength and ductility, which is suitable for many implant applications [10].

Mg itself is necessary for many metabolic processes (more than 600 enzyme reactions [11]), does not represent any further stress to the body, and also positively influences bone formation [12]. This is probably due to the fact that Mg has a direct influence on bone forming osteoblasts (OB) and bone resorbing osteoclasts (OC) [13]. Mg improves the viability of OB and increases the release of alkaline phosphatase (ALP) and osteocalcin (BGLAP), two proteins associated with bone formation [14]. This positive influence of Mg based implants could be shown *in vivo* [12] and the implants are already used medically by Syntellix AG (*e.g.* 2013: CE mark Europe).

These positive properties could be further enhanced by alloying elements such as silver (Ag) and gadolinium (Gd) [15,16]. Because Mg-based implants have a multiple positive influence on bone formation and similar mechanical properties to bone, they have a promising potential for new implant materials.

For the biological investigation of biomaterials, cell lines in mono- and cocultures or primary cells monocultures have mostly been used so far. In order mimic as close as possible the

natural system, it would be advantageous to use a coculture system consisting of primary cells, which regulate and differentiate themselves without addition of differentiation factors. This coculture system could be used to analyse some aspect of the future implant materials and determine how biomaterials can affect cell development and interaction. In other words, when targeting musculoskeletal applications, the effect of Mg and the different alloying elements can be investigated not only on OB and OC monoculture, but also on these cells interactions. Many studies have shown that from a certain concentration Gd is toxic to cells [17,18], on the contrary low concentrations have a positive effect on cells [19]. Therefore, the effect of Gd on coculture should also be investigated.

1.1 The musculoskeletal system

The bone as a living organ undergoes a permanent process of remodelling and adaptation to the daily mechanical stress throughout the organism's whole lifespan. The interaction between OB and OC is a major process involved in remodelling and repair processes. Normally, the bone resorption and formation are in a homeostatic balance, so old bone is continuously replaced by new one. Between 2 – 5 % of bone is being remodelled each year [20].

Bone is composed of around 60 % inorganic and 30 % organic components, and 10% water [21]. The inorganic component of the bone matrix primarily consists of (60 %) bone mineral or (crystalline) calcium hydroxyapatite $Ca_5(PO_4)_3(OH)$ [22]. Type I collagen fibres represent 90 % of the organic extracellular bone matrix. The remaining 10 % are non-collagenous or matrix proteins, which play a role in the mineralisation process and bone formation [23].

Bone remodelling and homeostasis are complex multifactorial processes. Bone, as mineral reservoir, play a role in the maintenance of circulating calcium (Ca) and phosphorous (P) level under hormonal control (Table 1). Numerous cells participate in the bone remodelling process. Cells of the OB lineage such as preosteoblasts, osteocytes and the lining cells, induce the activation of the bone remodelling cycle.

Table 1: Overview of major factors in the bone remodelling process

Molecule	Source	Effector Cell type	Main effects/functions	Reference
Receptor Activator of NF-κB Ligand (RANKL)	Cytokine expressed in several tissues and organs - osteoblasts and bone-marrow stromal cells	OC	- differentiation of osteoclast - fusion into multinucleated cells - activation and survival of osteoplastic cells	[24]
Calcitriol or vitamin D3	Proximal tubule of the nephron in the kidneys	OB and OC	Increase level of Ca in blood by: - enhancing the absorption of intestinal calcium and renal tubular reabsorption of calcium - promoting release of RANKL and osteoclast activation	[25]
Parathyroid hormone	Parathyroid glands	OB and OC	Increase level of Ca in blood by: - similar effects than calcitriol - increasing inorganic phosphate (Pi) kidney excretion leading to decrease circulation phosphorous level and hydroxyapatite dissolution	[26]
Calcitonin	Produced by parafollicular cells of the gland	OC	Decrease level of Ca in blood by: - mediating loss of the ruffled border - stopping the motility of osteoclast - inhibiting the secretion of proteolytic enzymes	[27]
Glucocorticoids	Hormones produced by the adrenal gland	Bone cells	Decrease bone formation rate and bone mineral density by: - essential for osteoblasts growth - promoting differentiation of OB - decrease activity of OB - increase osteoclast recruitment - support bone remodelling	[28]
Macrophage colony-stimulating factor	Bone marrow, OB, endothelial cells, fibroblasts, and mononuclear phagocytes	OC	- Proliferation, differentiation, and survival of monocytes, macrophages, and bone marrow progenitor cells / necessary for OC development	[29] [30]

1 Introduction

OB develop from the mesenchymal lineage of the bone marrow stroma and produce new bone matrix. They have a diameter between 20 – 30 µm, are located on the surface of new bone and form the osteoid. Osteoid is an uncalcified collagen rich protein mixture of the bone tissue and includes bone matrix proteins such as type I collagen and other non-collagenous proteins like osteocalcin, osteopontin and osteonectin [31]. Are the osteoid formed, inorganic salts are deposited in it and forms the mineralized bone. In this process the stiffness and compressive strength of the structure increases and its energy storage capacity decreases [32]. Once bone formation by mature OB is completed, OB can develop into either lining cells or osteocytes. OB activities, such as differentiation, are regulated by (i) autocrine and paracrine growth factors (*e.g*. platelet-derived growth factor, insulin-like growth factors, transforming growth factor-beta (TGF-β), basic fibroblast growth factor, and the bone morphogenetic proteins (BMP)) [33–36] and (ii) transcription regulation (*e.g*. runt related transcription factor 2 (RUNX2), osterix) [37,38].

One of the first enzymes released by OB is ALP, which provides the required P by cleaving organic phosphate compounds. The P ions can cross the membrane of the matrix vesicles released by the OB [39]. Intravesicular conditions favour the formation of HA crystals (*e.g.* high Ca and P concentrations). Growing crystals will then punctuate the vesicle membrane and finally grow out of the vesicle to form mineralised nodules [40]. The preosteoblasts, osteocytes and the lining cells also affect bone remodelling *via* shape changes and release of collagenase under the influence of parathyroid hormone (PTH) [41] and expression of macrophage colony-stimulating factor (M-CSF) and receptor activator of nuclear factor of kappa ligand (RANKL), which are important for OC development.

OC develop from hematopoietic stem cells and are responsible for bone resorption [42]. OC are giant multinucleated cells with a diameter of up to 100 µm and formed by the fusion of macrophage colony-forming units [43]. To start the resorption of bone matrix, OC form an actin ring/ruffled border necessary for the sealing zone on the bone surface delimiting or isolating a resorption lacunae. Thereafter, cells release protons and lysosomal enzymes such as collagenases, tartrate-resistant acid phosphatase (TRAP) and cathepsin K in the resorption lacunae [44]. The first step during bone matrix resorption is the digestion of collagen in order to remobilise hydroxyapatite crystals and to release Ca and P. Resulting digestion products are absorbed by the OC, transported and released at the basolateral side. Continuous remodelling of the actin ring allows OC movement across the bone surface during the bone resorption process. The functions and differentiation of OC are regulated by endocrine hormones and paracrine acting factors/cytokines. Among paracrine factors are granulocyte/macrophage colony-stimulating factor, M-CSF, RANKL as well as

proinflammatory cytokines such as interleukins (IL) and tumour necrosis factor (TNF) [45]. M-CSF and RANKL, have been shown to be essential for survival, differentiation and activation of OC [42]. M-CSF binds, to early OC precursors, to the colony-stimulating factor-1 receptor (c-Fms), initiating signal cascades necessary for survival and proliferation. RANKL is also essential for differentiation, activates the OC and is important for the OC resorption activity. When treated with M-CSF alone, no resorption activity was observed in macrophage populations [46]. Therefore, complete osteoclastogenesis is *in vitro* only possible when the cells are treated with both M-CSF and RANKL.

IL are a group of proteins that have very various effects on bone cells. For example, IL 1 is an inflammatory protein, activates the nuclear factor 'kappa-light-chain-enhancer' of activated B-cells (NF-κB) signalling pathway [47] and activates TNF receptor associated factor 6 (TRAF 6), which is an essential protein of the RANKL pathway [48]. Thus, IL 1 positively influences the development and activity of OC and induce the pit-formation activity [49]. IL 2 has also inflammatory properties and support bone resorption by OC. IL 2 stimulates the acid production and Ca release by OC *in situ* on mouse calvaria bones. The stimulation ends when IL 2 was removed from the system [50]. IL 4 on the other side inhibit the bone resorption *in vitro* [51] and *in vivo* [52]. IL 4 inhibits OC differentiation by the suppression of RANKL-induced NF-κB DNA binding in OC precursor. This suppression of IL 4 triggers a weaker receptor activation of NF-κB ligand and consequently a slower OC differentiation [53].

The total absence of M-SCF was determined in macrophage-deficient osteopetrotic mice (a genetic disease leading to denser bone) [54]. Similarly, the importance of RANKL for the OC differentiation was demonstrated in a RANKL-deficient mice model leading to osteopetrosis and revealed the absence of OC [55]. RANKL interacts with a receptor on OC precursor cells called receptor activator of NFκB (RANK). The binding of RANK and RANKL leads to an activation, differentiation, and fusion of hematopoietic cells of the OC lineage to OC and starts the process of bone resorption. Furthermore, the binding between RANK and RANKL also prolongs the survival of OC by suppressing apoptosis [24]. This interaction indicates that the process between bone resorption and bone formation is connected through RANKL. RANKL can be blocked by osteoprotegerin (OPG), a secretory dimeric glycoprotein belonging to the TNF receptor family. OPG acts as a soluble antagonist (decoy receptor) for RANKL and is mainly produced by cells of the OB lineage, but can also be produced by other cells like B-cells and dendritic cells [56–58]. On the other side, OC produce semaphorin 4D (SEMA4D), which inhibits the differentiation of OB. With SEMA4D, the OC probably control the location where the mature OB start the bone formation process [59]. Thus, SEMA4D is probably an essential factor for the event organisation of bone remodelling (Figure 1).

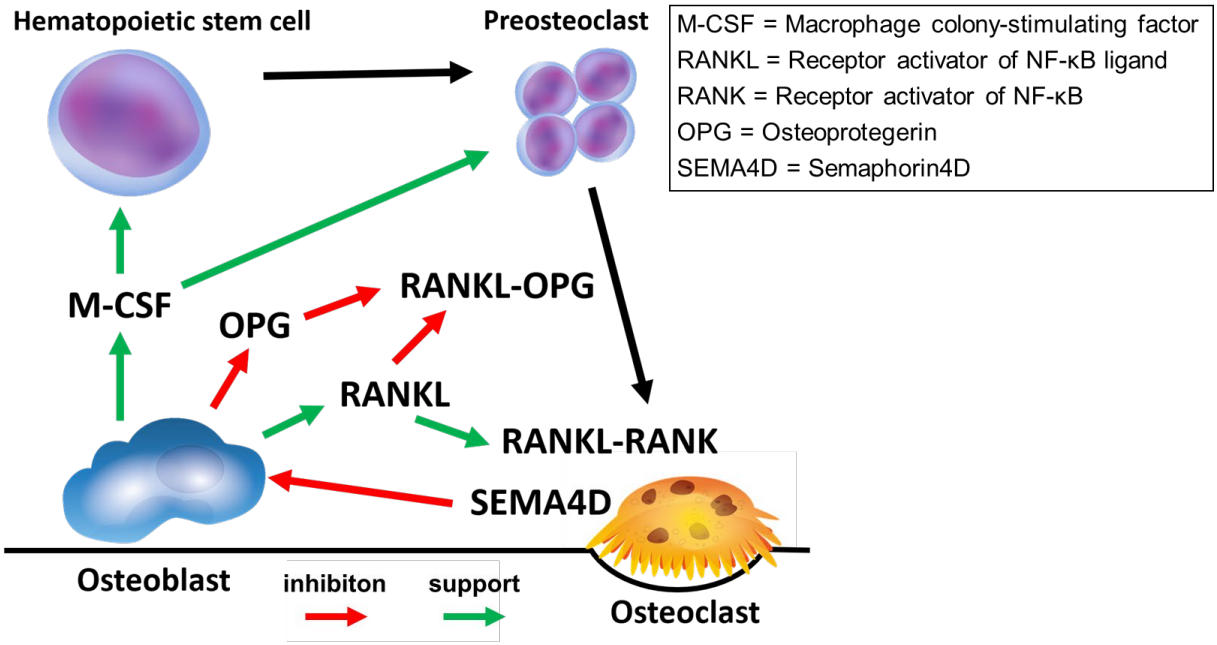

Figure 1: Crosstalk between osteoblast and osteoclast [24,54–59]

The remodelling process itself consists of three steps: resorption, reversal, and formation. The resorption starts with the migration of partially differentiated mononuclear preosteoclasts to the bone surface where they form multinucleated OC in the presence of RANKL and M-CSF. When the osteoclastic resorption of the bone occurred it comes to a reverse phase, meaning the migration of mononuclear cells on the bone surface begins. These mononuclear cells remove the collagen and prepare the surface for the OB migration. Mononuclear cells remain on the bone surface until the resorbed part is completely replaced by osteoid and other proteins by OB [60,61]. Finally, the bone surface is covered by flattened lining cells. The different stages of remodelling vary in time. The resorption takes approximately two weeks and the reversal takes, depending on the surface area, up to four or five weeks. Four months are needed until the new bone structure of the micro fracture is completely created [37]. A detailed molecular mechanism displaying the interaction of the osteoblastic and osteoclastic lineages was described by Raggatt *et al.* (2010) [62].

1.2 *In vitro* culture systems for orthopaedic implant material investigation

For the *in vitro* investigation of the cytocompatibility and effects of biomaterials or of Mg-based alloys more specifically, different culture systems are available, depending on the research question. In addition to the use of mono (one cell type) or coculture (2 and more cell types),

the model system can be divided by the type of cell selected: primary cells and (immortalised) cell lines.

Primary cells are usually obtained from donor samples (human, rodents or others) for each experiment or short experimental period. Most primary cell cultures have a limited lifespan but most closely represent the tissue of origin. In addition, their reaction or behaviour (*e.g.* proliferation rate) can vary largely depending on the donor [63]. Thus, although the cell behaviour is relatively natural, in large or long experiments the variance of the donor cells leads to a larger bias of the results. Therefore, several donors should be used for the experimental analysis.

Cell lines, on the other side, can be kept almost indefinitely in culture without any significant change in their behaviour, so the experiments are more comparable. However, most cell lines are immortalized and therefore have tumorigenic properties. If these cells are implanted in suitable animals (*e.g.* naked mice) they are able to form tumours [64]. In the past, most cell lines were obtained *in vitro* or *in vivo* from spontaneously or specifically (chemically or virally induced) tumours. Some cell lines have more or less retained their undifferentiated character [63]. Thus, cell lines are easier to handle, but due to their immortalisation the probability is lower that the observed processes are comparable to the in the *in vivo* system. Since the results are more reproducible, cell line systems should be used for *e.g.* toxicity screening. Thus, ethical principles can be followed that animal testing is reduced to a minimum [65,66].

1.2.1 Osteoblast mono culture models

In order to investigate the potential of Mg alloys for bone formation, human or murine OB are mainly used. One example, for the difference between primary cells and cell lines for OB is that the osteosarcoma cell line MG63 is less stable than OB at a higher pH [67].

MC3T3-E1 cells (mouse cell line) have been used for cytotoxicity testing of binary Mg alloys (aluminium (Al), tin (Sn) and zinc (Zn)). Treatment with different alloys such as Mg-1Al; Mg-1Sn or Mg-1Zn did not significantly reduce the viability of MC3T3-E1 [68].

Direct contact of primary human OB with the surface of Mg-2Ag for 14 days has led only initially (day 2) to increased cytotoxicity. On the third day, however, the cytotoxicity level was similar to that of Mg-Pure treated samples. Culture on Mg-Pure and Mg-10Gd surfaces did not show any cytotoxic effect [69].

Positive effects on cell adhesion, differentiation and proliferation were observed when Mg was incorporated into bone substitute materials such as Ca_3PO_4 or hydroxyapatite [70,71]. The

adhesion of OB to a collagen composite matrix could be increased compared to a Mg free control [72]. In another study not only the adhesiveness of human bone derived cells was improved but also the expression of type I collagen was increased. In this experiment, the cells were grown on a bio ceramic substrate which contains Mg (Al_2O_3-Mg^{2+}) and compared to an unmodified one (Al_2O_3) [73].

In order to have a direct comparison, different oteosarcoma-derived cell lines (MG63, Saos-2, and U2OS) with isolated primary OB grown directly on Mg-based implant materials. The individual samples were examined with regard to cell morphology, expression of focal adhesions and changes in gene expression. It turned out that the primary OB have increased above average in size. Furthermore, gene expression differed between the cell lines and the primary OB. While the gene expression of the primary OB, U2OS and MG63 for the osteoinductive genes and those necessary for the communication with the OC were highly regulated when cultured on Mg samples, only few differences to control (*i.e.*, primary OB) could be observed in the Saos-2 cells [74].

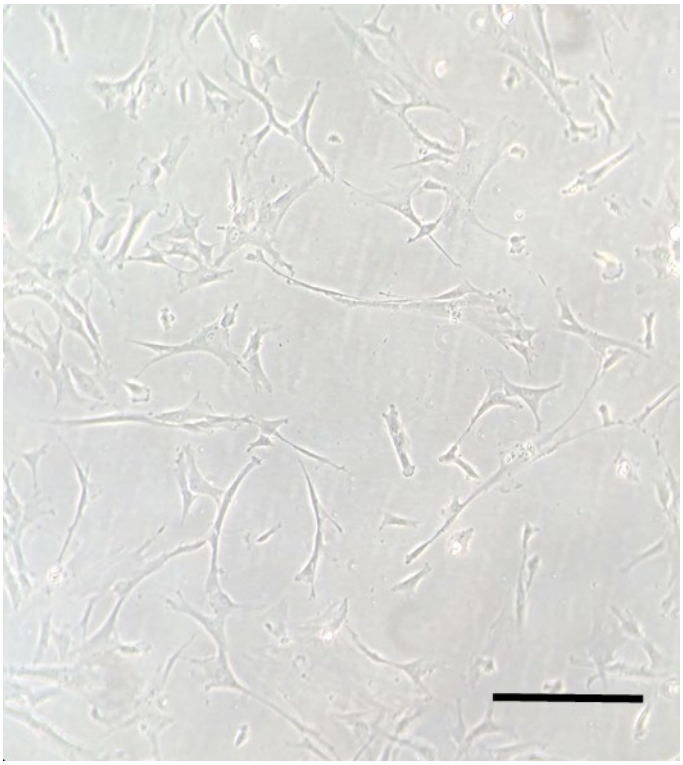

Figure 2: Primary monoculter HUCPV after 3 Days (scale bar: 100 µm)

The human umbilical cord perivascular cells (HUCPV; Figure 2) are an attractive alternative to cell lines or primary OB. The HUCPV are derived from Wharton's jelly, originate from the mesenchymal stromal cells [75] and can differentiate spontaneously into OB [76]. Furthermore, the HUCPV have a higher proliferation rate than human bone marrow mesenchymal stem cells and thus a larger number of cells can be generated and utilized until the zero growth point [77,78]. In addition, HUCPV maintain their mesenchymal stem cell character and have an extended life span in culture [79]. The differentiation into OB was proven in using flowcytometry, the detection of ALP and osteopontin. A later study has further shown that cells differentiated from HUCPV had the ability to form bones [80]. The study has also shown that HUCPV differentiates into cells that express *ALP*, *colagen 1*, *RUNX 2* and *bone sialoprotein* without the addition of osteogenic components (b-glycerophosphate, L-ascorbic acid and

dexamethasone). However, the expression of *ALP* and *bone sialoprotein* (BSP) is higher when osteogenic components are added and with the addition of osteogenic components, more bone mass was formed. The osteogenic differentiation of HUCPV cells can also be enhanced by 50 nm 1.25-dihydroxyvitamin D3 (vitamin D3) [81]. In addition, vitamin D3 influences Ca homeostasis, cell proliferation, differentiation and function [82]. Vitamin D3 interacts with the vitamin D3 receptor and triggers the expression on IGF-I witch induce the osteoblastogenesis [83].

1.2.2 Osteoclast mono culture model

Experiments utilizing OC are rather rare due to their complex behaviour and low tissue abundance. The amount of active OC in adult primate bone is only about 1 % [84]. Furthermore, the OC are mainly located on the calcified bone surface in the medullary canal. This makes it extremely difficult to obtain a sufficient number of active, primary OC for analyses. Thus, the discovery of RANK and M-CSF signalling system, which enables the *in vitro* generation of OC from their mononuclear precursors, has greatly simplified their availability [85].

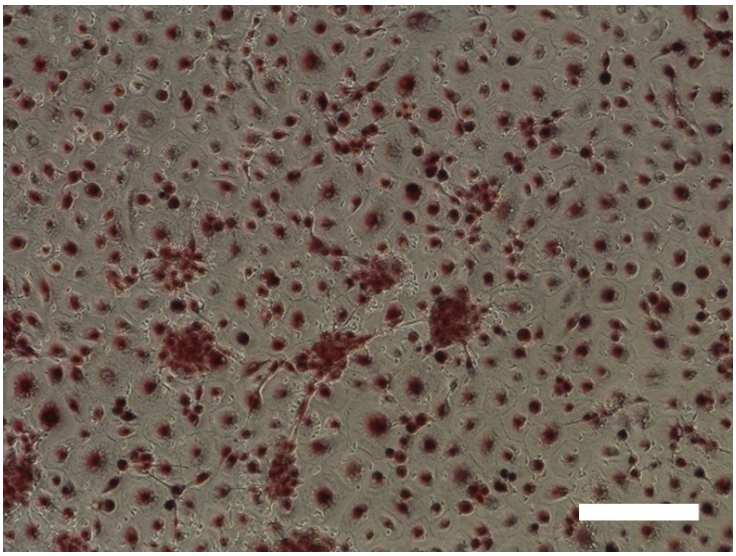

Figure 3: Picture of a TRAP stained PBMC monocluture after 14 days (scale bar 100 µm)

Peripheral Blood Monocular Cells (PBMC; Figure 3) are able to differentiate into OC [86]. The PBMC are originate from hemopoietic stem cells which are located in the bone marrow. To induce this differentiation, the cells have to be exposed to RANKL and M-CSF so the $CD14^+$ PBMC can differentiate into OC. Although these cells can be obtained relatively easy from human blood, it is not possible to multiply the cells undifferentiated in the laboratory and therefore they have to be isolated fresh for every experiment. The cells were already used for many study as monocultures with RANKL/M-CSF [87,88] or cocultures [89,90].

With addition of RANKL and M-CSF, the influence of different concentrations of Mg extracts (*e.g.* Mg-Pure, MgAg, etc.) on the vitality and differentiation of OC could be investigated.

Moreover, it was shown that OC alone were more sensitive to increasing Mg concentrations than if cultured together with OB [91,92].

1.2.3 Osteoblast-osteoclast coculture model

Both cell types are involved in the precisely coordinated process of bone remodelling and are thus believed to be the two most important or representative cells of this tissue [62]. Since most cytocompatibility studies are conducted with OB, the interaction between the cells and the role of OC for the success of biomedical implants remain underestimated [93].

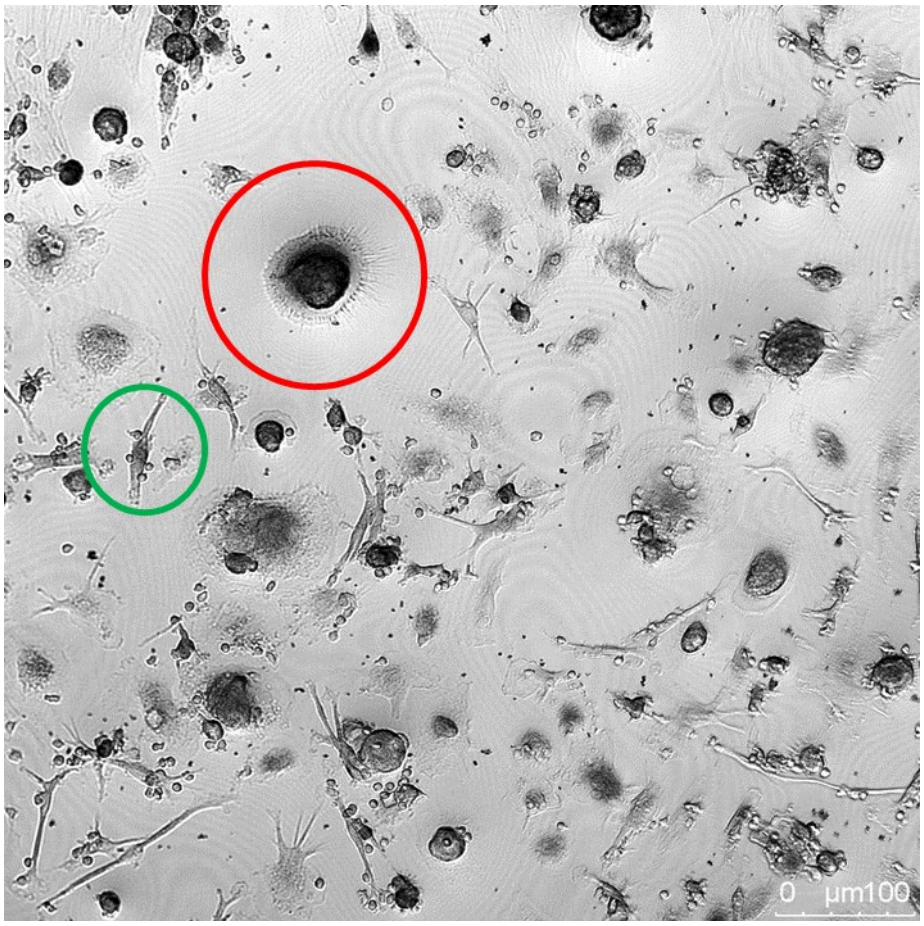

Figure 4: Confocal picture of a coculture consisting of differentiated HUCPV into OB (green circle) and PBMC into OC (red circle) after 28 days.

Therefore, new *in vitro* models are necessary, which not only observe the differentiation and activity of the OB but also that of the OC as well as the OB-OC crosstalk (Figure 4). Thus, an OB-OC coculture should be more similar to *in vivo* osseous conditions as mono cultures and thus allow a deeper investigation of how implant materials influence the communication between the bone forming OB and the bone resorbing OC.

There are some examples of highly complex coculture systems. In one study, a three-dimensional (3D) *in vitro* model of bone was developed by seeding murine primary OB (from C57Bl6/J mice) and OC precursors (from C57Bl/6-Tg(ACTB-EGFP)1Osb/J mice) on a resorbable porous ceramic scaffold based on silicon-stabilized tricalcium phosphate [94]. Such scaffold allowed bone cell interactions in a 3D environment that mimics the *in vivo* state better than traditional two-dimensional cultures.

Cocultures of OB and OC have already been used in various experiments to investigate *e.g.* the influence of different substances on the cells. In the following some examples are described in which context cocultures of OB and OC were used.

In another study a combination of murine OB (MC3T3-E1) and OC (primary monocyte from 8-week-old CD1 mice) were used [95]. It was investigated whether silk fibroin, chitosan and poly (L-lactic acid) affect the growth and differentiation of OB and OC in co- and monocultures. Furthermore, the materials degradation and the effect of the different cultures on the degradation rates were studied.

The expression of intercellular adhesion molecule-1 (ICAM-1) were investigated in a coculture of human OB-like cells and OC precursors [96]. ICAM-1 mediates adhesion between OB and OC precursors through interaction with leukocyte function-associated antigen-1. During the investigation it was determined whether the expression of ICAM-1 changes during the development of OC.

It was known that bisphosphonates such as zoledronic acid (ZOL) reduce resorption activity in monocultures of OC. Since no experiments with coculture have taken place up to this time, the effect of ZOL on coculture was investigated based on primary human OB and OC ($CD14^+$ human PBMC) [97]. ZOL was applied in an implant coating based on poly(D,L-lactide) in different concentrations (10-50 microM). ZOL has been shown to reduce TRAP-positive cells and positively influence OB differentiation depending on dose.

In 1999, a human coculture system was established consisting of OC precursors ($CD34^+$ haematopoietic stem cells from human bone marrow) and mesenchymal stem cells [98]. The OC in this coculture were able to express TRAP, calcitonin and show a bone resorption activity.

In addition, a coculture system of human monocytes and human mesenchymal stem cells (hMSCs) was established [99]. The cells were cultured on membrane-like structures of mineralized collagen I, which imitated the extracellular bone matrix. Both cell types were physically separated by transwell inserts without hindering the exchange of soluble factors. The development of the coculture was followed by determining the gene expression as well as

the ALP and TRAP activity. It turned out that the adipogenic differentiation of hMSCs is suppressed by the presence of OC.

1.3 Implant material in orthopaedic application

There are two types of orthopaedic metallic implant materials. The non-degradable implant materials, which are made of *e.g.* titanium or stainless steel alloys and the degradable implant materials, which consist of Mg, Zn, iron (Fe) or their alloys.

1.3.1 Non-resorbable Materials

Most implants currently used in orthopaedics are made of non-resorbable materials. They stay permanently in the body or must be explanted by an additional surgical procedure.

Mechanical characteristics

Non-absorbable titanium or steel are normally implanted for replacement or fixation of bone in human and veterinary medicine [100–102]. Titanium also has a higher stiffness in comparison to bone, which could induce stress shielding effects [103–105].

Toxological properties

Titanium could have a negative effect on (*e.g.*) the proliferation, functions of OB and the polarisation of macrophages [106,107]. Furthermore wear debris could lead to aseptic loosening and revision surgery [108]. Since permanent implants like stainless steel, titanium alloys etc. (316L stainless steel, Ti-6Al-4V, Co-Cr-Mo etc.) are also widely used, toxic metal ions such as chromium, cobalt or nickel can be released from these, which can lead to inflammation and are thus classified as harmful to the surrounding tissue [109–111].

1.3.2 Resorbable Material

In contrast to non-degradable materials, degradable materials dissolve in the body over time and releasing the alloying substances into the body. Because of that, it is necessary that the implant material consist of non-toxic and biocompatible elements.

Mechanical characteristics

Because of their mechanical properties, bioresorbable metals like Zn, Fe, and Mg alloys have a high potential in the numerous treatments of soft and hard tissue trauma and diseases [112].

Mg has a suitable combination of mechanical strength, ductility and tensile modulus in contrast to ceramics or polymers, (Table 2) and Mg particles have been reported to support bone regeneration without inducing inflammation [113].

Table 2: Mechanical properties of bone an implant materials [114–118]

	Bone	**Magnesium**	**Polymers**	**Titanium**	**Ceramics**
Tensile strength [Mpa]	35 - 283	160 - 250	16 - 69	170 - 950	83 - 306
Youngs modulus [Gpa]	17 - 20	41 - 45	0.4 - 7	110 - 127	150 - 420

The mechanical properties of Mg implants can be tailored by using different alloying elements or various processing techniques. Additionally to the mechanical properties, the alloying elements can also add some useful characteristics like antibacterial properties (please see Ch. 1.3.6 Page 16; Ch. 1.3.7 Page 17).

Toxological properties

A Zn and Fe overloads can lead to *e.g.* neurotoxicity and liver damage, respectively. However, hypermagnesemia is rare and is mainly due to iatrogenic artefacts, *e.g.* laxatives and anti-acids and advanced chronic kidney disease [119]. The effects of Mg^{2+} vary between species, strains, gender, and age [120].

1.3.3 Degradation processes

The degradation rate of alloys is very important. If the alloys degrade too quickly, implants can lose their integrity too fast and could damage the surrounding tissue [121]. Furthermore a fast release of alloying elements such as Al, Ag or manganese could induce toxic side effects [122]. Therefore, degradation rate of any bioresorbable metal-based biomaterials have to be measured. The issue of fast Mg-based degradation has already been identified in the first *in vivo* experiments as Mg implants had completely degraded within only 8 days [121]. This high degradation rate was probably due to impurities in the Mg implants: even small iron impurities can lead to a significant increased degradation and thus gas formation [123].

During degradation processes Mg is oxidised to Mg^{2+} and H_2O is reduced to OH^- and H_2 [124]. These degradation products are harmless, cause only minor changes in the blood composition and can be excreted through the urine without damaging the liver or kidneys [124,125]. However, a too rapid degradation of Mg-based biomaterials would lead to an excessive hydrogen evolution, local hydrogen saturation and hindered solubility and a shift to an alkaline pH.

1.3.4 Actual implant materials in clinical application

First reported uses of Mg as implant materials date from early twentieth century [126]. The Mg source and the production process at that time basically determined the purity of Mg and its alloys. Therefore, surgeons were mainly dependent on the local Mg alloys or the skills of the nearest Mg supplier [126].

Lambotte and Verbrugge perform clinical experiments on different children with supracondylar humerus fractures. The first experiments had to be aborted because of gas cavities, swelling and pain. It was understood that to prevent electrolytic corrosion Mg could only be implanted without other metallic implants [121]. After adjusting experimental settings, additional experiments were performed on four different children (7 - 10 years old). Because of the exclusively use of Mg all children healed without complication except the gas cavities, which disappeared after several weeks [121,127]. In 1940, two fractures of the upper arm were examined in people with needles made of Mg. In one case, the healing process went off without any special events. In the other case, however, the implant had to be removed after only 12 days due to the continuous formation of gas cavities [128]. One of the first patents in the field of degradable implants was filed in 1969 by Stroganov for the alloy consisting of the rare earth element cadmium with Mg or other elements in different compositions which showed an improvement in corrosion resistance [129].

Since then, some Mg-based implants have been introduced to the market. For example, the first Mg screw was developed by Syntellix in 2013 (CE mark Europe). A short time later, in 2016, BIOTRONIK SE & Co. KG recently developed (CE mark Europe) stent was used in a patient. This stent received Food and Drug Administration (FDA) approval for the US market at the beginning of 2017. Another Mg based screw with the composition of Mg-5Ca-1Zn was approved by the Korea Food and Drug Administration in 2015 [130]. In China, no approvals of Mg implants are known so far [131], but some interesting studies have been performed in recent years. The Chinese company Eontec started clinical trials in 2015. This study was published in 2016 and showed good results, but the implant was not stable enough [132].

1.3.5 Physiology and function of magnesium

In nature, Mg occurs in the form of salts (*e.g.* $MgCl_2$, $MgSO_4$ and $MgCO_3$), which have a high solubility equilibrium. Therefore, they have a high bioavailability. Mg acts as an activator of at least 200 enzymes and as a cofactor of 600 enzymes [133]. Mg is involved in a variety of essential processes such as deoxyribonucleic acid (DNA) replication, amino acid synthesis, glycolysis, stabilization of DNA as well as ribonucleic acid (RNA), proliferation, apoptosis and

much more [133,134]. The society “Deutsche Gesellschaft für Ernährung” (DGE) recommended daily intake of Mg 375 mg to 500 mg depending on age and gender. A normal Mg level in serum is 17-24 mg/L. This is only 1 % of the total amount in the human body [135]. The remaining 99 % are located in the cells. A healthy adult stores about 20 - 30 g Mg in the body [136].

Mg homeostasis is controlled *via* bony, renal and gastro enteral processes. First, Mg is absorbed mainly by the small intestine, partly by the large intestine *via* ion channels like transient receptor potential ion channel 6 and 7 (TRPM6 and TRPM7), and stored in the bone if there is an excess or excreted. In addition, Mg can also be stored in muscles and other soft tissues [137]. In order to maintain the physiological Mg level, about one third of the Mg stored in the bone and can be mobilized if necessary [138]. Finally, the kidneys play an elementary role in Mg homeostasis. It reabsorb about 95 % of the filtered Mg under physiological conditions and in case of an excess the Mg can be excreted together with the unabsorbed 5 % *via* urine and faeces [139].

Additionally, Mg is biologically and chemically related to some elements like Ca and potassium (K) [124,140]. Mg is a natural, non-competitive antagonist that uses the same voltage-dependent Ca channels and regulates Na-K pumps [141,142]. In addition, Mg not only promotes OB differentiation but also inhibits the release of inflammatory factors such as interleukin-1, tumour necrosis factor and substance P, thereby inhibiting OC activity [143].

Epidemiological studies, animal and human evidences suggested that a Mg deficiency (<1.2 Mg/dL) can lead to various inflammatory diseases such as osteoporosis, nerve dysfunctions, pathophysiological effects in cardiovascular pathology, the development of cardiomyopathic lesions and atherosclerosis [144–147]. In general a Mg deficiency results in inflammatory and/or oxidative stress, which can result in impaired cardiac function, inflammatory processes in lungs, activation of macrophages and an increase of inflammatory cytokines [139–143]. Since Mg is involved in a large number of metabolic processes, a supplementation with Mg, if it compensates a deficiency, can counteract the mentioned symptoms or cause them to disappear [148]. Mg supplements (*e.g.* $MgSO_4$ or $MgCl_2$) have been extensively investigated for their protective effect in inflammatory processes. $MgSO_4$ significantly reduced the bacterially induced inflammatory processes [149–151]. If the amount of Mg in the body is too high it can lead to disturbance of consciousness, hypotension and bradycardia [152,153].

1.3.6 Physiological influence and antibacterial properties of silver

Due to its antibacterial properties, Ag-containing or coated implants are a strategy to reduce the probability of infection after surgery. The antibacterial effect of Ag is also used in other areas such as wound dressings, cosmetics or antibiotics [154]. So far, only limited information is available on the toxic effects of Ag on mammalian cells and the existing studies mostly refer to Ag nanoparticles. As Ag^+ ions are also released in physiological fluids from nanoparticles, it is difficult to determine whether the effects are caused by ions or nanoparticles [155].

The nanoparticles are absorbed into the cell by endocytosis. The Ag^+ ions are released in the acidic environment of endosomes and secreted afterwards intracellularly. Free Ag^+ ions can be transported into the cell by the copper transporter 1 (CTR1) [156] and the divalent metal transporter (DMT1) [157]. After the Ag^+ ions has entered the cell, it promotes the production of reactive oxygen species (ROS) in the mitochondria [158]. ROS are necessary for various processes up to a certain point like immune defence and cell development (*e.g.* OC), but at higher concentrations they can irreparably damage DNA and proteins and lead to cell death [159,160].

At which concentration the cytotoxic effect of Ag occurs is not yet precisely determined. In some studies concentrations of 5 µg/mL were already toxic [161], in other publications only much higher concentrations led to toxic effects in different cell types [162]. The discussion whether Ag is more cytotoxic for bacteria than for mammalian cells is also controversial. While already shown, *Staphylococcus epidermidis* has a higher tolerance to Ag^+ ions than mice OB [163]. On the other side it could also be shown that Ag is toxic for *Candida albicans* at a similar level as for human fibroblasts (1 mg/L) and that Ag nanoparticles hinder the growth of the tested yeast at a concentrations between 2-16 mg/L. Ag^+ ions was already toxic for eukaryotic cells at a concentration of 1 mg/L, but the Ag nanoparticles only until a concentration of 30 mg/L [164]. Both *in vitro* and *in vivo* Ag coating has already led to an inhibited biofilm formation of the bacterium *Staphylococcus aureus* [165].

Ag alloys have also been tested *in vivo*. Mg-Ag-Y was on of the tested alloys. This alloy had similar elastic moduli, tensile, and compressive stress properties compared to native bone. The Mg-Ag-Y alloy was implanted for 6 weeks in non-fractured distal femora of Sprague Dawley® rats and compared to Mg implants. The following tests showed that there were no abnormal physiological changes. The degradation rate of the Mg-Ag-Y alloy was only half that of the Mg implants. However, an average of twice as much new bone was formed in individuals with Mg-Ag-Y alloys [166].

1.3.7 Usage of gadolinium and its influence on calcium channels

The element Gd belongs to the lanthanides, is 3-fold positively charged and does not physiologically occur in the body. Compounds made of Gd derivatives serve as contrast agents in magnetic resonance imaging (MRI) [167]. Systemic toxic effects like apoptosis, oxidative stress and transmetalation were only detected at doses above 1 mM [17]. In cell culture experiments, however, Gd strongly inhibited the voltage-dependent Ca channels at much lower concentrations [18]. There are no known Gd transporter. Instead, the Gd^{3+} ions block the voltage-dependent Ca channels and the Na/K pump [168]. Gd particles can be absorbed by endocytosis and the cell viability only decreased at a concentration of 28 µM Gd [169].

Gadolinium chloride ($GdCl_3$) was also shown to increase the proliferation rate of NIH 3T3 cells (mouse fibroblasts) *via* the Phosphoinositid-3-Kinasen (PI3K) and mitogen-activated protein kinase (MAPK) signal cascades. This study did not explain in detail at which point this signal cascade is initiated [170]. Nevertheless, it is known that Gd^{3+} ions activate the calcium sensing receptor (CASR) and thus imitate a high Ca level [171].

2 Motivation and objectives

It has already been shown *in vivo* that Mg has a positive influence on bone formation [172]. To investigate further the influence of different Mg-based alloys (Mg-Pure, Mg-2Ag and Mg-10Gd) *in vitro*, the focus of this study was to establish a more complex coculture system consisting of primary OB (HUCPV) and OC (PBMC) precursor cells. The focus was laid on the differentiation and communication of the two precursor cell types and to draw conclusions about changes by molecular means. Single element salts solutions were used as a control for the extracts. The aim of the salts was to show the influence of the different elements as accurately as possible, independent of the degradation products.

To this purpose, this work has been divided into the following sections:

- Establishment and characterisation of the coculture consisting of PBMC and HUCPV

- Monitoring the influence of different Mg based alloys on the coculture by monitoring different specific markers like HA formation as well as metabolic activity (*e.g.* TRAP and ALP).

- Evaluation of the influence of different Mg-based alloys on the expression of different factors like RANKL, M-CSF and SEMA4D responsible for the communication between OB and OC.

3 Material and Methods

The experiments were performed between February 2015 and April 2018 in the laboratory of the Department of Metallic Biomaterials of the Helmholtz Centre in Geesthacht.

3.1.1 Production of the Mg-based materials

Pure Mg (Mg-Pure) and various alloys of MgAg (Mg-2Ag, Mg-4Ag, Mg-6Ag and Mg-8Ag) and MgGd (Mg-5Gd and Mg-10Gd) were produced by the Magnesium Innovation Center (MagIC) of the Helmholtz-Zentrum Geesthacht. The pure Mg (99.99 %), Ag (99.99 %) and Gd (99.95 %) were used for the casting process.

Various casting techniques were chosen to produce the materials (MgAg: permanent mould gravity casting; Mg and MgGd: permanent mould direct-chill casting method). After the Mg melting process, the melt was kept at 720 °C for Ag and 680 °C for Gd and the corresponding amounts of the material (Ag and Gd) were added while stirring for 15 minutes. The melt was poured under an oxygen-poor atmosphere (2 wt.% sulphur hexafluoride (SF6) in an argon mixture). The processing parameters for T4 heat treatment and extrusion were different due to the variety of the material in order to achieve similar microstructures resulting in a moderate degradation rate. These parameters are specified in Table 3. Discs were made from the extruded bars. After processing, the alloys were analysed with scanning electron microscope (SEM) Desktop ProX (Phenom, Eindhoven, Netherlands) and used in form of discs with the dimensions 1 mm high and 9 or 12 mm in diameter.

Table 3: Processing parameters of the diffrent alloys [173–176]

Alloy	T4 Heat Treatment	Extrusion Speed in mm/s	Extrusion T in °C	additional T4 heat treatment	Ø final
Mg-Pure	x	0.7	300	x	9
Mg-2Ag	420 °C; 6 h	2.5	370	x	9
Mg-4Ag	420 °C; 6 h	0.7	300	x	12
Mg-6Ag	430 °C; 8 h	0.7	285	x	12
Mg-8Ag	430 °C; 16 h	0.7	300	450 °C; 8 h	12
Mg-5Gd	550 °C; 6 h	3.5	430	x	12
Mg-10Gd	550 °C; 6 h	3.5	370	x	12

The materials were used in the following for two different experimental setups. In the indirect assay, the cells were exposed to the degradation products of the materials. In the direct assay the cells were cultured directly on the material. The indirect assay was used to observe the

influence of alloying elements in more detail. By adjusting the Mg concentration to a uniform value, the influence of the alloying partners can be observed more accurately. On the other hand, the degradation of the alloys is a process which releases mechanical forces. These forces can also influence the behaviour of the cells. In addition, the mixing in the wells is rather slow. This causes concentration gradients in the solution during degradation of the materials, which can also affect the cells. The direct assay was performed to determine the effects of the above-mentioned influences on the cell behaviour and whether this type of cultivation could even lead to the death of the cells.

3.1.2 Extracts preparation

The cell culture media with Mg degradation products hereinafter called Mg extract (Mg-Pure, Mg-5Gd [5 wt% Gd], Mg-10Gd [10 wt% Gd], Mg-2Ag [2 wt% Ag], Mg-4Ag [4 wt% Ag], Mg-6Ag [6 wt% Ag] and Mg-8Ag [8 wt% Ag]) were prepared according to EN ISO standards 10993:5 [177] and 10993:12 [178]. The discs were cleaned for 20 min in n-hexane (Merck Millipore, Darmstadt, Germany), 20 min in acetone (Merck Millipore, Darmstadt, Germany), 3 min with 100 % ethanol (Merck Millipore, Darmstadt, Germany) and sterilized for 20 min in 70 % ethanol. Subsequently, the samples were dried for 1 h under sterile conditions and incubated in a defined ratio (0.2 g/mL) in α-minimum essential medium (α-MEM medium; Gibco - Fisher Scientific GmbH, Schwerte, Germany), supplemented with 10 % Fetal Bovine Serum (FBS; Gibco - Fisher Scientific GmbH, Schwerte, Germany) and 1 % Penicillin/Streptomycin (pen/strep; 10,000 U/mL; Gibco - Fisher Scientific GmbH, Schwerte, Germany). After 72 h under physiological conditions (5 % CO_2, 20 % O_2, 95 % humidity, 37 °C), the resulting Mg extracts were sterile filtered. The element concentrations were determined by inductively coupled plasma mass spectrometry (ICP-MS) by GALAB (GALAB Laboratories, Hamburg, Germany).

For the following experiments, the extracts were adjusted with cell culture medium to an Mg concentration of 10 mM. The resulting Mg extracts were characterized by the analysis of osmolality (Osmomat auto, gonotec, Berlin, Germany) and pH (Si series pH meter, Sentron, Leek, Netherlands)

3.1.3 Preparation of salt solutions

The ion concentration to which the extracts were adjusted (*e.g.* 10 mM Mg) was chosen as the initial concentration for the preparation of the salt solution. For the Ag solution the

concentration of Mg-6Ag (3.35 nM Ag) was used and for the Gd solution the concentration of Mg-10Gd (3.13 nM Gd). To prepare the Mg and Gd salt solution, $MgCl_2$ (Merck Millipore, Darmstadt, Germany) and $GdCl_3$ (Sigma-Aldrich Chemie GmbH, Munich, Germany) were dissolved in ultrapure water Type 1. For the Ag solution the Silver ROTI®STAR Standard (Element standard solution atomic absorption spectroscopy) was diluted with ultrapure water Type 1 to the appropriate concentration. The solutions were freshly prepared for every test series and stored at 4 °C until use.

3.1.4 Immersion test of different magnesium alloys

To determine their degradation rates, the samples were incubated with (n=3) and without cells (n = 3) for 28 days in α-MEM medium supplemented with 10 % FBS and 1 % pen/strep. Prior to incubation, samples were weighted and individual samples taken from the medium on days 3, 7, 14, 21 and 28 were washed with 100 % ethanol and stored in a vacuum oven (SalvisLab, Rotkreuz, Schwiss). To remove the degradation layer, the samples were treated 2 times for 10 min with 2 mol/L chromic acid (Sigma-Aldrich Chemie GmbH, Munich, Germany) and washed 2 times with ultrapure water Type 1. To determine the weight loss, the sample was weighted a second time after this treatment. The following formula was used to determine the mean degradation depth (Equation 1) and degradation rate (Equation 2).

Equation 1: Calculation of the mean degradation depth

$$\text{Mean degradation depth } (\mu\text{m}) = \frac{\Delta\text{mass loss (g)} \times \text{f}}{\text{Surface } (\text{cm}^2) \times \text{density } (\text{g/cm}^3)}$$

f: Unit conversion factor. To obtain the mean degradation depth in µm, this factor is 10000.

Equation 2: Calculation of the degradation rate

$$\text{Degradation rate in } \mu\text{m/day} = \frac{\text{Mean degradation depth } (\mu\text{m})}{\text{days} + \text{y}}$$

y: Mean degradation depth attributing to initial reactions (obtained from linear regression function) in µm.

3.1.5 Investigation of material cytocompatibility by Live/Dead staining

Live/Dead staining (Invitrogen, Darmstadt, Germany) was used to detect live and dead cells on the samples. The fluorescent dye calcein-AM is taken up by living cells and converted by esterases to fluorescein analogues, which show a green fluorescence. Ethidium homodimer -1

is unable to penetrate intact cell membranes and thus only binds to the DNA of dead cells (red fluorescence). For the Live/Dead staining, the medium was removed after 3, 7, 14, 21 and 28 days and washed with medium without FBS.

Afterwards the medium was replaced by medium which was mixed with the dye solutions (calcein (2,7-Bis((*N*,*N*-bis(carboxymethy)amino)methyl)fluorescein; 2500:1) and ethidium homodimer (5,5'-[1,2-ethanediylbis(imino-3,1-propanediyl)]bis(3,8-diamino-6-phenyl); 1000:1)). The samples were incubated for 20 min at 37 °C and the staining solution was replaced by α–MEM medium without FBS. The images were taken immediately with a confocal microscope DM600 CS (Leica, Wetzlar, Germany). Samples without cells were used as negative control.

3.2 The cell culture system

3.2.1 Isolation of peripheral blood mononuclear cells (PBMC)

PBMC were isolated by Ficoll density gradient centrifugation (Figure 5) from TRIMA filter samples (from healthy donors; Institute of Transfusion Medicine at the University Hospital Eppendorf (UKE), Hamburg, Germany). The used anticoagulant was citrate dextrose solution (2.13 % free citrate ion ACD-A, which was added by the UKE at the time of donation). The human blood (approx. 10 mL) obtained from the TRIMA filter was diluted 1:5 with phosphate buffered saline solution (PBS; 155.17 mM NaCl, 1.059 mM KH_2PO_4, and 2.97 mM Na_2HPO_4-$7H_2O$; Biochrom AG, Berlin, Germany), was carefully coated on the Ficoll-Paque (Amersham Biosciences, Uppsala, Sweden) and centrifuged at 350 g without brake for 30 min. At the interface of the Ficoll- and PBS phase, the required monocyte-enriched PBMC fraction was trapped and was carefully collected with a 1000 µL pipette. The cells were washed twice with PBS, counted afterwards and used immediately.

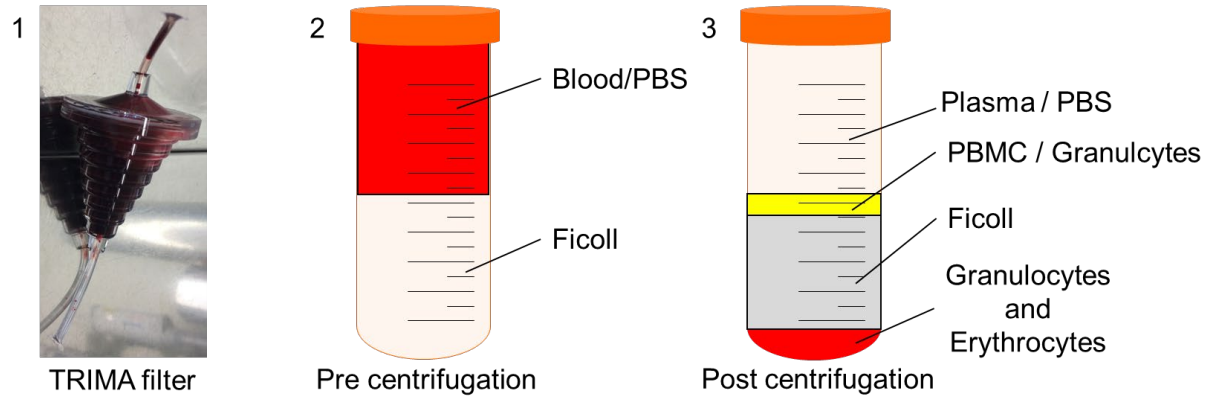

Figure 5: PBMC isolation by density gradient centrifugation

3.2.2 Isolation of human umbilical cord perivascular cells (HUCPV)

The isolation of HUCPV cells was performed according to the protocol of Sarugaser *et al.* [179]. The isolation and application of HUCPV were approved by the Ethics Committee of the Hamburg Medical Association (Hamburg, Germany) PV4058. The preserved umbilical cord (acquired from the Perinatal Centre Asklepios Klinikum Altona, Hamburg, Germany) was cut into approx. 5 cm large pieces. The artery was isolated from the Wharton's jelly and a closed vascular loop was formed. This loop should ensure that only the cells from the perivascular region migrate into the culture bottle so that the culture is not contaminated with the cells from inside of the arteria. The vascular loop was placed in a T175 cell culture flask and incubated for 10 days in α-MEM medium supplemented with 15 % FBS (Gibco - Fisher Scientific GmbH, Schwerte, Germany) and 1 % pen/strep (Gibco - Fisher Scientific GmbH, Schwerte, Germany). After the cells outgrowth, the medium was changed every 2 to 3 days. At 80 % confluence, the cells were separated with a cell scraper and resuspended in fresh medium. The process is shown in Figure 6.

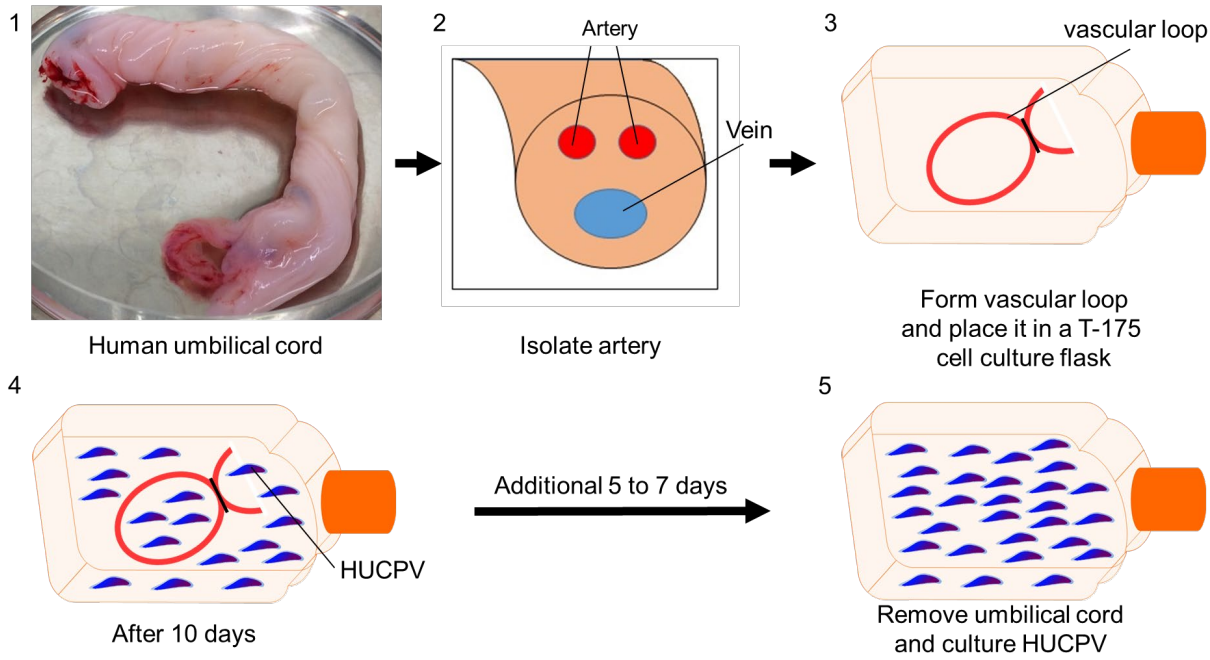

Figure 6: HUCPV isolation from the human umbilical cord

3.2.3 Cell culture conditions for osteoblasts and osteoclasts

The cells were cultured in α-MEM medium (Life technologies, Darmstadt, Germany) supplemented with a 1 % dilution of pen/strep (10,000 U/mL; Gibco - Fisher Scientific GmbH, Schwerte, Germany) and various FBS (either stem cell FBS (scFBS); for HUCPV from Merck

Millipore, Darmstadt, Germany or OC FBS for PBMC and coculture from Gibco - Fisher Scientific GmbH, Schwerte, Germany) at 37 °C, 5 % CO_2, 20 % O_2 and 20 % humidity (BBD 6220; Thermo Scientific, Darmstadt, Germany). To detach the cells from the culture vessel, the cells were washed with PBS (Thermo Fisher Scientific, Darmstadt, Germany) and incubated for 5 min in 0.05 % trypsin/Ethylenediaminetetraacetic acid (EDTA; Gibco - Fisher Scientific GmbH, Schwerte, Germany). The trypsin reaction was stopped with cell culture medium (ratio 1:1.5) and the cells were centrifuged at 1,500 rpm (Heraeus, Hanau, Germany) for 5 min. The supernatant was removed and the cells were resuspended in cell culture medium. Then the cells were counted and seeded either for further cultivation or for the planned experiments.

For freezing, the cells were centrifuged with 1,500 rpm (Rotina 430, Andreas Hettich, Schwerin, Germany) and the supernatant was replaced by the freezing medium (FBS supplemented with 10 % Dimethyl sulfoxide (DMSO) (Sigma-Aldrich Chemie GmbH, Munich, Germany)) to obtain a cell concentration of $2x10^6$/mL. The cells (1 mL of the cell DMSO solution) were aliquoted into a 2 mL screw vessel (cryogenic vessel), slowly cooled to -80 °C (1 °C/h) with a freezing container filled with Isopropanol and afterwards stored in liquid nitrogen. The cells were reactivated by thawing in a water bath (SV 1422, Memmert GmbH, Schwabach, Germany) at 37 °C, 9 mL cell culture medium added and centrifuged with 1,500 rpm (Rotina 430, Andreas Hettich, Schwerin, Germany). The supernatant was discarded, the cells were resuspend in the cell culture medium and placed in the culture vessel.

3.2.4 Optimized coculture protocol for PBMC and HUCPV cells

For the coculture the cells were seeded in a density of one HUCPV to 100 PBMC cells (for a 24-well cell culture plate per well: $1x10^4$ HUCP and $1x10^6$ PBMC). Only HUCPV with a passage between 8 and 13 were used for the experiments. For differentiation, the cells were cultured in α-MEM medium supplemented with 10 % FBS (Life Technologies, Darmstadt, Germany) and 50 nM vitamin D3 (Sigma-Aldrich Chemie GmbH, Munich, Germany) at 37 °C, 5 % CO_2, 20 % O_2 and H_2O saturation for up to 28 days with medium change every 2 to 3 days.

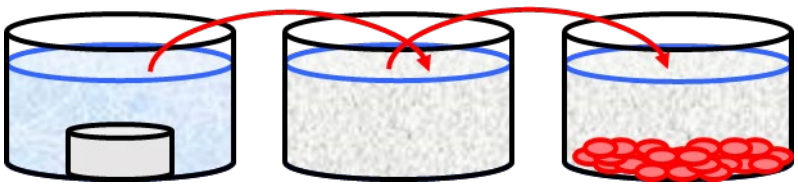

Figure 7: Process of indirect assay with extract preparation

For the indirect assay (Figure 7), either the Mg extracts or salts were added to the medium. To determine the influence of the salts or solutions and the degradation products of the Mg-Pure, MgGd or MgAg alloys, samples and cell culture supernatants were taken after 3, 7, 14, 21 and 28 days (Figure 8).

For the direct assay, the cells were grown directly on the surface of the samples. For this purpose, the alloys were preincubated with cell culture medium supplemented with FBS for 72 h in agarose coated wells of a 24-well cell culture plate. The material were pre-incubated for 72 h instead of 24 h, as preliminary tests showed that after 72 h far more cells can attached to the material. The cells were let adhere (in a 15 µL drop of media) on the sample surface and incubated at 37 °C for 30 min. Finally, 1 mL medium was added carefully and the cells were incubated for up to 28 days with medium change every 2-3 days. Here also, samples were taken after 3, 7, 14, 21 and 28 days (Figure 8).

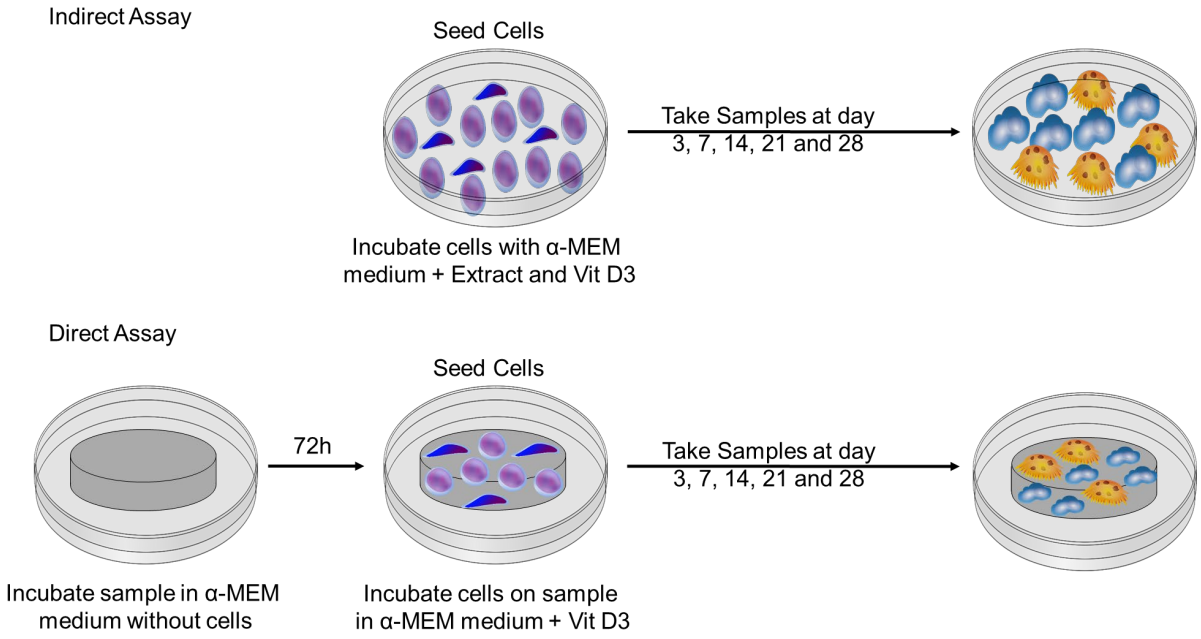

Figure 8: Schematic illustration of the experimental set-up of the indirect and direct coculture assays

3.3 Biochemical tests

Primary cells were used for the study. To optimize the known issue of donor variation and to obtain relevant and representative results, several HUCPV and PBMC donors were selected. For each experimental run 1 HUCPV donor and 2 different PBMC donors were used (biological replicates = 2). Each experimental set-up was performed 3 times and measured 3 times each

(technical replicas = 3). The allocation of the different donors in the different experiments can be seen in the following Table 4.

Table 4: Overview of the donors used in the experiments

Type	Experiment	OB donor	OC donor	Technical replicates	Total replicates
Pre-tests	Medium Test	A24	1 - 2	3	6
	Ratio Test	A24	3 - 4		
	Differentiation Test	A24	5- 6		
Extract	Mg-Pure, Mg-8Ag, Mg-5Gd	A80	7 - 8		
	Mg-Pure, Mg-6Ag, Mg-10Gd	A80	9 - 10		
	Mg-Pure, Mg-2Ag, Mg-4Ag	A80	11 - 12		
Salt	$MgCl_2$, $AgHNO_3$, $GDCl_3$	A80	13 - 14		
Resorption	all materials	A80	15 - 16		
PLC	all materials and salts (except Mg-8Ag)	A93	17 - 18		
Direct Assay	Mg-Pure, Mg-10Gd	A93	19 - 20		
	Mg-Pure, Mg-2Ag	A93	21 - 22		

Table 5 illustrates which analyses were performed on the cells from indirect and the direct assay. The detailed description of the different tests are described below.

Table 5: Analysis performed on indirect and direct assay

Analysis	Indirect assay	Direct assay
Immersion test		X
Live/Dead staining		X
DNA quantification	X	X
Metabolic activity	X	
ALP activity	X	X
TRAP activity	X	X
Resorption activity	X	
TRAP/DAPI costaining	X	
HA Staining	X	
PCR	X	

3.3.1 DNA quantification

As the nucleus of PBMC and HUCPV always contain the same amount of DNA, DNA quantification can served as an indicator of cell count and was also used as a normalization factor. The DNA isolation is based on the principle of alkaline lysis of cells. The protocol from Truett *et al.* were used and adapted [180]. Alkaline lysis was first described in 1979 [181]. In principle, NaOH shifts the pH value far into the alkaline range resulting in a lysis of cell membranes and cleavage of hydrogen bonds between the complementary DNA strands. Normally, sodium dodecyl sulphate is also used to dissolve the membrane. In this protocol, however, the cell membrane is additionally destroyed by heat.

The DNA content was quantified using the fluorometric properties of bisbenzimide. Bisbenzimide (Sigma-Aldrich Chemie GmbH, Munich, Germany) interacts with thymine and adenine rich regions of double-stranded DNA [182]. RNA, which does not usually occur in double-stranded form and does not contain thymine, does not influence the measurement.

DNA was quantified after 3, 7, 14, 21 and 28 days in the direct and indirect tests. The cell culture medium was removed and the cells were washed 2 times with sterile ultrapure water Type 1. Cells were treated with 200 µL lyisis buffer (25 mM NaOH; Sigma-Aldrich Chemie GmbH, Munich, Germany and 0.2 mM EDTA; Sigma-Aldrich Chemie GmbH, Munich, Germany) for 5 min. Subsequently, the lysate was heated to 95 °C for 1 h with shaking at 1,000 rpm (Thermomixer, Eppendorf, Hamburg, Germany) and cooled down to 20 °C with shaking at 700 rpm. 200 µL neutralization buffer (40 mM Tris/HCl pH 5.5; Sigma-Aldrich Chemie GmbH, Munich, Germany) was added and the samples were centrifuged at 13,000 rpm (Biofuge Pico, Heraeus, Hanau, Germany) for 1 min. The samples were diluted in a ratio of 1:5 with dilution buffer (2.5 mM NaCl, 19 mM sodium citrate pH 7.0) and 50 µL of the diluted DNA was mixed with 50 µL working buffer (2 M NaCl, 15 mM sodium citrate pH 7.0; Merck Millipore, Darmstadt, Germany). Defined quantities of calf thymus DNA (Sigma-Aldrich Chemie GmbH, Munich, Germany) were used as standards in the range of 150 ng/L and 2.34 ng/L. The bisbenzimide working solution (2 µg/mL bisbenzimide in the working buffer) was added in a volume of 50 µL and incubated in the dark for 15 min. Finally, the samples were measured fluorometrically (excitation: 355 nm, emission: 460 nm) with the microplate reader Victor 3 (Perkin Elmer, Waltham, USA) and the amount of DNA was calculated using the following formula (Equation 1).

Equation 3: Calculation of the DNA amount from the fluorometrically data

$$DNA\ amount\ in\ \mu g/mL = \frac{Fluorescence - Y}{X} * 5$$

X: Slope

Y: Point of intersection with the Y axis

5: Dilution factor

3.3.2 Measurements of metabolic activity

Water-soluble tetrazolium salt (WST-1; Roche Diagnostic GmbH, Mannheim, Germany) was used to detect the metabolic activity of the cells. WST-1 is reduced to formazan at the surface of the plasma membrane of the mitochondria by the nicotinamide adenine dinucleotide (NADH) oxidase. The NADH is produced during mitochondrial electron transport and is thus directly linked to the metabolic activity of viable cells. The tetrazolium salt is reduced to a dark yellow formazan derivative, which absorbance can be measured at a wavelength of 450 nm. The cell culture medium supernatant was removed after 3, 7, 14, 21 and 28 days of culture, replaced by a 10 % WST-1 dye solution in fresh cell culture medium and incubated for 30 min under cell culture conditions (at 37 °C, 5 % CO_2). Pure cell culture medium without cells was used as blank and cells without treatment (only cell culture medium) were used as control. Afterwards, 100 µL of the supernatants were transferred in triplicates to a 96-well plate and measured immediately with a microplate reader (Tecan Reader; Berthold Technologies GmbH, Bad Herrenalb, Germany) at 450 nm with a reference wavelength of 620 nm. Equation 4 was used to calculate the metabolic activity of the samples compared to control. Since the amount of WST-1 converted depends mainly on the number of mitochondria and thus also on the number of cells, the activity was calculated on the basis of DNA quantity in Equation 5.

Equation 4: Calculation of the metabolic activity in % of control

$$\text{Absorbance in \% of control} = \frac{\text{Sample - Blank}}{\text{Absorbance amount of Control}} * 100$$

Sample: Absorbance sample

Control: Absorbance control

Blank: Absorbance blank

100: Multiplication factor to get results in %

Equation 5: Calculation of the by DNA normalised metabolic activity in % of control

$$\text{Normalised absorbance in \% of control} = \frac{\left(\frac{\text{Sample - Blank}}{\text{Sample DNA}}\right)}{\left(\text{Average of } \frac{\text{Control}}{\text{Control DNA}}\right)} * 100$$

Sample: Absorbance sample
Control: Absorbance control
Blank: Absorbance blank
100: Multiplication factor to get results in %
Control DNA: DNA amount of control
Sample DNA: DNA amount of sample

3.3.3 Measurement of alkaline phosphatase

As ALP, a marker of OB, can be secreted into the environment, its activity can be detected in the supernatant. The conversion of the substrate p-Nitrophenyl phosphate by ALP is shown in Figure 9. The supernatant was measured after 3, 7, 14, 21 and 28 days using the ALP kit from BioAssay System (Hayward, USA). For the analysis, 50 µL samples (in triplet), 200 µL calibrator (kit) and 200 µL ultrapure water Type 1 were transferred into a 96 well plate (Greiner Bio-One, Kremsmünster, Austria). Afterwards, 150 µL working solution (consisting of kit components: assay buffer, Mg acetate and pNPP liquid) were added to the sample. Then, the plate was inserted into a microplate reader (Tecan Reader; Berthold Technologies GmbH, Bad Herrenalb, Germany), read immediately (T0) and after 4 min (T4).

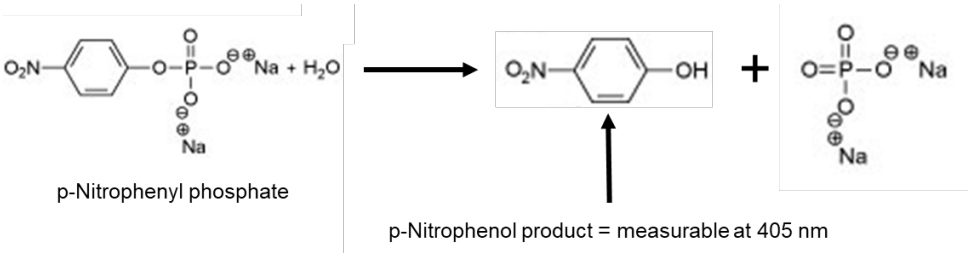

Figure 9: Chemical equation of the ALP assay

The ALP activity was calculated in IU/L=µmol/(L*min) by using the following formula (Equation 6).

Equation 6 Calculation of ALP activity

$$\text{ALP activity} = \frac{(\text{OD}_{\text{sample}}\ \text{t4} - \text{OD}_{\text{sample}}\ \text{t0}) * (\text{Reaction Volume})}{(\text{OD}_{\text{calibrator}} - \text{OD}_{\text{water}}) * \text{Sample Volume} * \text{t}} \times 35.3$$

OD: Optical density

3.3.4 Measurements of tartrate-resistant acid phosphatase

Due to the fact that OC exhibit high TRAP activity [183,184], this marker was used to track the differentiation of PBMC cells into OC. Samples were taken after 3, 7, 14, 21 and 28 days. The enzyme activity was detected in the supernatant with a TRAP staining kit (Kamiya Biomedical Co, Tukwila, USA). Even a few information is available, the most probable reaction of the substrate is shown in Figure 10. The source material fast red violet LB salt is slightly violet and turns red due to the reaction with the TRAP modified naphthol AS-mix phosphate. For the measurement, 15 µL of the samples (in triplicate) were mixed with 85 µL of the chromogenic substrate in a 96-well plate. Subsequently, the samples were incubated at 37 °C for 3 h and the absorption was immediately measured by microplate reader (Tecan Reader; Berthold Technologies GmbH, Bad Herrenalb, Germany), at 405 nm with reference wavelength at 620 nm.

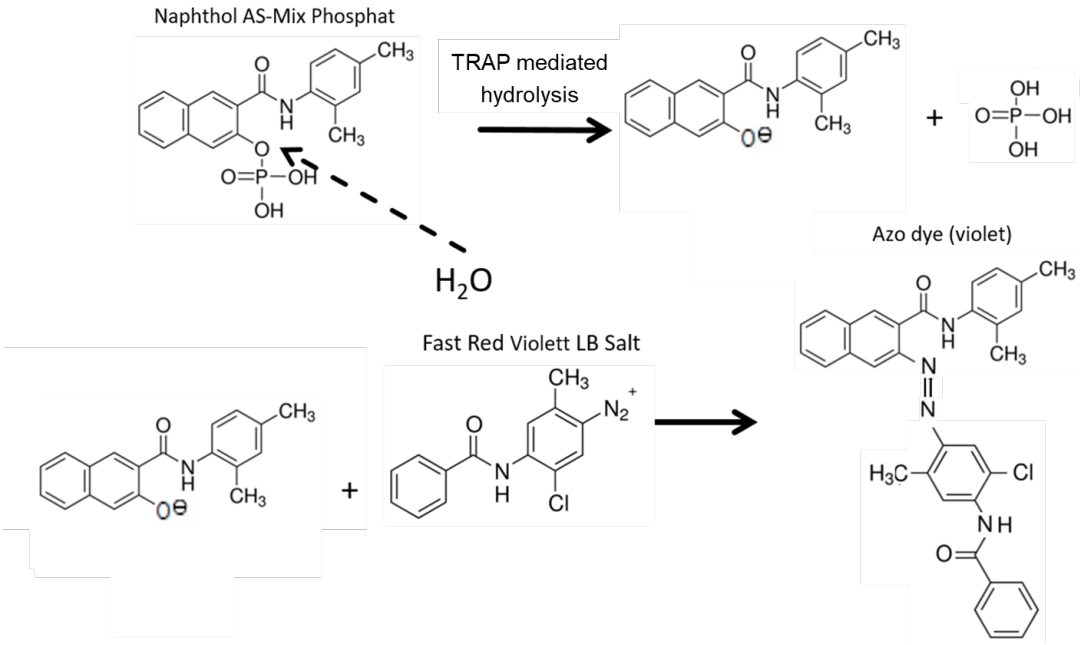

Figure 10: Possible chemical equation for TRAP activity measurement

To visualize the formation of TRAP-positive and polynuclear cells, the cells were stained with TRAP-staining kit and 4-6-diamidino-2 phenylindole (DAPI). The staining was performed after 14, 21 and 28 days with two biological replicates (donor) per material sample. The cells were washed with PBS (Biochrom AG, Berlin, Germany), fixed and permeabilized with 100 % methanol (LGC Standards, Bury, United Kingdom) for 10 min at room temperature. The cells were rinsed 3 times with ultrapure water Type 1 and stained with the chromogenic solution from the TRAP staining kit (Kamiya Biomedical Co, Tukwila, USA). After 1 h the reaction was stopped by replacing the staining solution with ultrapure water Type 1. To visualize the cell nuclei, the cells were incubated for 15 min with a 5 µg/mL DAPI (Sigma-Aldrich Chemie GmbH,

Munich, Germany) solution in the dark (DAPI binds to AT-rich areas in the cell nucleus). Subsequently, OC development was monitored using the microscope (Eclipse Ti, Nikon, Tokyo, Japan) with bright field view and DAPI filter (excitation: 340 - 380 nm; emission: 435 - 485 nm).

3.3.5 Resorption activity of OC

Despite a proven TRAP activity, it is possible that the cells do not resorb bones. Therefore, it is necessary to detect OC activity using a resorption assay, where the resorption of mineralized material is measured. The formation of a resorption pits on dentin allows the ultimate demonstration of OC activity. For this, the coculture was cultured for 28 days on dentin chips (duplicate; n=4) cut by ivory (from Bundesamt für Naturschutz). Afterwards the cells were removed by a 10 min treatment in sodium hypochlorite 10 % w/v in ultrapure water Type 1. Afterwards, the dentin chips were washed with ultrapure water Type 1 and wiped with a paper towel. The dentin chips were incubated in 70 % ethanol and dried. Afterwards chips were incubated for 2 min in 1 % toluidin blue (Merck Millipore, Darmstadt, Germany) and rinsed again 5 times with ultrapure water Type 1. Finally, the dentin chips were analysed with a confocal 3D laser-scanning microscope VK-X200 (Keyence, Neu-Isenburg, Germany). The evaluation was carried out with the VK Analyser version 3.4.0.1.

3.3.6 Hydroxyapatite staining as indicator for mineralisation

Hydroxyapatite staining was performed after 14, 21 and 28 days of extract cultivation using the kit OsteoImage™ Mineralization Assay (Lonza, Basel, Switzerland). Cells were fixed with 100 % methanol (LGC Standards, Bury, United Kingdom) for 10 minutes before staining and washed once with wash buffer. The staining solution was added and the cells incubated protected from light for 30 minutes. Afterwards, the cells were washed twice for 5 min with wash buffer and finally observed with the inverted microscope Eclipse Ti (Nikon, Tokyo, Japan) (excitation 492 nm, emission 520 nm). To measure influence of materials on mineralisation, ratio of the number of green pixels on an area of 0.28 mm^2 of the sample to the control (average of 4 areas) was calculated and expressed as percentages (Equation 7).

Equation 7: Calculation of the mineralisation activity

$$\text{Pixel amount in \% of control} = \frac{\text{Sample}}{\text{Average Control}} * 100$$

Sample: Green pixel amount in samples
Control: Green pixel amount in control
100: Multiplication factor to get results in %

3.3.7 Gene expression of markers for OB and OC activity (RT-qPCR)

The polymerase chain reaction (PCR) is a method for amplifying DNA of interest. The PCR can be used to multiply DNA or as method to determine the amount of messenger RNA (mRNA). However, since mRNA is not heat-stable, it must first be converted into complimentary DNA (cDNA) using reverse transcriptase. The cDNA thus obtained can be used for RT-qPCR. One PCR cycle consists of a denaturation, an annealing and an elongation phase.

(i) Denaturartion

The reaction chamber is heated to 98 °C. At this temperature the hydrogen bonds of the complementary bases are released. This causes the DNA strands to separate from each other.

(ii) Annealing

The length of the primer determines the duration of this phase. The longer the primers are, the longer the accumulation takes. This phase usually lasts between 20 and 40 seconds. The temperature in the annealing phase depends on the GC content of the primers and is normally between 50-65 °C. The higher their GC content, the higher the annealing temperature. If the temperature is too low, unspecific binding may occur. If the temperature is too high, the high thermal movement of the primers can prevent them from binding. The optimal temperature is normally between 5-10 °C around the melting point of the primer sequence.

As the polymerase also has an activity at lower temperatures (70 °C ~ 2800 bp/min; 55 °C ~ 1400 bp/min) [185], the annealing and elongation phase can be combined in the course of the PCR program.

(iii) Elongation

Specific segments of DNA, flanked by 5' and 3' primers is copied by the Taq DNA polymerase (Taq = *Thermus aquaticus*). The duration of this phase depends on the temperature and the length of the DNA strand to be copied (see above).

As the DNA segments double with each cycle, RT-qPCR can be used to calculate the initial amount of the sequence of interest. A reporter (*e.g.* sybr green) is added to the reaction mixture, which only interacts with double-stranded DNA and emits a fluorescent signal, which is measured after each cycle.

RNA extraction including cell digestion was performed after 3, 7, 14, 21 and 28 days with the RNeasy Mini Kit (Qiagen GmbH, Hilden, Germany) according to manufacturer instructions. The RNA concentration was estimated by measuring the absorbance at 260 nm with a

Nanodrop (Thermo Scientific, Darmstadt, Germany) and the amounts were adjusted for cDNA synthesis. With the Sensiscript Kit (Qiagen GmbH, Hilden, Germany) and oligo dT Primer (Qiagen GmbH, Hilden, Germany) the cDNA synthesis was carried out according to the manufacturer instructions. The qPCR was used to determine the gene expression by the reporter sybr green (SSO Fast; BioRad, Munich, Germany). The qPCR was performed in the Bio-Rad CFX96 instrument (BioRad, Munich, Germany).

Three different housekeeping genes were selected for normalization (*Actin beta* (*β-ACTIN*), *Glyceraldehyde-3-phosphate dehydrogenase* (*GAPDH*) and *ER membrane protein complex subunit 7* (*EMC7*)). Several markers were used to observe the cell interaction of OC and OB (*SEMA4D*, *RANKL* and *M-CSF*). Osteogenesis (*RUNX2* and *ALP*) and differentiation of OC (*Nuclear factor of activated T-cells cytoplasmic 1* (*NFATC1*) and *Cathepsin K* (*CTSK*)) were also determined. Finally, the signal cascade of the calcium sensing receptor (*CASR*, *Phospholipase C gamma 2* (*PLCG2*), *Mitogen-activated protein kinase 1* (*MAPK1*) and *Protein phosphatase 3 catalytic subunit alpha* (*PPP3CA*) were followed.

The primer sequences presented in Table 6 were created using Primer Blast (NCBI, Bethesda, USA) and purchased from Eurofins Scientific (Hamburg, Germany). The results were evaluated by CFX-Manager 3.1 (BioRad, Munich, Germany) using the ΔΔCq method (expressed relative gene expression value normalized to the control group only medium or Mg-Pure extract).

Table 6: PCR Primers

Group	Target name / NCBI RefSeq			
	Abbreviation	**Forward**	**Reverse**	**Amplicon length (bp)**
Referemce genes	Actin beta / NM_001101			
	β-ACTIN	CTTCCTGGGCATGGAGTC	TGATCTTCATTGTGCTGGGT	134
	Glyceraldehyde-3-phosphate dehydrogenase / NM_002046			
	GAPDH	GTCGGAGTCAACGGATTTG	TGGGTGGAATCATATTGGAA	143
	ER membrane protein complex subunit 7 / NM_020154.2			
	EMC7	TGCCCTATCCTCTCCAAATG	CCCCACGATTCCCTTTTAAT	67
Cell Marker	Alkaline phosphatase / NM_000478			
	ALP	TAAAGCAGGTCTTGGGGTGC	AGTGTCTCTTGCGCTTGGTC	133
	Cathepsin K			
	CTSK	CCCGCAGTAATGACACCCTT	AAAGCCCAACAGGAACCACA	127
	Bone gamma-carboxyglutamate protein / NM_199173.5			
	BGLAP	ATGAGAGCCCTCACACTCCT	TGGACACAAAGGCTGCAC	115
Transcription Factors	Nuclear factor of activated T-cells cytoplasmic 1 / NM_172387.1			
	NFATC1	CACCAAAGTCCTGGAGATCCCA	TTCTTCCTCCCGATGTCCGTCT	132
	Runt related transcription factor 2 / NM_001024630.3			
	RUNX2	TCTGGCCTTCCACTCTCAGTA	TGGATAGTGCATTCGTGGGT	134
Communication	Colony stimulating factor 1 / NM_172210			
	M-CSF	TGCAGCGGCTGATTGACA	GATCTTTCAACTGTTCCTGGTCTACA	81
	Semaphorin 4D / NM_006378			
	SEMA4D	TCTTCAATGTGCTGCGGGAT	CTGTGGGGTGAAGAGTGCAT	83
	TNF superfamily member 11 / NM_003701			
	RANKL	ATACCCTGATGAAAGGAGGA	GGGGCTCAATCTATATCTCG	202
	Tumor necrosis factor receptor superfamily, member 11b / NM_002546.4			
	OPG	CGCTCGTGTTTCTGGACAT	GGACATTTGTCACACAACAGC	112
CASR Pathway	Calcium sensing receptor / NM_001178065.1			
	CASR	CTCACCTTTGTGCTGTCTGTC	CTCCCCCTCAATGATCCCTT	93
	Phospholipase C gamma 2 / NM_002661			
	PLCG2	CAGGGTGGAGGAGCTCTTTG	TGGCGATGGACTGGTTCTTC	110
	Mitogen-activated protein kinase 1 / NM_002745			
	MAPK1	ATTACGACCCGAGTGACGAG	ACTGGGAAGAAGAACACCGA	200
	Protein phosphatase 3 catalytic subunit alpha / NM_000944.4			
	PPP3CA	CTGTTGAGGCTATTGAGGCTGA	TGCCGTTAGTCTCTGAGGTG	186

3.3.8 CASR downstream analysis by blocking Phospholipase C (PLC)

In order to analyse the impact of Mg-degradation products on the CASR signal cascade PLCG2 as downstream factor of CASR was inhibited with the PLC inhibitor D609 (Figure 11; APExBIO, Houston, USA). The coculture was seeded and exposed to the salts or extracts after one day, with and without PLC Inhibitor (50 ng/mL) for the whole experiment. The RNA was taken after 1, 2 and 3 days of treatment and the HA was stained on the 1st and 3rd day.

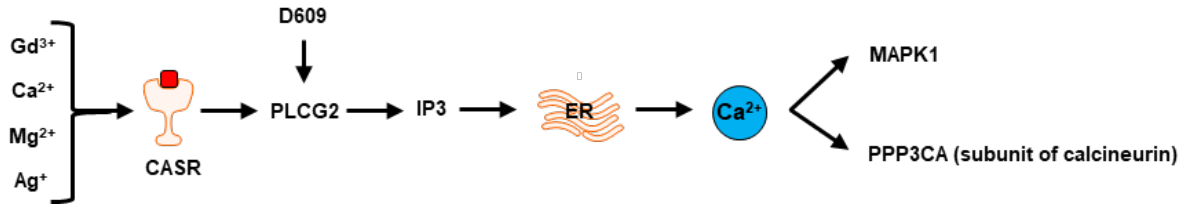

Figure 11: Schematic illustration of the location where the PLC inhibitor influences the CASR pathway [186–188,171,189–192].

3.4 Statistical analyses

The analysis of was performed with SigmaPlot 12.5 (Systat Software GmbH, Erkrath, Germany) using the one-sided repeated variance analysis (RM ANOVA) with the Holm-Sidak post-hoc test. This test was used because it allows comparison in pairs as well as comparison to the control group. It is also more powerful than the Tukey or Bonferroni test. Thus, it is possible with the Holm-Sidak test to find differences, which the others (Tukey or Bonferroni) do not reveal. Significance was accepted if the probability value was < 0.05.

For RT-PCR, to detect differential expression, t-test method ($P \leq 0.05$) was employed and directly calculated by CFX Manager Software (Bio Rad, Munich, Germany; version 3.0).

4 Results

4.1 Establishment and characterization of the coculture

Primarily the different cell types, OC developing from PBMC and OB differentiating from HUCPV, need specific conditions for optimal growth. However, since HUCPVs normally grow in a different FBS than PBMCs, a first test was conducted to demonstrate the influence of FBS on cell growth and viability. The cells were cultured for 21 days in α-MEM medium with different FBS and concentrations (10 % OC FBS, 15 % OC FBS, 15 % stem cell FBS (scFBS)). The experiment has shown that both cell types can be successfully cultured in all FBS varieties and concentrations (Figure 12; A). It was noticed that, as expected, higher FBS concentrations favour cell proliferation, requiring a change of the cell ratio to overcome the fast proliferation of HUCPV. However, it is important that the ratio of the cells remains approximately constant, since too large fluctuations could influence the test results. For this reason, an OC differentiation protocol with 10 % OC FBS was applied. This also has the advantage that it already used for differentiate of PBMCs to OC [92].

In addition to the FBS choice, the ratio between PBMC and HUCPV is also important factor for a successful differentiation. Literature review revealed that coculture ratios can vary between 1:50 and 1:100. To determine the optimal ratio, PBMC and HUCPV were cultured at different concentrations for 28 days (Figure 12; B). It was shown that the DNA content between the different cell ratios does not differ significantly. The TRAP activity of the cells also differed not significantly (Figure 12; D). Since both DNA content and TRAP activity were highest at a ratio of 1:100, this ratio was used in the following experiments.

Finally, it was determined whether a prior differentiation period for the HUCPV favours the differentiation of PBMC cells. Therefore, HUCPV cells were treated with vitamin D3 for 0, 7, 14 or 21 days and PBMC cells were added afterwards (Figure 12; C). TRAP activity was assessed after 28 days. TRAP activity was the highest without prior treatment of HUCPV cells with vitamin D3. Therefore, HUCPV and PBMC were seeded concomitantly.

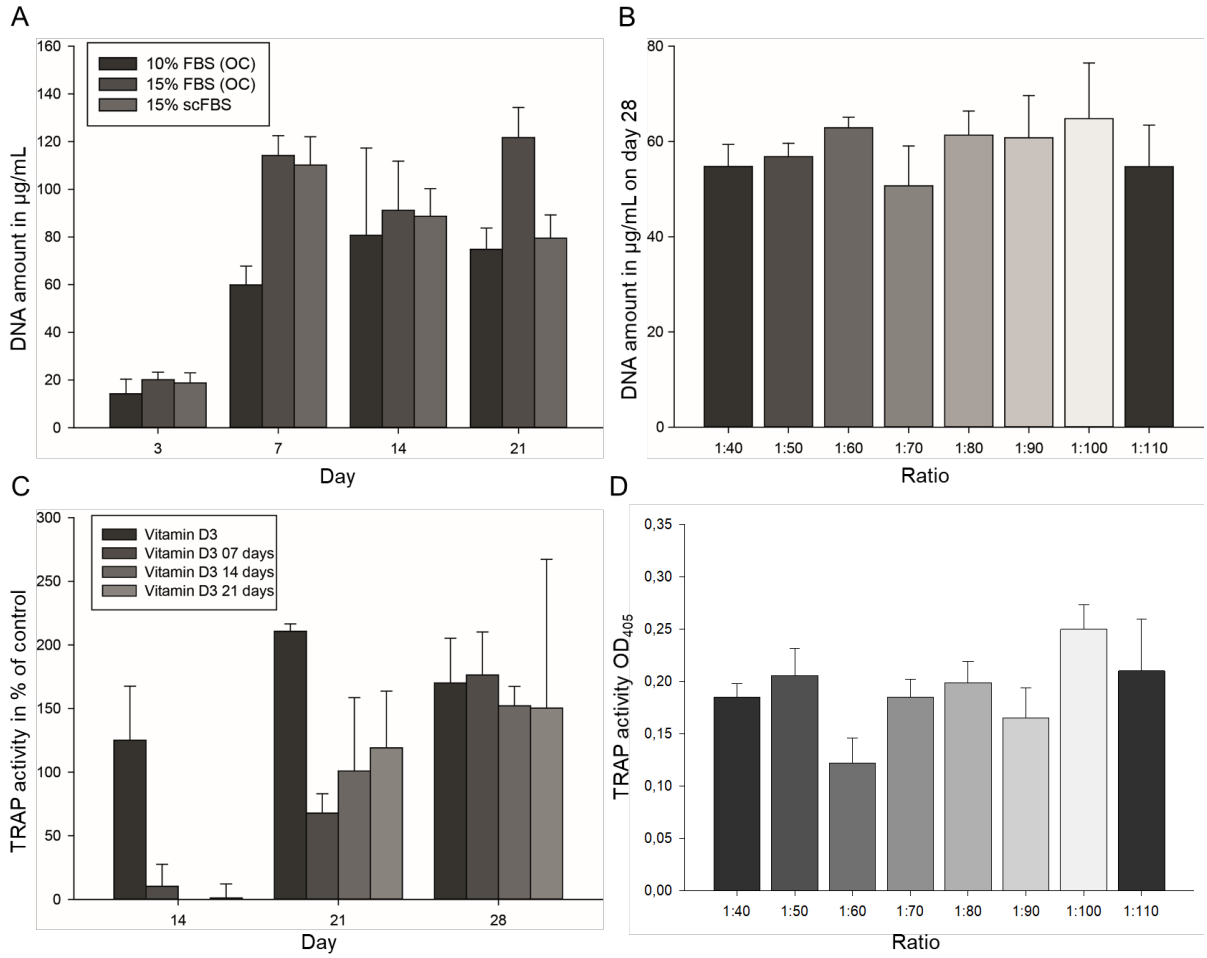

Figure 12: Evaluation of various culture conditions for further coculture experiments. A: Test of α-MEM medium with different kinds of FBS and concentration; B: Different ratio of cells (HUCPV:PBMC) for the coculture experiments; C: Effect of preincubation of HUCPV with vitamin D3 on the TRAP production of OC; D: Effect of cell ratio of HUCPV and PBMC on the TRAP production of OC. Bars represent mean ± standard deviation (SD) n = 6. no significant differences (Holm-Sidak post-hoc test)

During the following experiments, it turned out that the passage of the HUCPV cells is essential for a good development of the OC. When used for the coculture HUCPV cells of passage 1 and 10, the TRAP/DAPI costaining shows a clear difference in phenotype (Figure 13). In the coculture with the early HUCPV passage, well spread cell can be observed. However, if HUCPV cells of a later passage were used, clearly morphologic different cell types can be identified (Figure 13; C & D). Utilizing elder HUCPV passages, well-developed large OC with many cell nuclei can be identified (red marks). Therefore, only passages of HUCPV cells between 8 and 13 were used in the experiments.

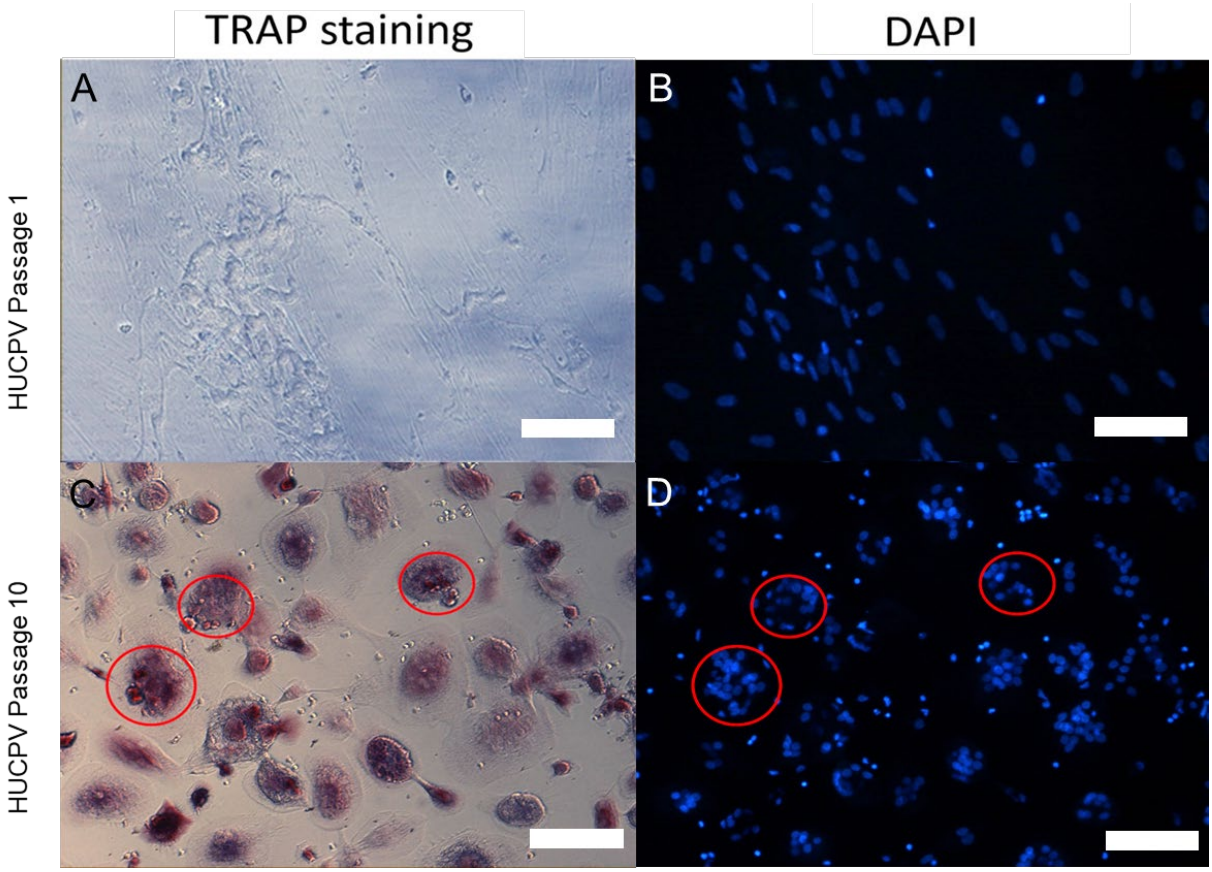

Figure 13: Pictures of TRAP/DAPI costaining of the coculture with different HUCPV passages on day 28. Scale bar 100 µm. Images were captured using bright field (A and C) and DAPI filter (B and D) microscopy. A and B: HUCPV passage 1; C and D: HUCPV Passage 10.

Summarizing the results of the coculture establishment experiments, the following standard parameters have been selected for the further experiments:

- 10 % standard OC FBS
- Culture start with a ratio of 1:100 HUCP:PBMC
- No artificial pre-differentiation of HUCPV - Both cell seeded concomitantly
- Age of HUCPV passage 8-13

4.2 Influence of Mg extracts on the coculture

To characterise the extracts and ensure consistent experimental conditions, the Mg, Ag and Gd contents were measured by ICP-MS (Table 7).

Table 7: Results of the ICP-MS sample analysis

Material	GALAB Report ID	Magnesium in mg/mL	Silver in mg/mL	Gadolinium in mg/mL
Mg-Pure	P2016121590	442	<0.02	<0.02
Mg-Pure	P2016123694	1340	<0.02	<0.02
Mg-Pure	P2016125974	560	<0.02	<0.02
Mg-2Ag	P2016125975	465	0.2	<0.02
Mg-4Ag	P2016125978	1480	2.2	<0.02
Mg-6Ag	P2016125977	1710	2.6	<0.02
Mg-8Ag	P2016113682-01	1170	3.3	<0.02
Mg-8Ag	P2016123695	1080	2.8	<0.02
Mg-5Gd	P2016113683-01	1470	<0.02	0.69
Mg-10Gd	P2016125976	1680	<0.02	3.4

All extracts were adjusted to a Mg concentration of 10 mM in order to be able to compare the different extracts. Furthermore, the pH value and osmolality were determined of the diluted extracts (Table 8).

Table 8: Characterisation of the different extract solutions (calculated by weight, ** represents the values for different Mg extracts)*

Material	Mg (mM)	Ag (nM)	Gd (nM)	pH	Osmolality in osmol/Kg
α-MEM	0.82	<0.02	<0.02	7.60	0.29
Mg-Pure **	10.00	<0.02	<0.02	8.40	0.30
$MgCl_2$	10.00*	<0.02	<0.02	7.60	0.32
Mg-2Ag	10.00	0.96	<0.02	7.80	0.29
Mg-4Ag	10.00	3.35	<0.02	7.80	0.30
Mg-6Ag	10.00	3.42	<0.02	8.00	0.31
Mg-8Ag **	10.00	5.84 ± 0,02	<0.02	8.30	0.31
$AgNO_3$	<0.02	3.42*	<0.02	7,60	0.30
Mg-5Gd	10.00	<0.02	0.73	8.10	0.31
Mg-10Gd	10.00	<0.02	3.13	8.00	0.31
$GdCl_3$	<0.02	<0.02	3.13*	7.90	0.29

The degradation rate decreases with increasing Gd content and also increases with increasing Ag content. The pH in the MgAg extracts increase with increasing Ag content. In the Gd extracts, it is the other way round. The pH in the prepared solutions ($MgCl_2$, $GdCl_3$ and $AgNO_3$) is lower than the extract corresponding to the ion content (Table 8).

To investigate the influence of extracts and salts on the coculture, samples were taken after 3, 7, 14, 21 and 28 days and analysed for proliferation (DNA content), metabolic activity (WST-1), mineralization (ALP; OB activity) and resorption (TRAP; OC activity).

4.2.1 Effect of different salt solutions and related Mg extracts

In order to investigate the effect of the alloying elements and their origins, the coculture was exposed to solutions ($MgCl_2$, $AgNO_3$ or $GdCl_3$) or extracts (Mg-Pure, Mg-6Ag or Mg-10Gd), and compared to cells without any added solution (control). The DNA content of samples treated with extract is always higher than that of samples treated with corresponding salts (Figure 14). Significantly differences were measured between Mg-6Ag and $AgNO_3$ as well as between Mg-10Gd and $GdCl_3$ at day 14, 21 and 28.

The Ag salt $AgNO_3$ had the strongest inhibitory effect indicated by a low DNA content. The treatment with Mg-6Ag extract had no effect on the DNA content compare to the control.

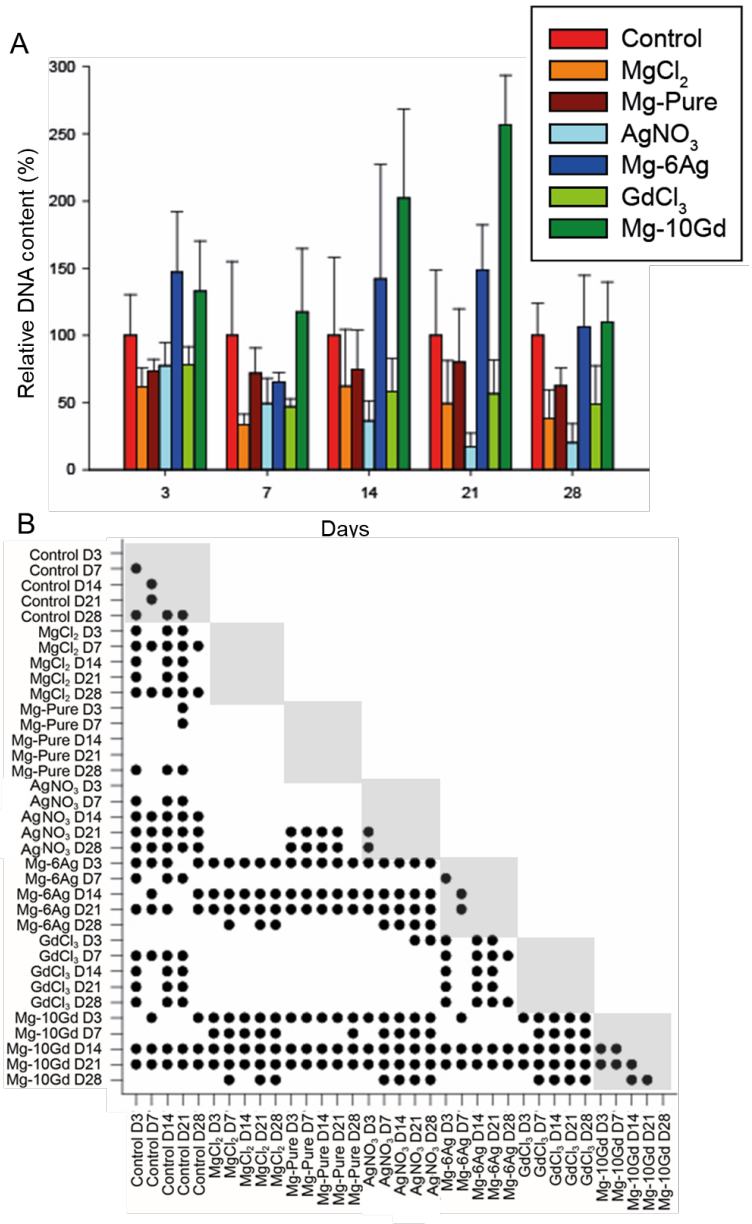

Figure 14: DNA content of the cells after treatment with solutions ($MgCl_2$ $AgNO_3$ and $GdCl_3$) or extracts (Mg-Pure, Mg-6Ag and Mg-10Gd). The coculture (n=6) was incubated for 28 days in cell culture medium and samples were taken on days 3, 7, 14, 21 and 28. A: Bar charts, Bars represent mean ± standard deviation (SD). B: statistical significances (Holm-Sidak post-hoc test). Dots indicate significant differences between different treatments (p =< 0.05). Grey blocks represent the difference within one condition or for one material over all time points.*

The metabolic activity (Figure 15) of the samples was comparable or lower than the one of the control up to day 14. On day 7 all samples had a significantly lower metabolic activity than the control except for the cells treated with Mg-Pure extract. Treatment with $GdCl_3$ leads to a significantly higher metabolic activity compared to the control from day 21. $AgNO_3$ induced a decreased activity over the whole period compared to the control, as observed for DNA content.

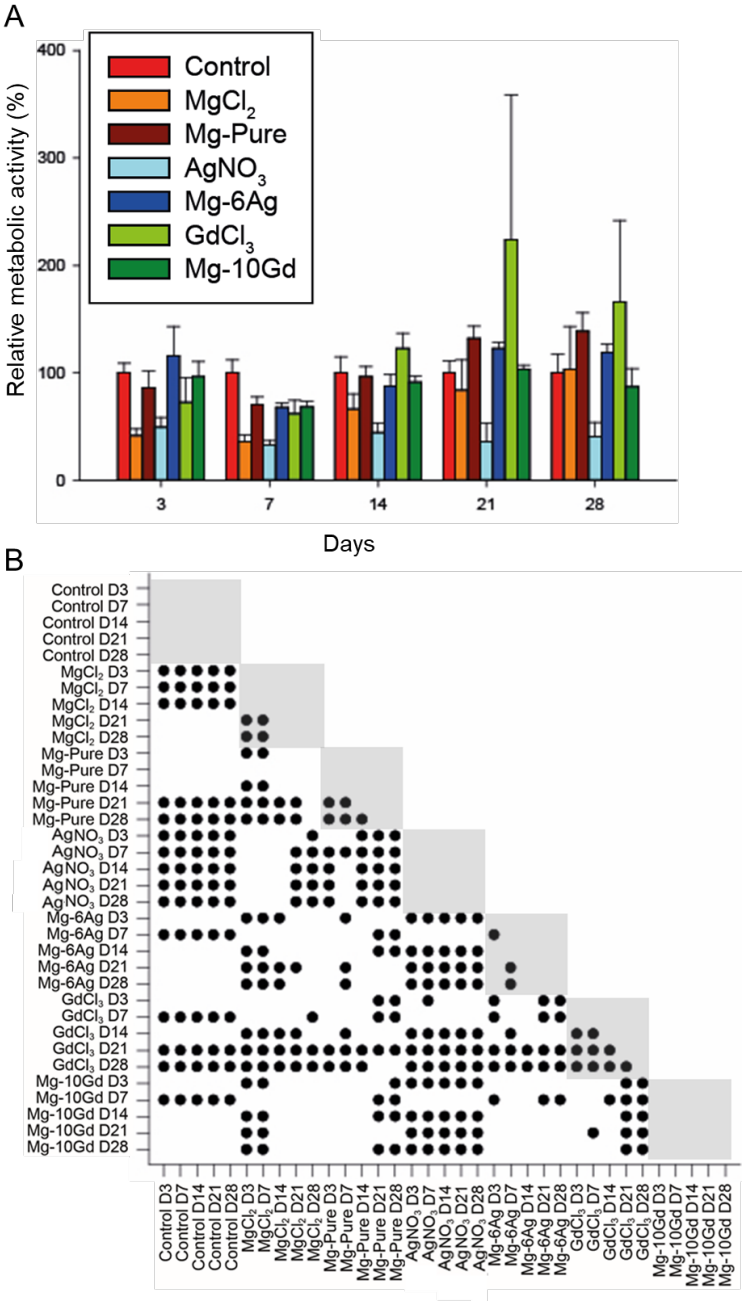

Figure 15: Metabolic activity of the cells after treatment with solutions ($MgCl_2$ $AgNO_3$ and $GdCl_3$) or extracts (Mg-Pure, Mg-6Ag and Mg-10Gd). The coculture (n=6) was incubated for 28 days in cell culture medium and samples were taken on days 3, 7, 14, 21 and 28. A: Bar charts, Bars represent mean ± standard deviation (SD). B: statistical significances (Holm-Sidak post-hoc test). Dots indicate significant differences between different treatments (p =< 0.05). Grey blocks represent the difference within one condition or for one material over all time points.*

In order to compare the mineralization potential of the differentiated OB, the ALP activity was measured and a significant increase could be demonstrated for the Mg-Pure and Mg-10Gd extract treatments (compared to the control) from day 14 as shown in Figure 16.

The samples treated with $MgCl_2$ showed a significant increase in ALP activity at day 3, which is unusual as an increase in ALP activity is normally measured after 14 days. This increase can also be seen with $MgCl_2$ at day 14. The samples treated with $AgNO_3$ and $GdCl_3$ as well as with Mg-6Ag showed no significant difference compared to the control during the whole test period.

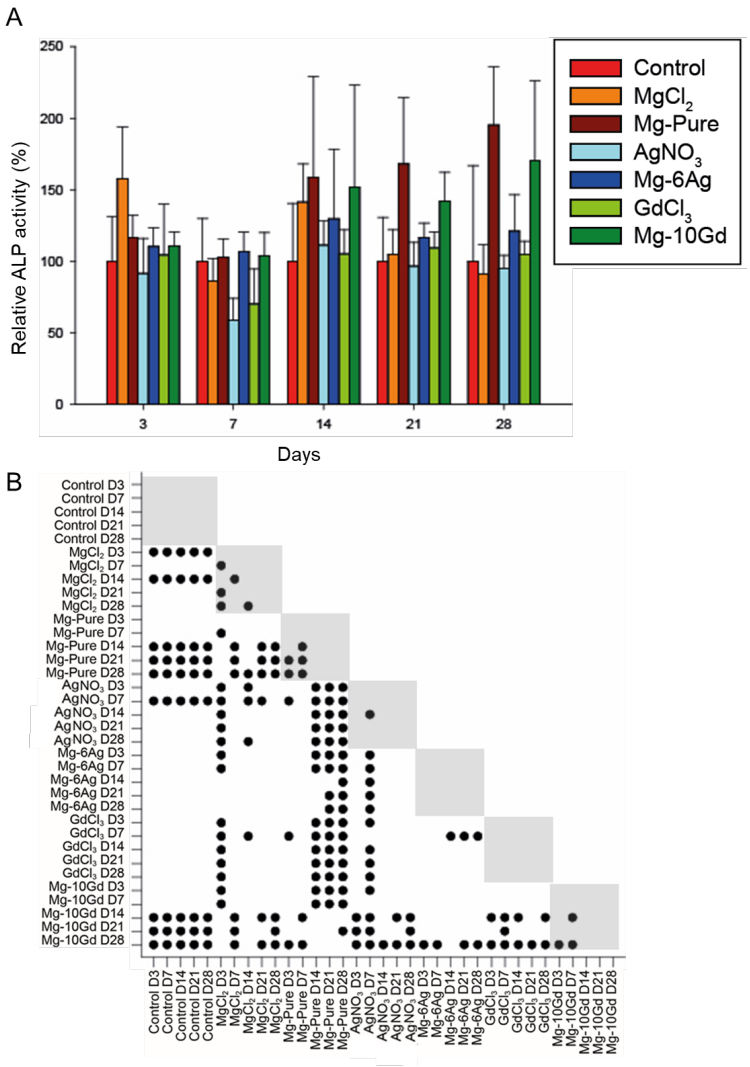

Figure 16: ALP activities of the cells after treatment with solutions ($MgCl_2$ $AgNO_3$ and $GdCl_3$) or extracts (Mg-Pure, Mg-6Ag and Mg-10Gd). The coculture (n=6) was incubated for 28 days in cell culture medium and samples were taken on days 3, 7, 14, 21 and 28. A: Bar charts, Bars represent mean ± standard deviation (SD). B: statistical significances (Holm-Sidak post-hoc test). Dots indicate significant differences between different treatments (p =< 0.05). Grey blocks represent the difference within one condition or for one material over all time points.*

The enzyme activity of TRAP represents the activity of present OC. The extracts appear to inhibit TRAP production in the cells during the early experimental phase. However, a significantly higher TRAP activity was measured in the samples treated with Mg-6Ag and

Mg-10Gd extracts at day 14 and 21. The samples treated with the Mg-Pure extract showed a significant reduction in TRAP activation on day 28 (Figure 17).

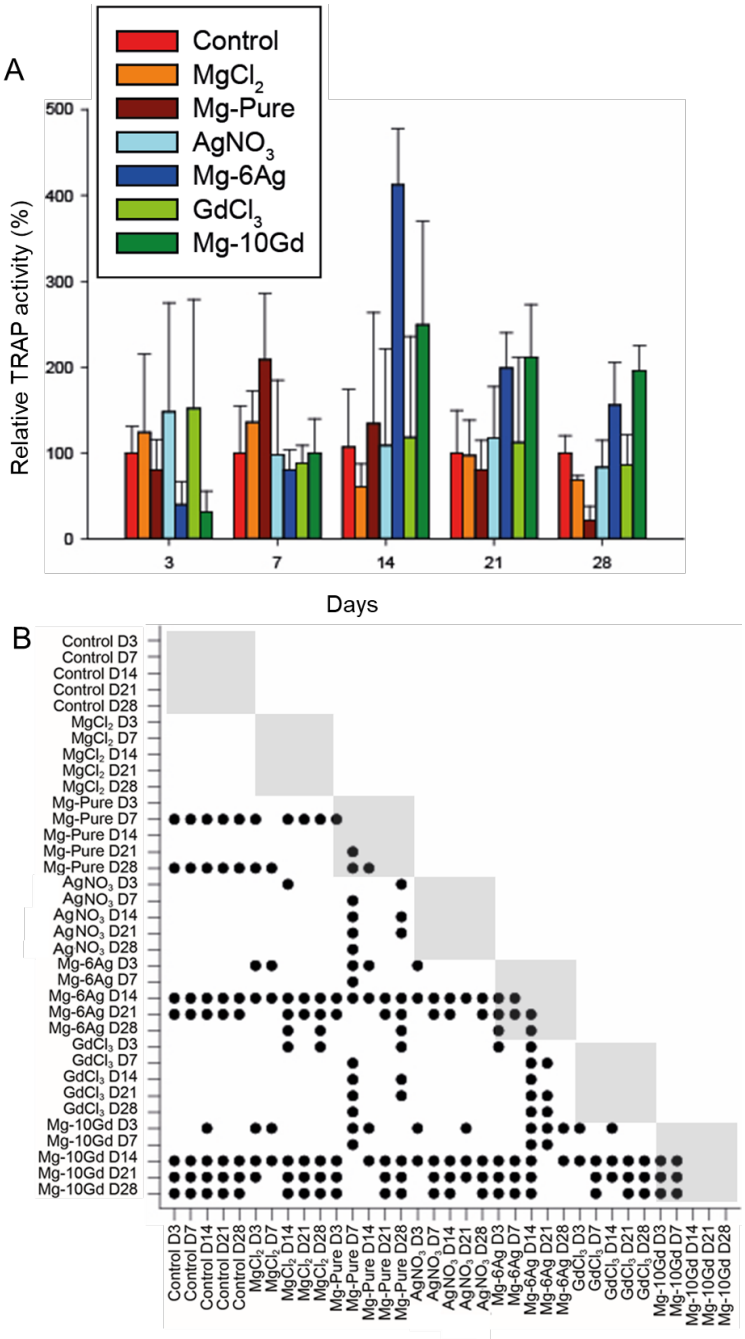

Figure 17: TRAP activities of the cells after treatment with solutions ($MgCl_2$ $AgNO_3$ and $GdCl_3$) or extracts (Mg-Pure, Mg-6Ag and Mg-10Gd). The coculture (n=6) was incubated for 28 days in cell culture medium and samples were taken on days 3, 7, 14, 21 and 28. A: Bar charts, Bars represent mean ± standard deviation (SD). B: statistical significances (Holm-Sidak post-hoc test). Dots indicate significant differences between different treatments (p =< 0.05). Grey blocks represent the difference within one condition or for one material over all time points.*

4.2.2 Effect of different MgAg extracts

In order to investigate the impact of increasing content of the alloying element, different MgAg extracts were compared. The DNA content of cocultures exposed to Mg-Pure and Mg-6Ag extracts was less decreased than the other extracts at day 28. Extracts of materials with the highest Ag content showed the most pronounced reduction of DNA content thus cell number. Similarly, treatment with Mg-6Ag showed a significantly higher impact on DNA content compared to Mg-2Ag and Mg-4Ag extracts at day 14 (Figure 18).

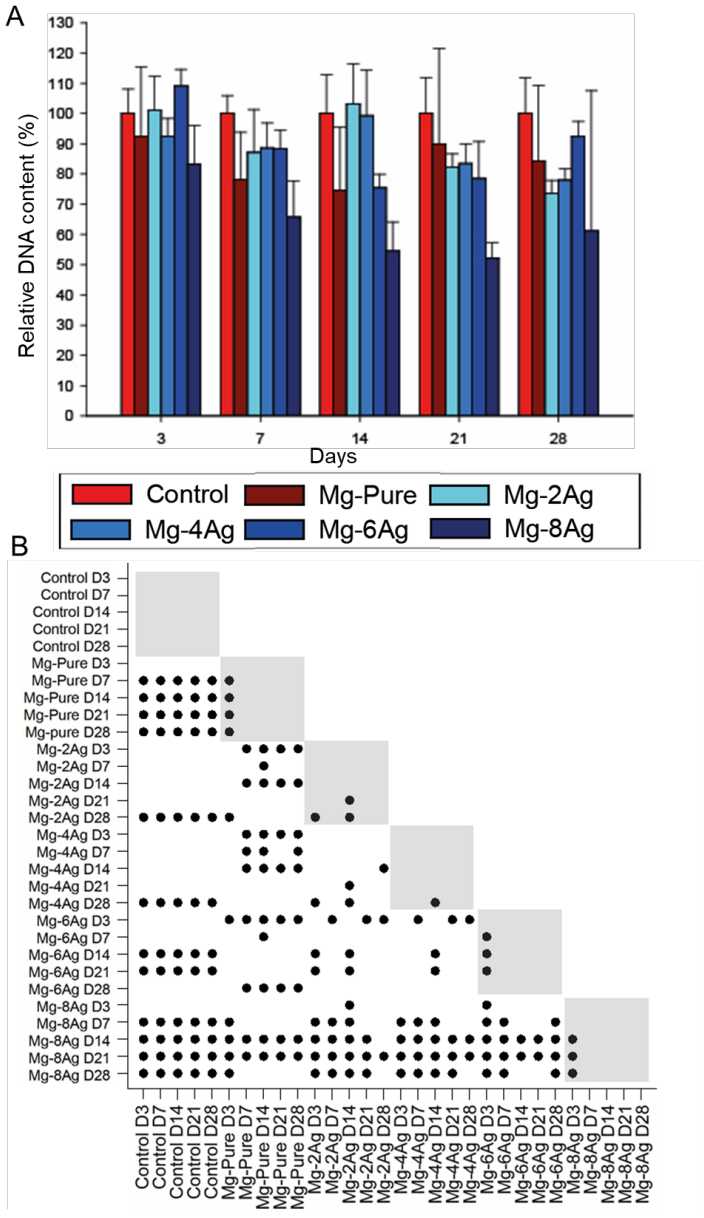

Figure 18: DNA content of the cells after treatment with extracts (Mg-Pure, MgAg). The coculture (n=6) was incubated for 28 days in cell culture medium and samples were taken on days 3, 7, 14, 21 and 28. A: Bar charts, Bars represent mean ± standard deviation (SD). B: statistical significances (Holm-Sidak post-hoc test). Dots indicate significant differences between different treatments (p =< 0.05). Grey blocks represent the difference within one condition or for one material over all time points.*

As already observed with DNA content, Mg-8Ag appears to affect negatively cell activity, as the metabolic activity in the samples treated with the extract was significantly reduced across the entire course of the experiment. The samples treated with Mg-Pure extract had a decreased metabolic activity, which however in the course of the experiment reached the activity of the control. Samples treated with Mg-2Ag and Mg-4Ag showed the highest activity at day 14 (Figure 19).

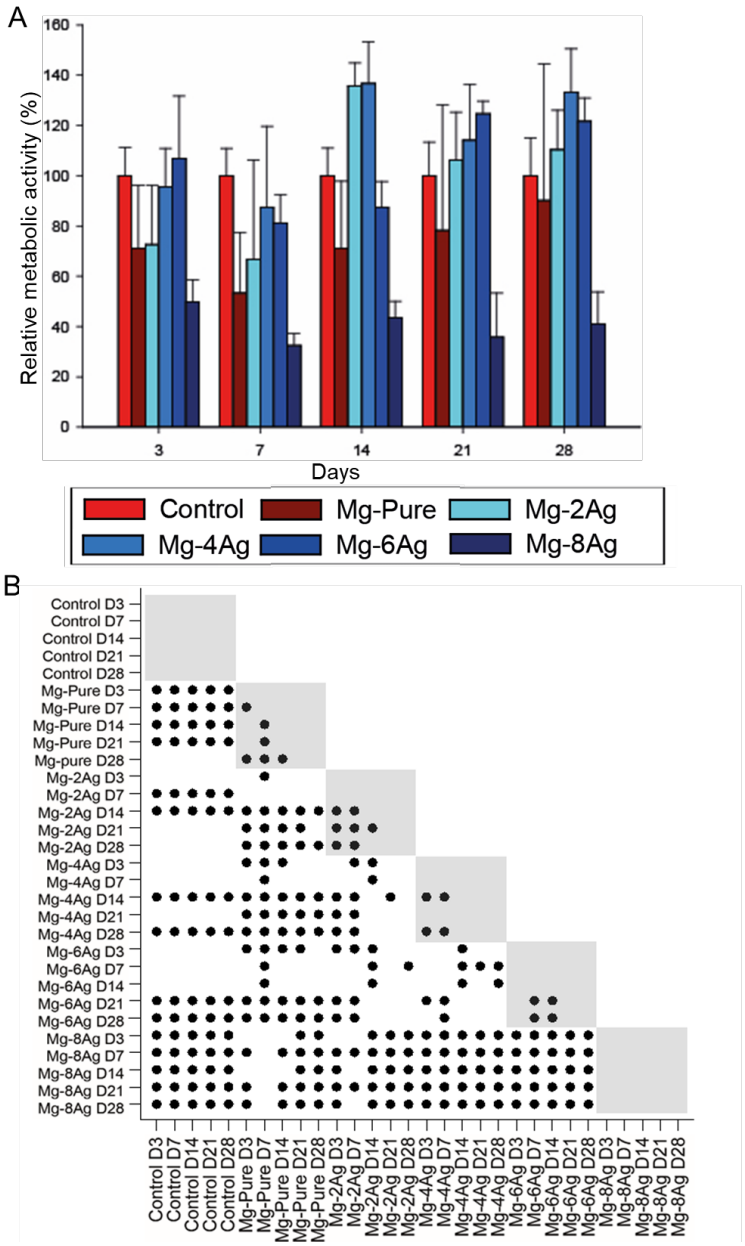

Figure 19: Metabolic activity of the cells after treatment with extracts (Mg-Pure, MgAg). The coculture (n=6) was incubated for 28 days in cell culture medium and samples were taken on days 3, 7, 14, 21 and 28. A: Bar charts, Bars represent mean ± standard deviation (SD). B: statistical significances (Holm-Sidak post-hoc test). Dots indicate significant differences between different treatments (p =< 0.05). Grey blocks represent the difference within one condition or for one material over all time points.*

Treatment with MgAg extracts seemed to have little effect on ALP activity. Only at day 14, the samples treated with Mg-4Ag and Mg-6Ag showed a significantly higher ALP activity than the control. Since both Mg-2Ag and Mg-8Ag showed a lower ALP activity, it can be assumed that there is an optimal MgAg composition regarding the modulation of ALP activity (Figure 20).

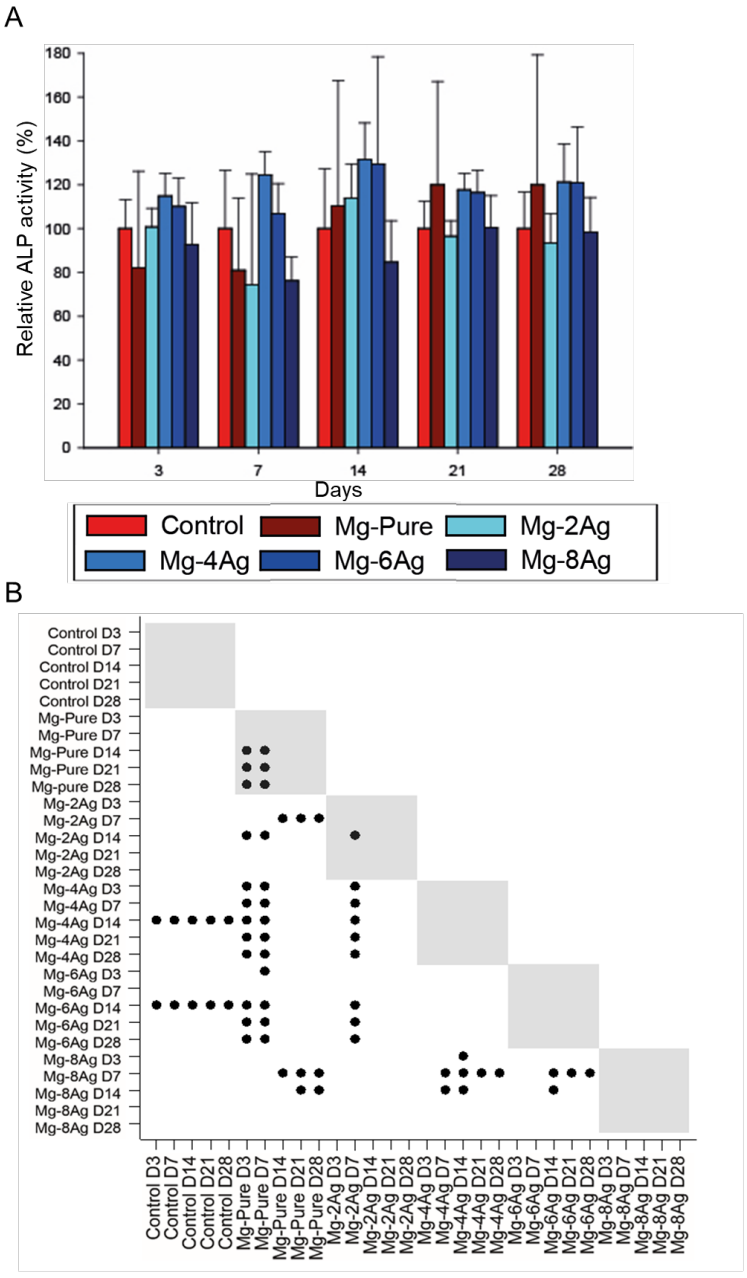

Figure 20: ALP activity of the cells after treatment with extracts (Mg-Pure, MgAg). The coculture (n=6) was incubated for 28 days in cell culture medium and samples were taken on days 3, 7, 14, 21 and 28. A: Bar charts, Bars represent mean ± standard deviation (SD). B: statistical significances (Holm-Sidak post-hoc test). Dots indicate significant differences between different treatments (p =< 0.05). Grey blocks represent the difference within one condition or for one material over all time points.*

Furthermore, treatment of the coculture for 14 days with Mg-6Ag extracts also induces the TRAP activity (Figure 21).

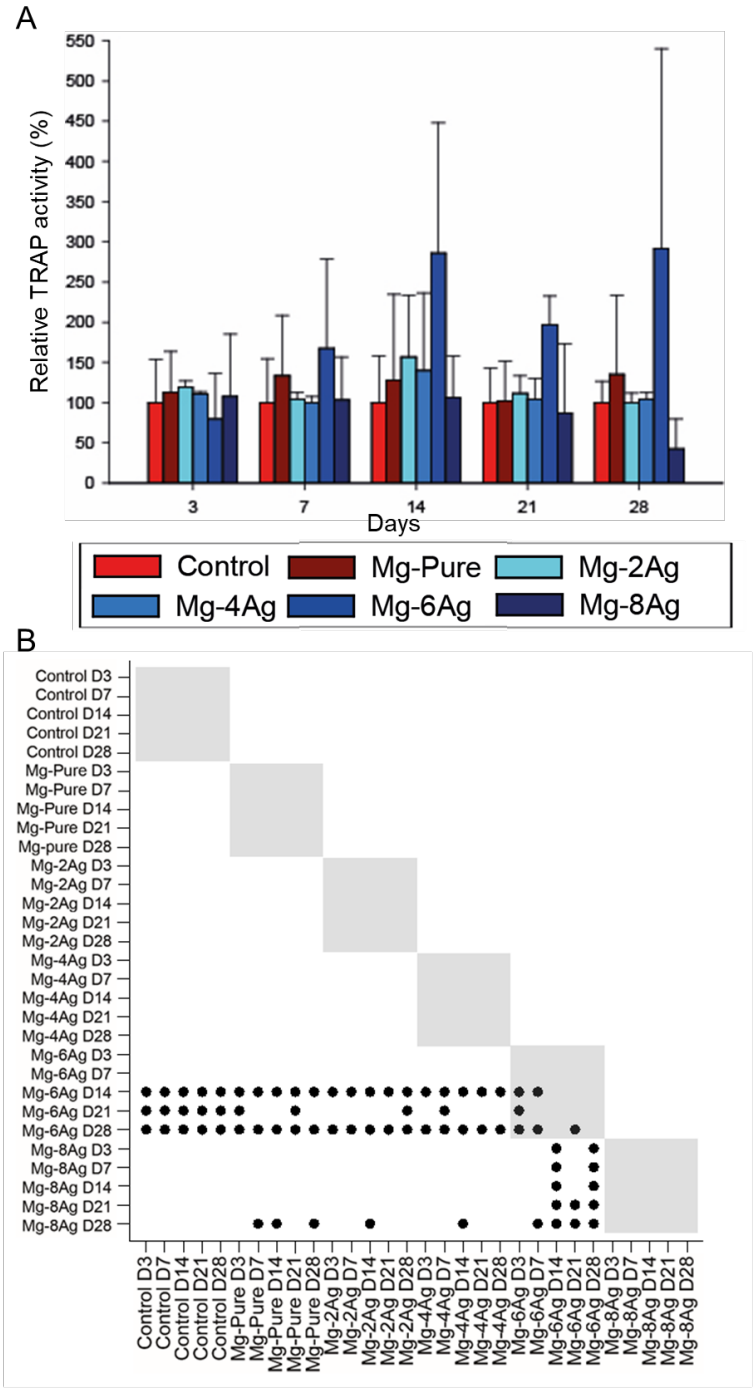

Figure 21: TRAP activity of the cells after treatment with extracts (Mg-Pure, MgAg). The coculture (n=6) was incubated for 28 days in cell culture medium and samples were taken on days 3, 7, 14, 21 and 28. A: Bar charts, Bars represent mean ± standard deviation (SD). B: statistical significances (Holm-Sidak post-hoc test). Dots indicate significant differences between different treatments (p =< 0.05). Grey blocks represent the difference within one condition or for one material over all time points.*

4.2.3 Effect of different MgGd extracts

Mg-10Gd appeared to have a more positive effect on cell proliferation than Mg-5Gd. Over the whole duration of the experiment, the DNA contents of samples treated with Mg-10Gd extract were higher than those treated with Mg-5Gd. This result was significant until day 14 (Figure 22). However, compared to the cell culture media control, only a significant increase of the Mg-10Gd treatment at day 3 could be observed. As shown in the previous MgAg experiments also in this part Mg-Pure seemed to have an inhibitory effect on cell proliferation. Like Mg-Pure also Mg-5Gd extracts seemed to decrease the cell proliferation.

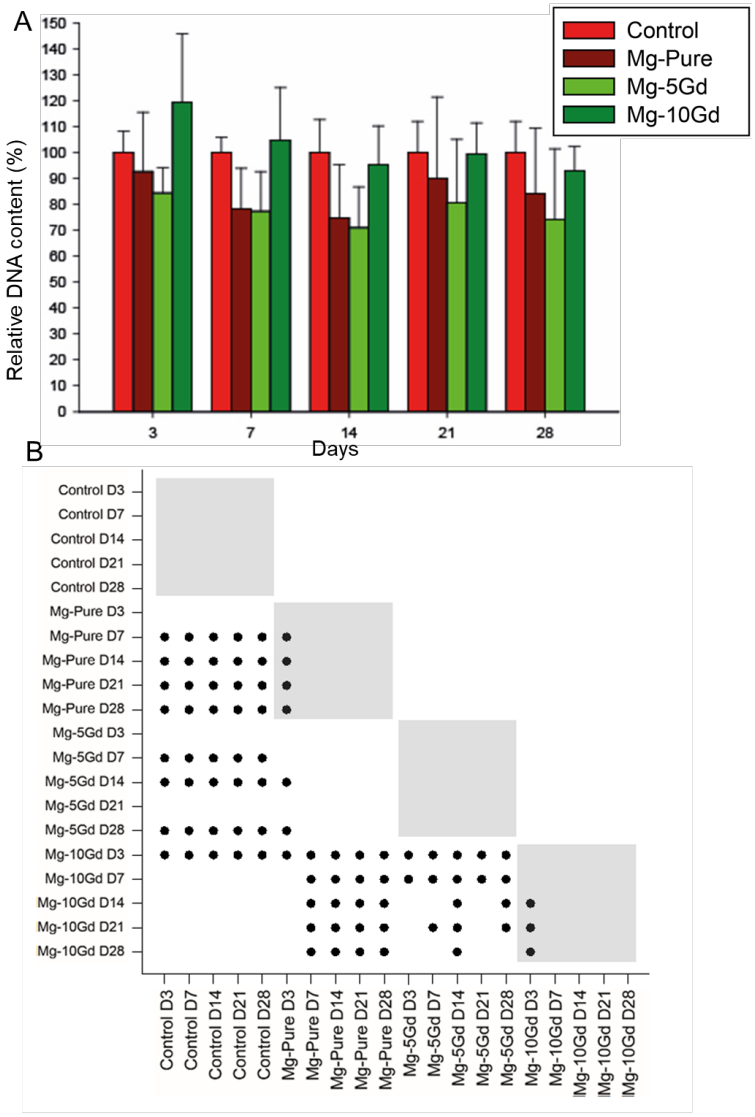

Figure 22: DNA content of the cells after treatment with extracts (Mg-Pure, MgGd). The coculture (n=6) was incubated for 28 days in cell culture medium and samples were taken on days 3, 7, 14, 21 and 28. A: Bar charts, Bars represent mean ± standard deviation (SD). B: statistical significances (Holm-Sidak post-hoc test). Dots indicate significant differences between different treatments (p =< 0.05). Grey blocks represent the difference within one condition or for one material over all time points.*

Mg-5Gd extract supported the metabolic activity of the cells at day 21 and 28 (statistical significance). The samples treated with Mg-10Gd showed a slight increased (not significant) activity at the beginning, then remained rather constant compared to control (Figure 23).

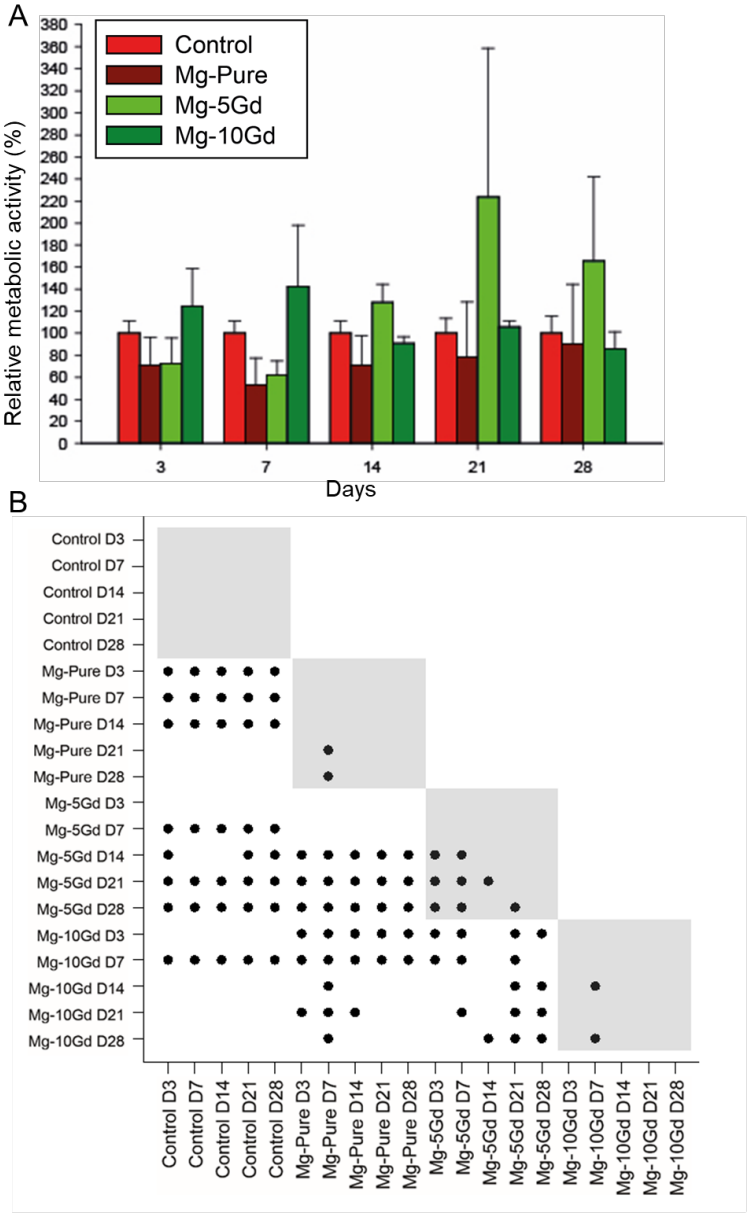

Figure 23: Metabolic activity of the cells after treatment with extracts (Mg-Pure, MgGd). The coculture (n=6) was incubated for 28 days in cell culture medium and samples were taken on days 3, 7, 14, 21 and 28. A: Bar charts, Bars represent mean ± standard deviation (SD). B: statistical significances (Holm-Sidak post-hoc test). Dots indicate significant differences between different treatments (p =< 0.05). Grey blocks represent the difference within one condition or for one material over all time points.*

The samples treated with Mg-10Gd extract exhibited a significantly higher ALP activity than the control from day 14. No significant difference between control and Mg-5Gd treatment (Figure 24) could be found over the whole period.

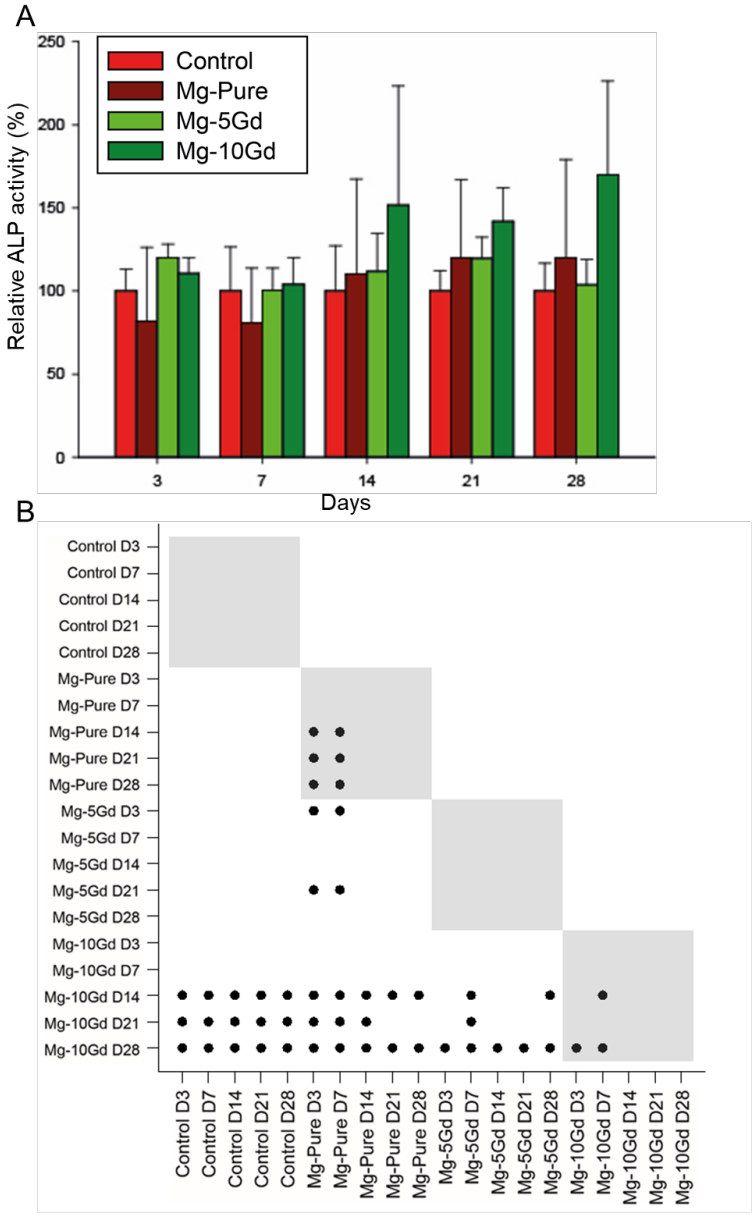

Figure 24: ALP activity of the cells after treatment with extracts (Mg-Pure, MgGd). The coculture (n=6) was incubated for 28 days in cell culture medium and samples were taken on days 3, 7, 14, 21 and 28. A: Bar charts, Bars represent mean ± standard deviation (SD). B: statistical significances (Holm-Sidak post-hoc test). Dots indicate significant differences between different treatments (p =< 0.05). Grey blocks represent the difference within one condition or for one material over all time points.*

The coculture exposed to Mg-10Gd extract had a significant higher TRAP activity from day 7 compared to the relative control, Mg-Pure and Mg-5Gd treatment (Figure 25).

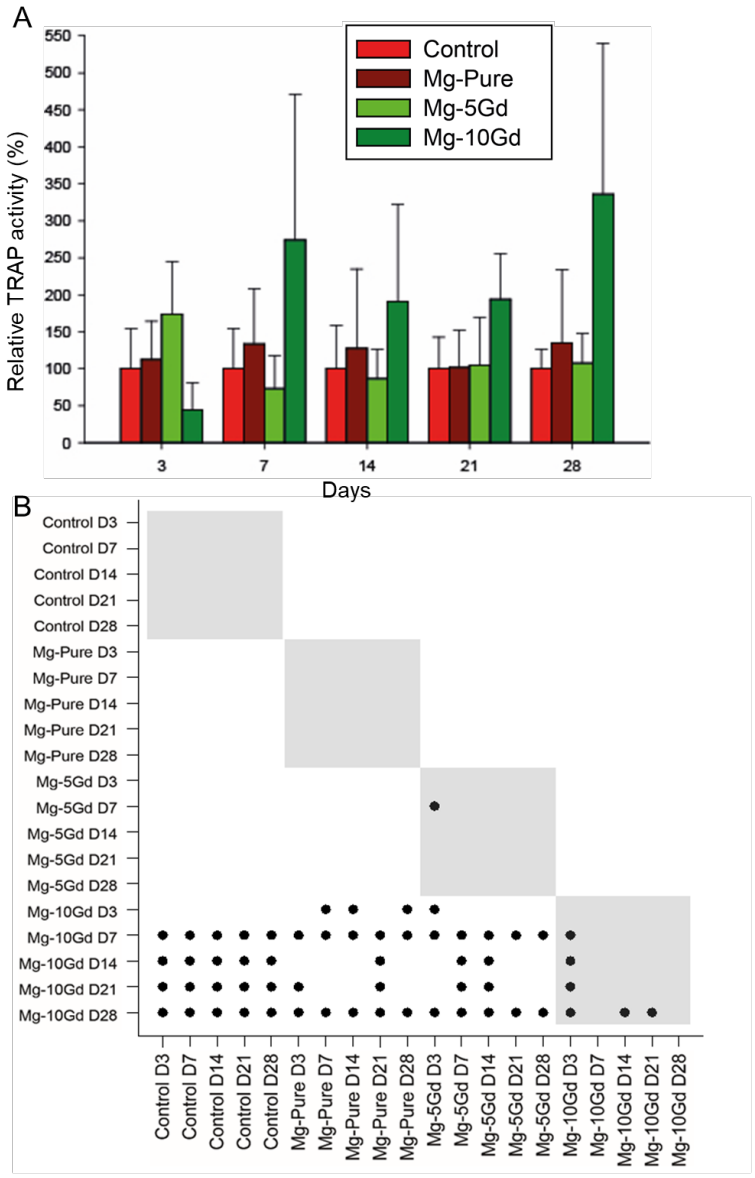

Figure 25: TRAP activity of the cells after treatment with extracts (Mg-Pure, MgGd). The coculture (n=6) was incubated for 28 days in cell culture medium and samples were taken on days 3, 7, 14, 21 and 28. A: Bar charts, Bars represent mean ± standard deviation (SD). B: statistical significances (Holm-Sidak post-hoc test). Dots indicate significant differences between different treatments (p =< 0.05). Grey blocks represent the difference within one condition or for one material over all time points.*

4.2.4 Impact of extracts on differentiation of osteoclasts (TRAP staining)

To verify that the coculture contained both OB and OC, intracellular TRAP staining was performed with a DAPI nuclear counterstaining after 14, 21 and 28 days. On day 28, the untreated (control) OC could be identified as cells were TRAP positive (strong red colour) and contained more than 2 nuclei (Figure 26; A and B). Same cell morphology could also be

detected after treatment with Mg-Pure extracts. The cells were similar in size to those in the control and contained several cell nuclei (Figure 26; C and D). The OC in the samples treated with Mg-6Ag are smaller and there are many cells visible which contain only one nucleus (OB or monocytes) (Figure 26; E and F). The high occurrence of mononuclear cells could indicate that the differentiation of the cells is delayed. However, differentiated cells were visible in the samples treated with Mg-10Gd extract. The OC were smaller than in the control, but the cells contained several cell nuclei and a red coloration of the cells can be recognized (Figure 26; H and I).

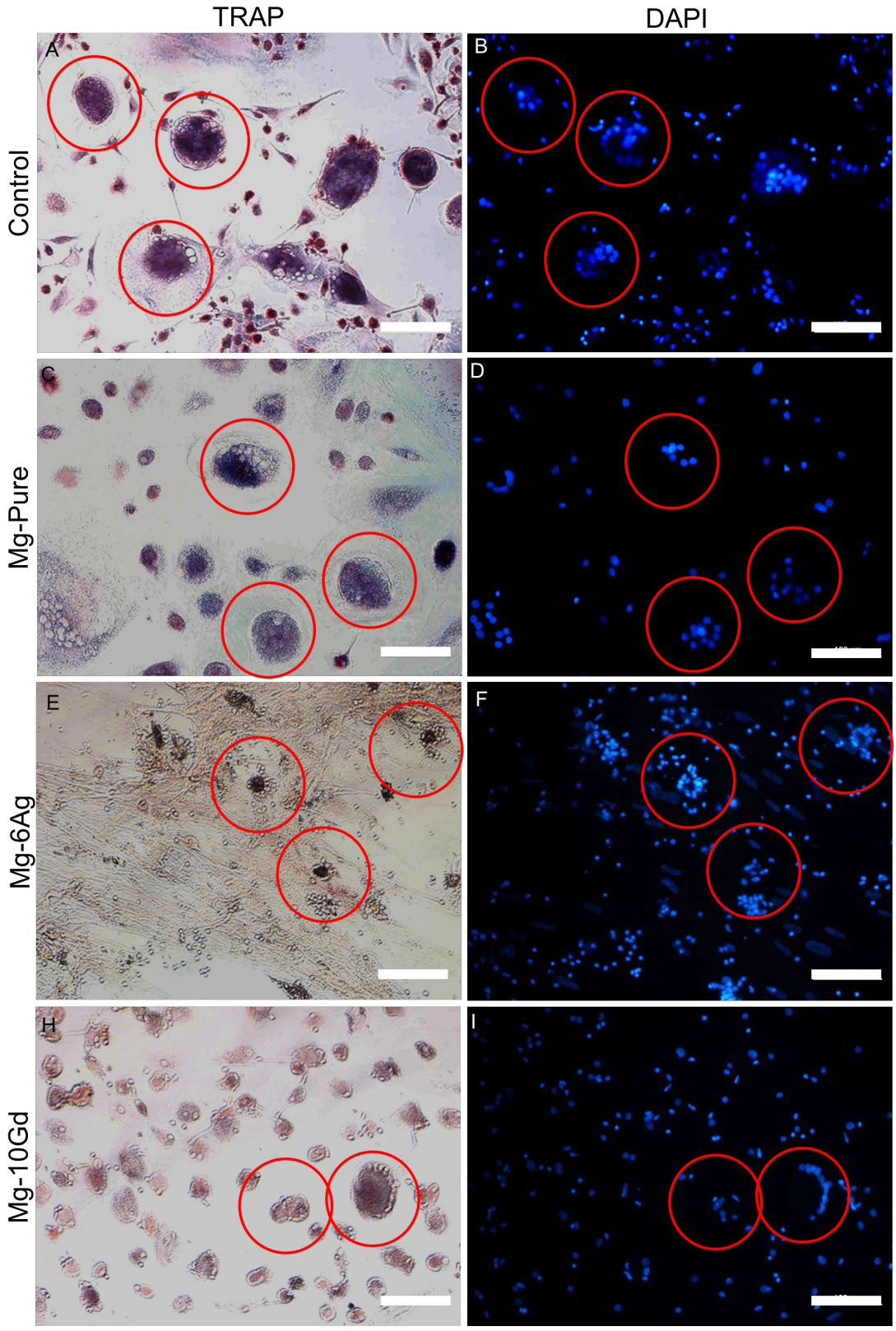

Figure 26: Representative pictures of TRAP/DAPI costaining of the coculture with different extract treatments at day 28. Scale bar 100 µm. Images were captures either using bright field (A, C, E and H) and DAPI fluorescence (B, D, F and I) microscopy. A and B: Control; C and D: Mg-Pure; E and F: Mg-6Ag; H and I: Mg-10Gd. OC examples are marked with a red circle.

4.2.5 Visualization of mineralization by hydroxyapatite staining

Mineralisation is a rather late process in osteogenesis and HA is produced by OB. To visualise the osteogenic effect of 10 mM Mg-solutions ($MgCl_2$, $GdCl_3$ and $AgNO_3$) and extracts (Mg-Pure, Mg-6Ag and Mg-10Gd) a HA staining (OsteoImage™) was performed on day 14, 21 and 28 (HA appears green). Since the result of the HA coloration has not changed over the course of the experiment, only the images from day 28 are displayed in Figure 27.

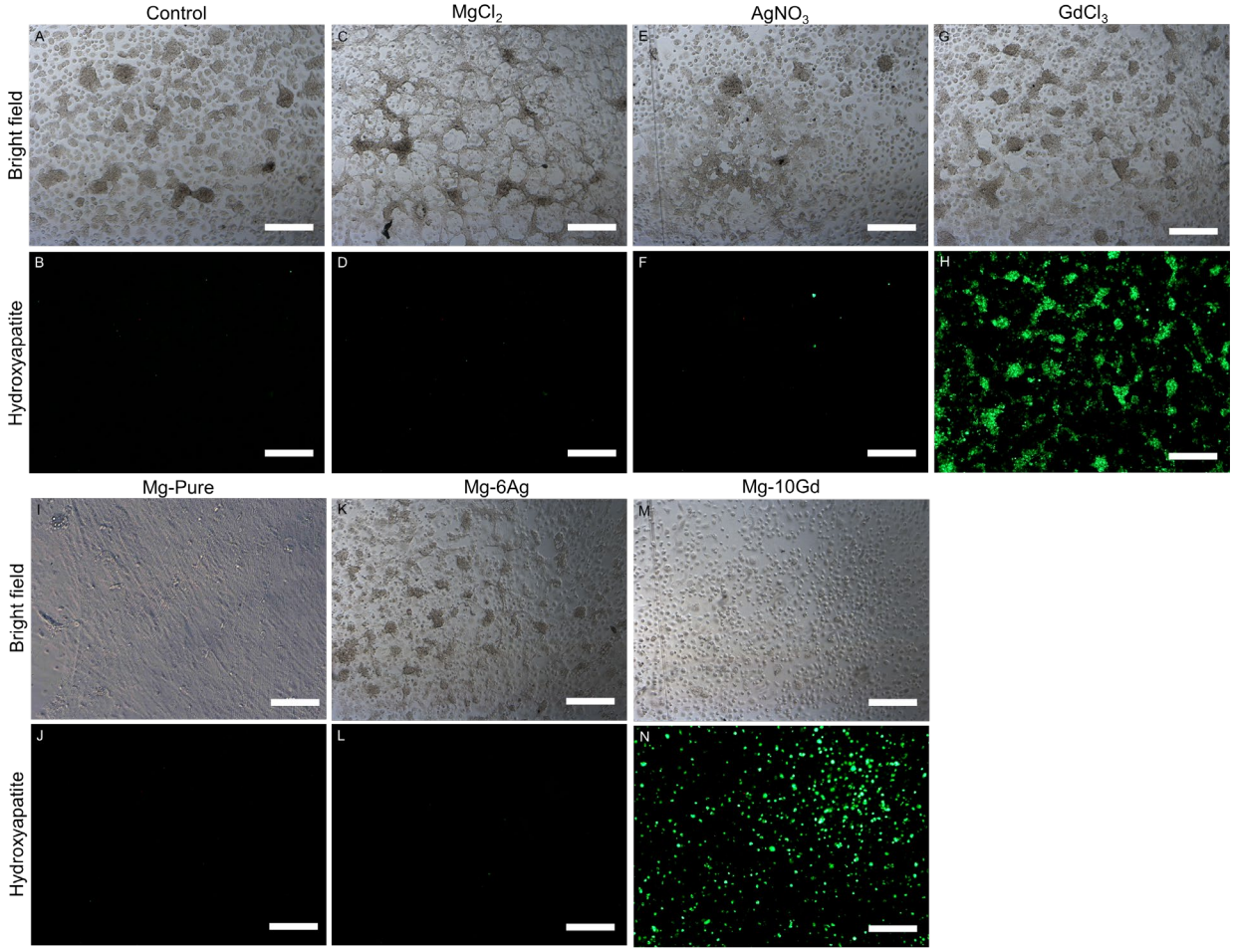

Figure 27: Representative pictures of HA staining of the coculture with different treatments at Day 28 Scale bar: 500 µm. Images were captures either using bright field (A, C, E, G, I, K and M) or fluorescence (B, D, F, H, J, L, and N) microscopy. A and B: Control; C and D: $MgCl_2$; E and F: $AgNO_3$; G and H: $GdCl_3$; I and J: Mg-Pure; K and L: Mg-6Ag; M and N: Mg-10Gd.

The treatment with Mg-Pure, Mg-6Ag, $AgNO_3$ and $MgCl_2$ showed no difference compared to the untreated cell control. However, a strong signal increase was measured in the Mg-10Gd and $GdCl_3$ exposed samples. To have a better overview, a quantification of the signals is presented in Figure 28. $MgCl_2$ showed a lower intensity of the HA staining signal than Mg-Pure and Mg-6Ag were lower than $AgNO_3$. It is also noticeable that treatment with $GdCl_3$ and Mg-10Gd leaded to a higher HA formation. It appears that both Ag and Mg had an inhibitory

effect on HA formation, which is more noticeable in Mg-6Ag extract. This would also explain why Mg-10Gd had a weaker staining signal than $GdCl_3$. Nevertheless, the results implied that the Gd could support the formation of HA.

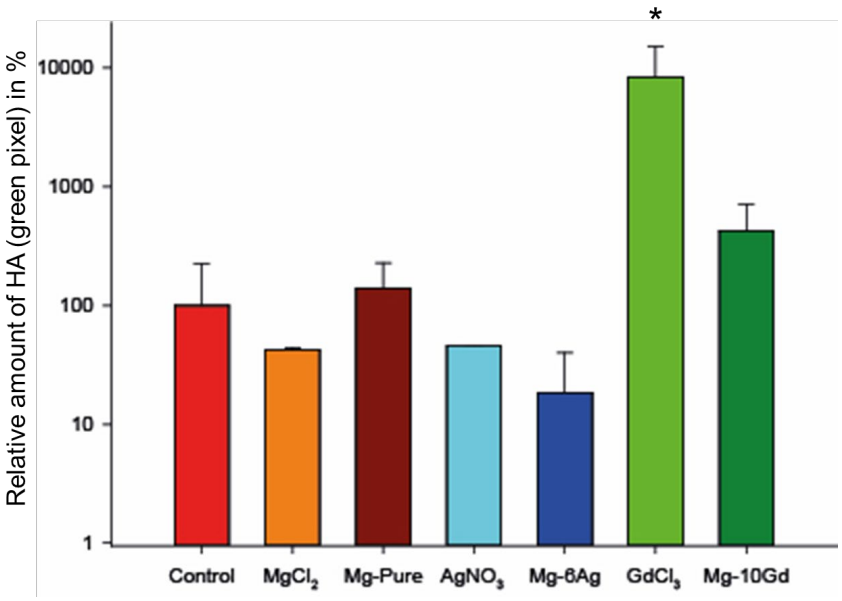

Figure 28: FITC signal of HA staining of the coculture with different treatments at Day 28. FITC signal strength was measured in green pixels (Bars represent mean ± standard deviation (SD). Stars indicate statistically significant difference between treatment and corresponding control (p =< 0.05))*

4.2.6 Resorption activity of OC

In order to verify the resorption activity of the developed OC a functional test utilizing dentin as ersatz of human calcified tissue was applied. The TRAP/DAPI staining indicates that both cell types appeared in the coculture system. As ultimate activity test, the cells were cultured on dentin chips for 28 days with pure media or extracts. Topographical views of resorption pits from randomly chosen sites in dentin slices were presented in Figure 29.

This figure showed that the resorption patterns were influenced by the extracts. When comparing the resorption pattern of Mg-Pure with the control, a similar number and size of the pits can be found. In comparison, the pits of Mg-10Gd are smaller but more numerous. Ag apparently reduces the resorption capacity of the OC. While visible resorption pits were still present during the treatment with Mg-Pure extract, in the Mg-6Ag extract treated samples almost no resorption activity can be recognized.

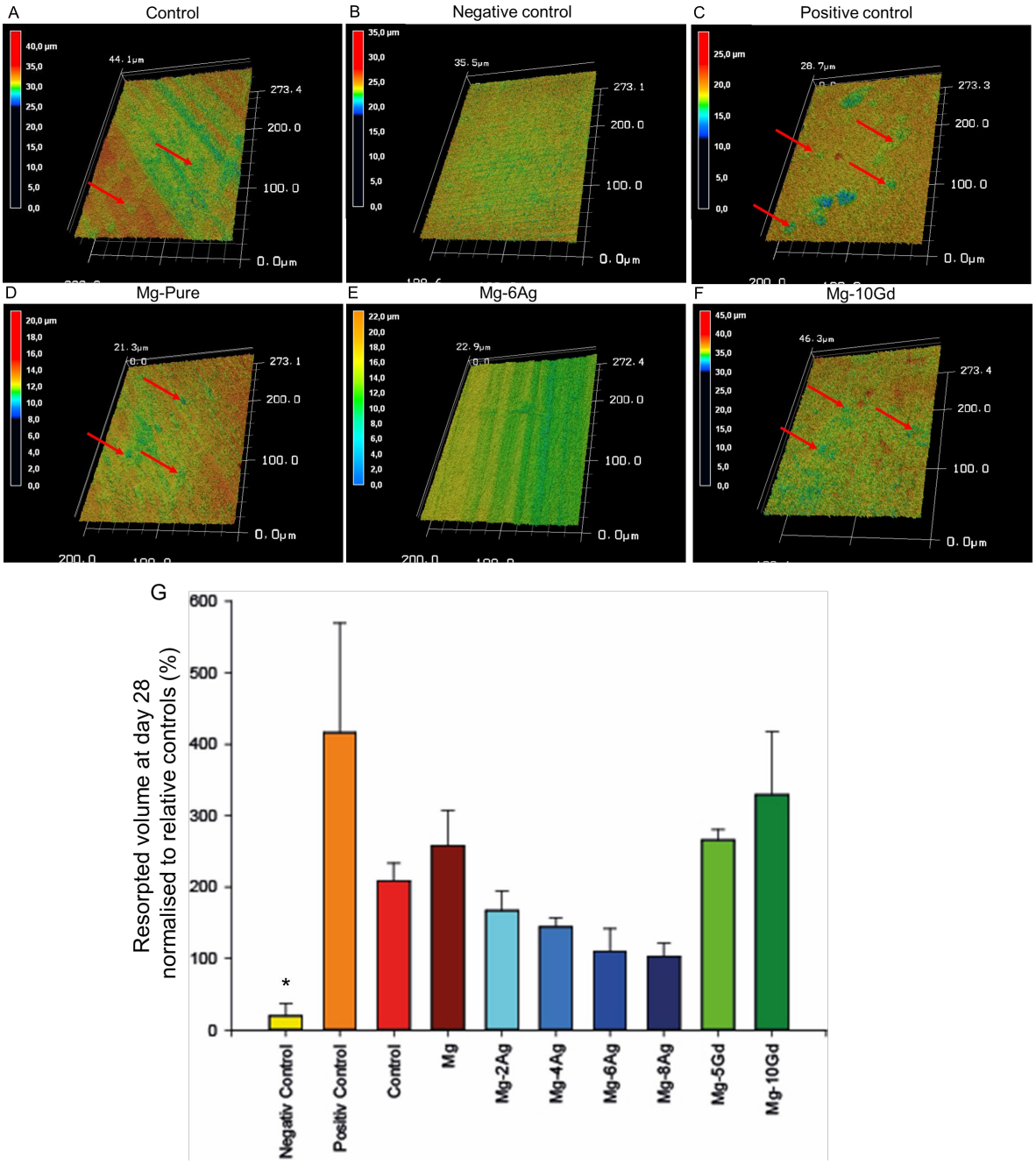

Figure 29: Topographical views of resorption pits (day 28) of the coculture after treatment with the Mg extracts. A: positive control (coculture treated with RANKL and M-CSF); B: negative control (no cells); C: Control (α-MEM cell culture medium; D: Mg-Pure; E: Mg-6Ag extract; F: Mg-10Gd extract; G: resorbed pit volume (Positive control: PBMC with RANKL and M-CSF; Mg-Pure and Mg-10Gd: with extract normalised to 10 mM Mg).

The MgAg extracts seemed to have a dose depended inhibitory effect. (Figure 29, G). Compared to the control, Mg-Pure extracts and especially the Mg-10Gd expressed a positive influence on the OC resorption activity.

4.2.7 Effect of Mg-extracts on the expression of cell specific markers

Specific markers of OB-OC differentiation and communication were analysed in order investigate the influence of single salt solutions ($MgCl_2$, $GdCl_3$ and $AgNO_3$) and extracts (Mg-Pure, Mg-2Ag, Mg-4Ag, Mg-6Ag and Mg-10Gd). The gene expression pattern from day 3 to day 28 is presented in Figure 30 **(Communication),** Figure 31 **(Transcription factors)** and Figure 32 **(Cell marker only day 28)**. In addition, detailed data from all measurement days (gene expression analyses) can be found in Supplementary Table 1 (Page 119) where fold expression values were compared to regulation threshold and significance levels indicated.

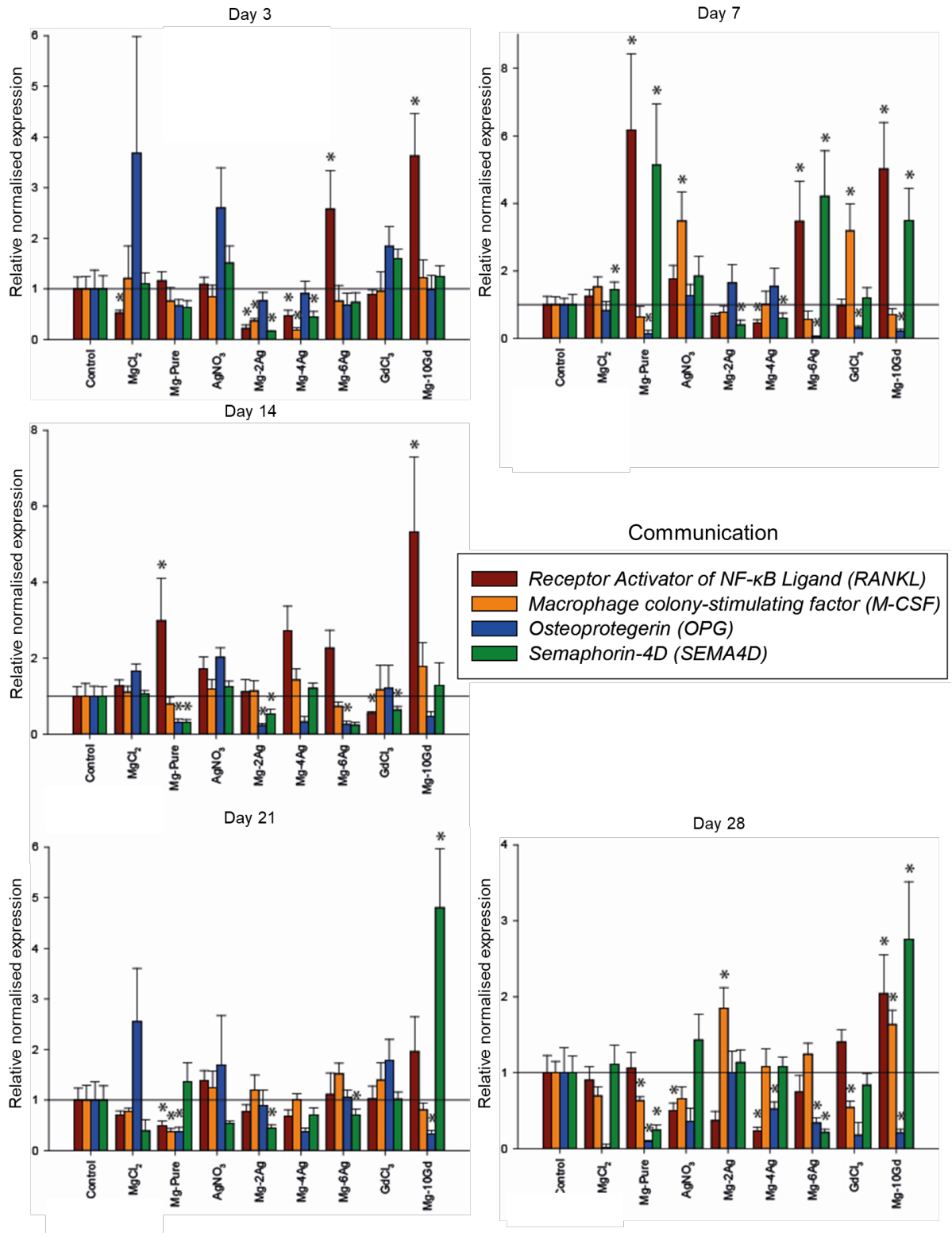

Figure 30: Evaluation of gene expression of single salt solutions ($MgCl_2$, $GdCl_3$ and $AgNO_3$) and extracts (Mg-Pure, Mg-2Ag, Mg-4Ag, Mg-6Ag and Mg-10Gd) normalised to control at 3, 7, 14, 21, and 28 days. Bars (n=6) represent mean ± standard deviation (SD). Stars indicate statistically significant (t-test) difference between treatment and corresponding control (p =< 0.05).*

Day 3: The expression of *RANKL* (+18.9) one of the most important proteins of communication between OC and OB was in the presence of $MgCl_2$ is significantly lower than in the control. This effect, however, was not observed with Mg-Pure. The expression of the communication relevant genes of the samples treated with Mg-2Ag and Mg-4Ag was decreased in contrast to the control. The genes *RANKL* (Mg-2Ag: -4.57 Mg-4Ag: -2.13), *M-CSF* (Mg-2Ag: -2.73; Mg-4Ag: -5.15) and *SEMA4D* (Mg-2Ag: -6.26; Mg-4Ag: -2.22) were significantly reduced by both material types. A small amount of Ag seems to inhibit the initial OB development at least by *SMEA4D*. The expression of *SEMA4D* as result of Mg-6Ag treatment was already comparable to the control whereas the expression of *RANKL* (Mg-6Ag: +2.58) was increased. This effect does not seem to occur with $AgNO_3$.

It is also interesting that the expression of *RANKL* (+3.63) was significantly increased in the samples treated with Mg-10Gd. The expression of *RANKL* under treatment of $GdCl_3$ was comparable to the control. It was observed that the expression of *OPG* in the samples treated with salts is higher than in the samples treated with the corresponding extracts.

Day 7: In the samples treated with Mg-Pure extract, the majority of genes are regulated to favour OC development (*RANKL*: +6.16; *SEMA4D*: +5.19; *OPG*: -6.59). This effect could not be observed in the samples treated with $MgCl_2$ or only to a small extent (*SEMA4D*: +1.45).

The expression of *SEMA4D* was significantly decreased at low Ag concentrations (Mg-2Ag: -2.48; Mg-4Ag: -1.68) and significantly increased at higher Ag concentrations (Mg-6Ag: +4.21). However, this may also be due to the different OC donors, as the Ag content in the two extracts does not differ so much. It is also interesting that the expression of *M-CSF* in the samples treated with the extracts was comparable to the control, the one of *M-CSF* in $AgNO_3$ was significantly increased ($AgNO_3$: +3.48). While the samples treated with $GdCl_3$ showed a significant increase in the expression of *M-CSF* (+3.19) and a significant decrease in *OPG* (-3.39), the samples treated with the extract Mg-10Gd showed a significant increase in the expression of *RANKL* (+5.02) and *SEMA4D* (+3.49) and a significant decrease in *OPG* (-4.8).

Day 14: The samples treated with Mg-Pure had a significantly higher expression of *RANKL* (+2.99) and the expression of *SEMA4D* (-3.24) and *OPG* (-3.31) was significantly lower than those treated with control. This difference was not obvious in samples treated with $MgCl_2$. The samples treated with Mg-2Ag and Mg-6Ag show a significant reduction in the expression of *OPG* (Mg-2Ag: -3.21; Mg-6Ag: -3.73) and Mg-2Ag additionally in the *SEMA4D* expression (-1.86). Since this difference was not visible in $AgNO_3$, it is probably due to the contained Mg and that only as an extract, since $MgCl_2$ did not show any significant difference to the control. As with all samples treated with the extracts, an increase in *RANKL* expression can also be

observed in the samples treated with Mg-10Gd. However, this increase differed significantly (*RANKL*: +5.32) from control. The samples treated with $GdCl_3$ showed a significant reduction in *RANKL* (-1.81) expression. In addition, *SEMA4D* expression in $GdCl_3$ treated samples was significantly reduced (*SEMA4D* -1.56).

Day 21: The samples treated with Mg-Pure showed a significant reduction in *RANKL* (-2.04), *M-CSF* (-2.67) and OPG (-2.68) compared to the control. These changes were not visible in $MgCl_2$ treated cell culture samples. The gene expression with Mg-2Ag and Mg-6Ag showed a significant reduction of *SEMA4D* (Mg-2Ag: -2.25; Mg-6Ag: -1.42). These changes could not be detected in the samples treated with $AgNO_3$. The samples treated with the Mg-10Gd extract showed a significant reduction in *OPG* expression (-3.02) and a significant increase in *SEMA4D* expression (+4.80). This influence was not visible in the samples treated with $GdCl_3$.

Day 28: Samples in the presence of Mg-Pure extracts showed a significant reduction in *OPG* expression (-10.73), *M-CSF* (-1.58) and *SEMA4D* (-4.09). The *RANKL* expression was lower for all samples treated with MgAg extracts and significant for $AgNO_3$ (-1.98) as well as Mg-4Ag (-4.28). Additionally, *OPG* expression was susceptible towards treatment with Mg4-Ag (*OPG*: -1.91) and Mg-6Ag (*OPG*: -2.96). The *OPG* expression appears to negatively correlate with the Ag content. In addition, samples treated with Mg-2Ag showed a significantly higher *M-CSF* (+1.85) expression and samples in presence of Mg-6Ag showed a significant decrease in *SEMA4D* (-4.66) expression. The expression pattern of the samples treated with Mg-10Gd and $GdCl_3$ was very similar. The pattern for Mg-10Gd extract treatment varied with an increase for *RANKL* (+2.04), *M-CSF* (+1.68) as well as *SEMA4D* (+2.76) and a decease for OPG (-4.78)

Summary: Ag initially had a positive effect on *RANKL* expression with increasing concentration. This influence continued more or less over the whole experiment. The expression of *RANKL* was higher in the samples treated with Mg-Pure and Mg-10Gd extracts than in the corresponding salts $MgCl_2$ and $GdCl_3$ solutions.

Ag seemed to reduce the observed factors for communication in general. Over the whole experiment, *OPG* and *SEMA4D* were usually less expressed than in the control. *RANKL* and *M-CSF* were also less exposed at the beginning. However, the expression of these two genes was either comparable to the control or more strongly expressed from day 14 onwards. In contrast, Gd seems to have an enhancing effect on communication factors except on *OPG* expression.

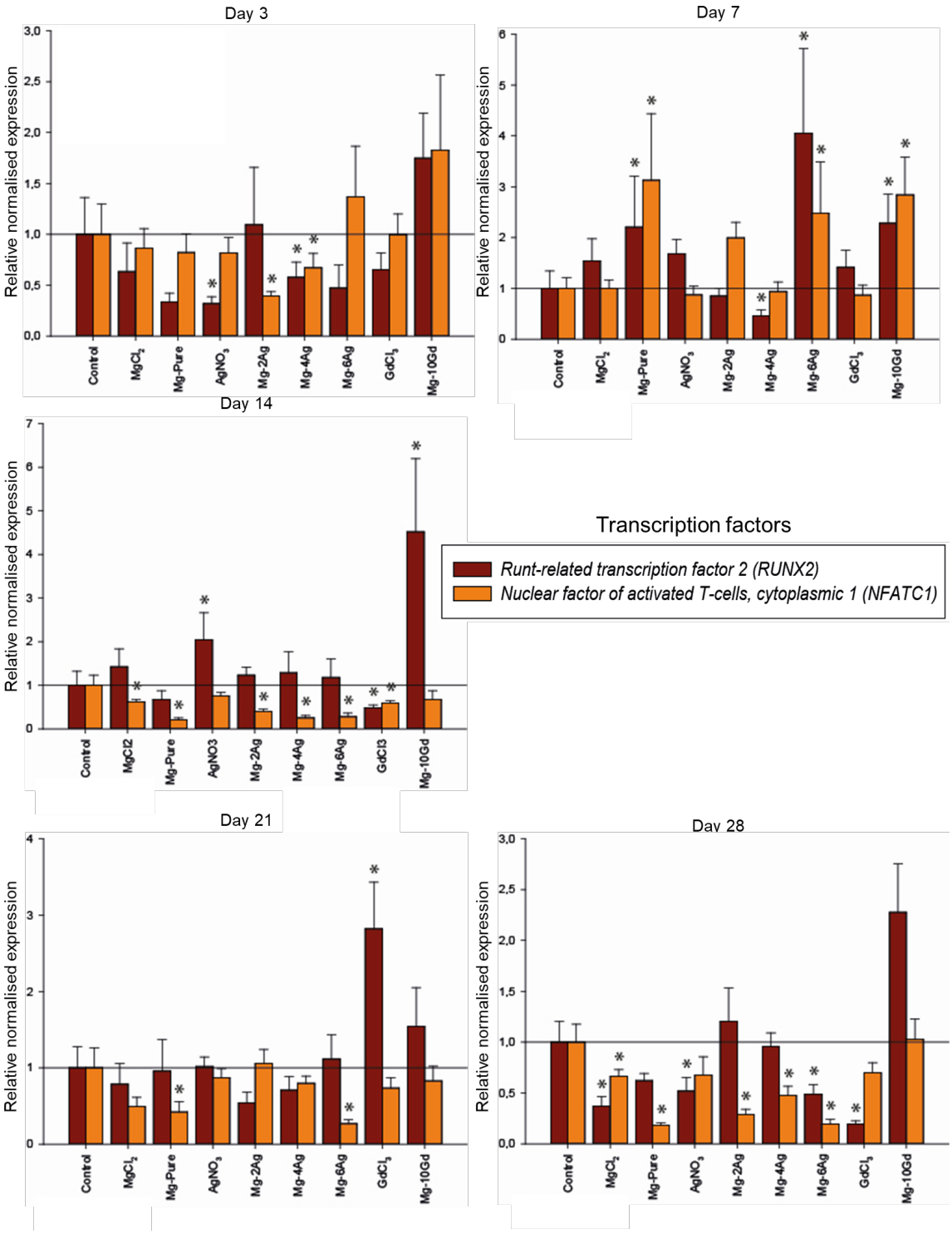

Figure 31: Evaluation of gene expression of single salt solutions ($MgCl_2$, $GdCl_3$ and $AgNO_3$) and extracts (Mg-Pure, Mg-2Ag, Mg-4Ag, Mg-6Ag and Mg-10Gd) normalised to control at different timepoints (3, 7, 14, 21, and 28 days). Bars (n=6) represent mean ± standard deviation (SD). Stars indicate statistically significant (t-test) difference between treatment and corresponding control (p =< 0.05).*

Day 3: Sample in the presence of $AgNO_3$ showed a significantly reduced expression of *RUNX2* (-3.31). Although, the treatment with the comparable extract Mg-6Ag led to a similar expression

pattern, there was no significant change measured. Treatment with Mg-2Ag led to a significantly reduced expression of *NFATC1* (-2.54). Mg-4Ag on the other side caused a reduced expression of both transcription factors (*RUNX2*: -1.73; *NFATC1*: -1.49). In the end, the other extracts and salts did not show any significant change at this measuring point.

Day 7: Treatment of the samples with Mg-Pure significantly increased the expression of both genes (*RUNX2*: +2.21; *NFATC1*: +3.31). The presence of $MgCl_2$ or $AgNO_3$ did not lead to any significant change compared to control. Treatment with the corresponding extract Mg-6Ag led to a stronger expression of both genes (*RUNX2*: +4.06; *NFATC1*: +2.48). On the other side, Mg-4Ag led to a significantly lower expression of *RUNX2* (-2.16). The samples treated with Mg-10Gd showed a significant increase in the expression of both *RUNX2* (+2.28) and *NFATC1* (+2.84).

Day 14: Treatment with both $MgCl_2$ and Mg-Pure resulted in a significantly decreased expression of *NFATC1* ($MgCl_2$: -1.49: Mg-Pure: -4.77). Ag treatment resulted in a reduction in *NFATC1* expression in all samples with Mg-2Ag (-2.54) and Mg-4Ag (-3.99), respectively. In addition, presence of $AgNO_3$ (+2.04) the *RUNX2* expression was significantly increased. Treatment of the samples with $GdCl_3$ significantly reduced the expression of both genes (*RUNX2*: -2.05; *NAFTC1*: -1.48). On the other hand, the samples in presence of Mg-10Gd had a significantly higher expression of *RUNX2* (+4.52).

Day 21: At this measuring point there were hardly any significant changes. Only for control treatment with Mg-Pure and Mg-6Ag led to a significant reduction in *NFATC1* (Mg-Pure: -2.37 Mg-6Ag: -3.70) expression. The treatment of the samples with $GdCl_3$ induced a significant increase in the expression of *RUNX2* (+1.95).

Day 28: The presence of $MgCl_2$ and Mg-Pure resulted in a significant reduction of *NFATC1* expression ($MgCl_2$: -1.51: Mg-Pure: -5.44). In addition, treatment with $MgCl_2$ resulted in a significant reduction in *RUNX2* (-2.27) expression. The MgAg extracts caused a significant reduction of *NFATC1* expression (Mg-2Ag: -3.51; Mg4-Ag; -2.21: Mg-6Ag: -5.16). Furthermore, a significant decrease in the expression of *RUNX2* in Mg-6Ag (-2.05) treated samples was measured. This significant reduction was also observed in presence of $AgNO_3$ (-1.93). Treatment of $GdCl_3$ resulted in a significant reduction in *RUNX2* (-5.17) expression and the Mg-10Gd extract had the opposite effect.

Summary: Exposition to Mg-10Gd had a positive influence on the *RUNX2* expression, meaning a support of OB differentiation. This pattern was not detected in samples treated with $GdCl_3$. The influence of Ag on the measured transcription factors seemed to be very dependent on the duration of the experiment. On day 3 the *NFATC1* expression increased with increasing

Ag content while the expression of *RUNX2* decreased. Consequently, because of the decreased *RUNX2* expression could the OB differentiation be slower. NFATC1 is important for both OC and OB development, thus in that way the differentiation of both cell types could be supported. On day 14 the *NFATC1* expression decreased with increasing Ag content while *RUNX2* remained almost constant. On day 28, the *RUNX2* expression decreased again with increasing Ag content, while the *NFATC1* remained almost constant. Later the *RUNX2* expression was constant or decreased, thus the OB differentiation may be slower as in the control.

In a final step, the cell markers on day 28 were determined to show the development status of coculture at the end of the experiment.

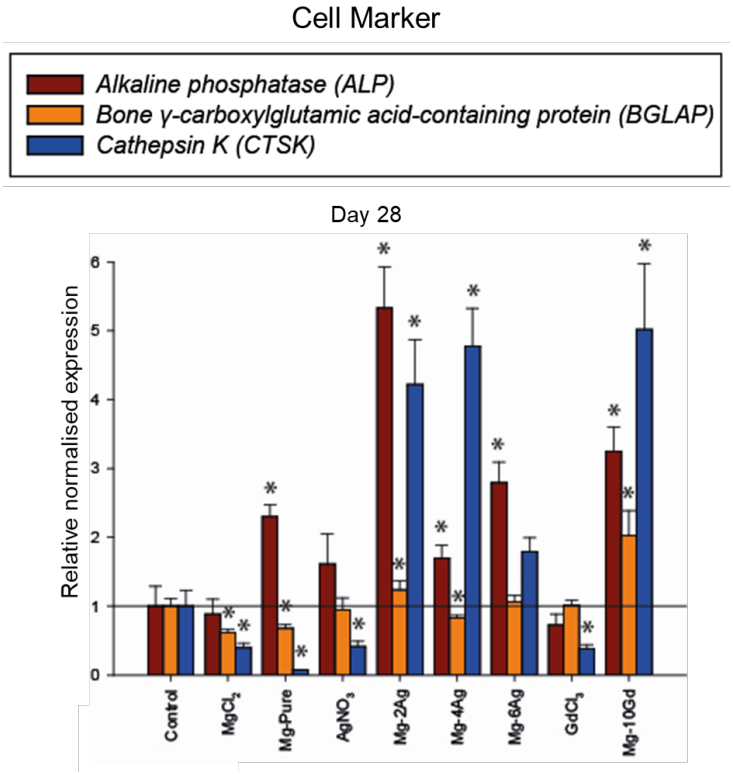

Figure 32: Evaluation of gene expression of single salt solutions ($MgCl_2$, $GdCl_3$ and $AgNO_3$) and extracts (Mg-Pure, Mg-Pure, Mg-2Ag, Mg-4Ag, Mg-6Ag and Mg-10Gd) normalised to control at day 28. Bars (n=6) represent mean ± standard deviation (SD). Stars indicate statistically significant (t-test) difference between treatment and corresponding control (p =< 0.05).*

Treatment with $MgCl_2$ and Mg-Pure has led to a similar expression pattern. Despite of, a significant increased expression of *ALP* (+2.30). Treatment with both $MgCl_2$ and Mg-Pure reduced the expression of *BGLAP* ($MgCl_2$: -1.63; Mg-Pure: -1.47) and *CTSK* ($MgCl_2$: -2.51; Mg-Pure: -13.48). Considering the Ag containing materials, only the presence of $AgNO_3$ led to a significant reduction in *CTSK* (-2.41) expression. The expression of *CTSK* was significantly

increased in both cocultures treated with Mg-2Ag (+4.22) and Mg-4Ag (+4.78). Furthermore, *BGLAP* was significantly upregulated (+1.24) in samples with Mg-2Ag. However, the expression was significantly decreased compared to the control (-1.21) if Mg-4Ag added to the medium. The *ALP* expression was significantly increased with the treatment of all MgAg extracts (Mg-2Ag: +5.33; Mg-4Ag: +1.70; Mg-6Ag: +2.79). Treatment with $GdCl_3$ resulted in a significant reduction in *CTSK* (-2.63) expression. But with Mg-10Gd, significantly increased the expression of *CTSK* (+5.02). In addition, Mg-10Gd led to a significant increase in *ALP* expression (+3.25).

Summary: The MgAg alloys seemed to have an activating effect on the expression of both ALP (marker for OB) and CTSK (marker for OC). In addition, the treatment with Mg-10Gd extract triggered a higher expression of all cell markers measured in this expression. On the other hand, this effect could not be observed with $GdCl_3$.

4.2.8 Influence of extracts on the calcium sensing receptor pathway

Via HA staining and microscopic monitoring, Gd had been shown to support HA formation (4.2.5 Visualization of mineralization by hydroxyapatite staining; Page 55). However, these results were not supported by the *RUNX2* expression pattern. In order to elucidate the influenced process in detail, the pathway of CASR was selected, because this receptor is present on OB and OC, translates the external Ca level into an intracellular Ca signal and therefore it is an important factor for maintaining the bone structure. Furthermore, it is known that Gd can act as an antagonist of Ca for receptor binding.

Day 3: Treatment with $MgCl_2$ led to a significant reduction in expression of *CASR* (-1.52) and the expression in the samples with Mg-Pure showed a significant reduction of *PLCG2* (-1.91). Although there were no significant changes in the samples with $AgNO_3$, numerous significant changes could be measured in the samples treated with MgAg extracts. The treatment of the samples with Mg-2Ag and Mg-4Ag led to a significant reduction of *PPP3CA* (Mg-2Ag: -2.44; Mg-4Ag: -1.45). In addition, the expression of *CASR* was decreased on the presence of Mg-2Ag (*CASR*: -3.97) and the expression of *MAPK1* was decreased with Mg-4Ag (*MAPK1*: -1.85). In contrast, treatment with Mg-6Ag was more pronounced towards an increase in *CASR* (+2.40). The presence of Mg-10Gd in coculture medium resulted in a significant increase in *CASR* (+6.39) expression, but this difference could not be observed with $GdCl_3$.

Day 7: Treatment with $MgCl_2$ and Mg-Pure extracts resulted in a significantly increased expression of *MAPK1* (+1.29; *Mg*: +3.50). In addition, the expression of *CASR* was significantly

increased (*CASR*: +10.52) by pure Mg. The presence of $AgNO_3$ only resulted in a significant increase of *PLCG2* (+1.75). The expression of *CASR* was significantly reduced with both Mg-2Ag and Mg-4Ag (Mg-2Ag: -2.09; Mg-4Ag: -5.10). Moreover, the expression of *PLCG2* was significantly reduced with Mg-2Ag (*PLCG2*: -1.80). Otherwise, treatment with Mg-2Ag led to a significant increase in *PPP3CA* expression (+2.93) and the presence of Mg-6Ag resulted in a significant increase in the expression of *CASR* (+6.62), *PLCG2* (+2.83) and *MAPK1* (+2.36). Treatment of the cells with $GdCl_3$ led to a significant reduction in the expression of *CASR* (-1.38), but to a significant increase in the expression of *PLCG2* (+1.32) and *MAPK1* (+1.30). The Mg-10Gd extract led to a significant increase in the expression of *CASR* (+5.74), *PLCG2* (+2.39) and *PPP3CA* (+5.51).

Day 14: The presence of $MgCl_2$ resulted in a significant reduction in *PPP3CA* (+3.10) expression and a significant increase in *MAPK1* (+1.77) expression. Mg-Pure significantly reduced expression of *CASR* (-9.98) and $AgNO_3$ led to a significant increase in *PLCG2* expression (+1.59). *PLCG2* expression was significantly reduced by treatment with Mg-2Ag (*PLCG2*: -1.82) and Mg-4Ag (*PLCG2*: -1.65). Mg-6Ag led to a significant increase in *MAPK1* (+2.05). Treatment with $GdCl_3$ significantly reduced the expression of *CASR* (-2.27) and Mg-10Gd led to a significant increase in *MAPK1* (+4.59) and *PPP3CA* (+3.70) expression.

Day 21: Continuously, in presence of $MgCl_2$ the MAPK1 expression is significantly increased (+2.93). Mg-Pure, on the other hand, led to a significant reduction in *PLCG2* expression (-8.75). Treatment with $AgNO_3$ significantly increased the expression of *MAPK1* (+1.54). If the cell culture medium contains Mg-2Ag or Mg-4Ag the expression of *PLCG2* is significantly reduced (Mg-2Ag: -2.15; Mg4 Ag: -2.99). Additionally, *MAPK1* (-1.79) expression was significantly reduced and *CASR* (+5.74) expression significantly increased in the presence of Mg-2Ag. The treatment of the samples with Mg-6Ag only led to a significant reduction in *PLCG2* expression (-3.13) and $GdCl_3$ led to a significant increased *PLCG2* expression (+1.68). Whereas with Mg-10Gd no significant genetic change could be measured.

Day 28: Finally, the treatment with $MgCl_2$ significantly reduced the expression of *CASR* (-1.72) and *MAPK1* (-2.66). The presence of $AgNO_3$ resulted in a significant reduction of *PLCG2* (-1.57) and *MAPK1* (-2.58). If the cell culture medium contains Mg-2Ag, however, led to an increase in *PLCG2* (+3.29) expression. The other MgAg extracts did not result in any significant change of the coculture. If the coculture medium contains $GdCl_3$ the *PLCG2* was significantly increased (+1.23) and the expression of *MAPK1* was significantly decreased (-1.56). Treatment with Mg-10Gd extract led to a significant reduction of *PCLG2* (-3.03) expression.

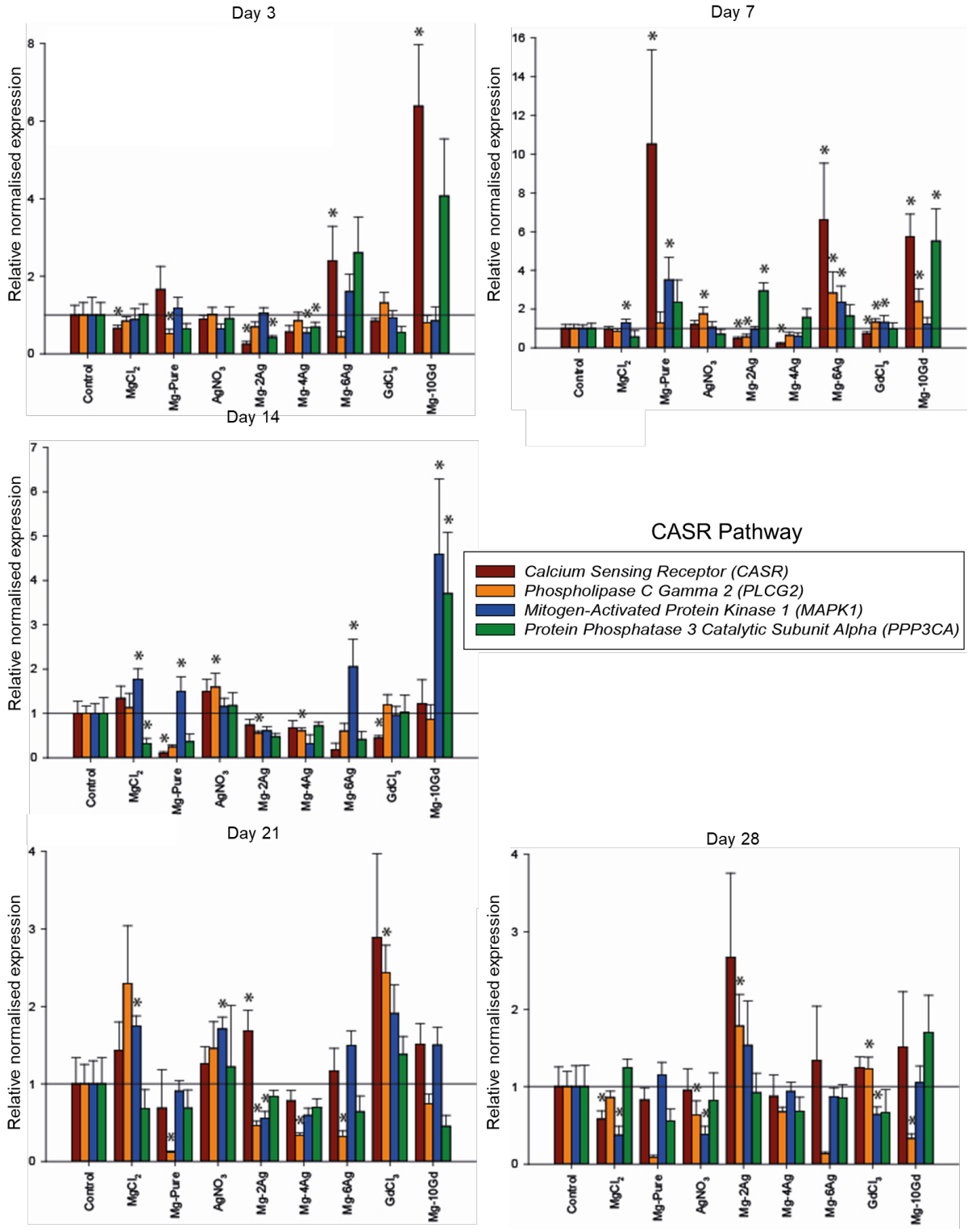

Figure 33: Evaluation of the CASR signal cascade gene expression of the cells treated with solutions ($MgCl_2$, $GdCl_3$ and $AgNO_3$) and extracts (Mg-Pure, Mg-6Ag and Mg-10Gd) normalised to control at day 28. The coculture was incubated for 28 days with the different Mg extracts and salts in α-MEM medium with 10 % FBS and 1 % pen/strep. Bars (n=6) represent mean ± standard deviation (SD). Stars indicate statistically significant (t-test) difference between treatment and corresponding control (p =< 0.05).*

4 Results

Summary: Mainly Mg-10Gd extract had positively influence on the expression of different selected factors involved in the CSAR pathway. The $GdCl_3$ salt seemed to have a positive effect on expression CSAR pathway, but this effect did not occur until day 21 and is less pronounced. Apart from Mg-6Ag, MgAg alloys had a higher inhibitory effect on the CASR pathway selected markers than the control. A significant increase of *PLCG2* in Mg-2Ag can only be observed on day 28. In addition, Mg-Pure showed only an initial (day 7) positive effect on the *CASR* expression. In the following days an inhibitory effect of *CASR* expression was observed.

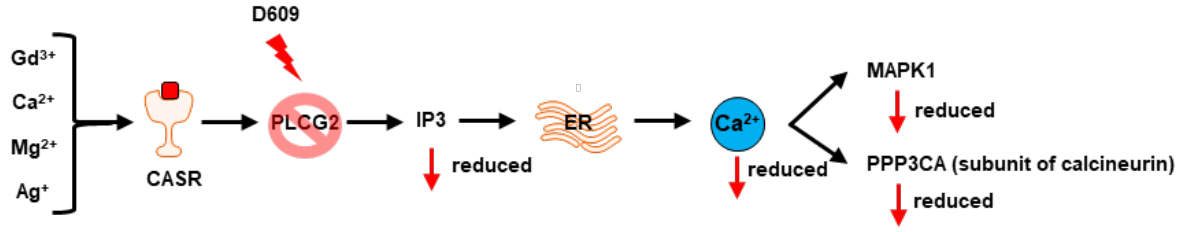

Figure 34: Excepted influence of PLC inhibitor D609 on the CASR signal cascade [186–188,171,189–192].

The previous HA staining have shown that Gd appeared to have a positive effect on HA formation. In addition, *PLCG2* expression was increased at day 7 in samples treated with Gd (extract and salt) and also increased in $GdCl_3$ treated samples at day 21 and 28. This protein links the CASR, sensing the extracellular Ca level, with the mobilisation of inositoltrisphosphat 3 (IP3) to initiate the intercellular Ca secretion from the endoplasmic reticulum (ER). The released Ca ions trigger various proteins such as MAPK1 or Calcineurin (subunits of calcineurin are PPP3CA, PPP3CB, PPP3CC). This pathway (Figure 34) is therefore an important element for maintaining bone homeostasis and an inhibition of PLCG2 should result in a reduced HA formation and expression of genes downstream of PLCG2. To further demonstrate a link between Mg, Ag or especially Gd and the CASR cascade, the coculture exposed to Mg-Pure, Mg-6Ag and Mg-10Gd extracts as well as $MgCl_2$, $AgNO_3$ and $GdCl_3$ were also treated with the PLC inhibitor D609, which was selected to block the signal of CASR at the step of PLCG2 [193].

Table 9: Summary qPCR results of the coculture with or without PLC inhibitor. Stars (*) indicate degree of significance (= p =< 0.05; ** = p =< 0.001; *** = p =< 0.0001).*

	Alloy	Mg-Pure				Mg-Pure + D609			
	Gene	CASR	PLCG2	MAPK1	PPP3CA	CASR	PLCG2	MAPK1	PPP3CA
Day 1	Regulation	-2,26	-3,24	-2,47		-2,22	-2,49		
		↓	↓	↓		↓	↓		
	p-Value	1,20E-05	1,66E-02	3,31E-03		1,30E-05	1,25E-02		
		***	*	**		***	*		
Day 2	Regulation	2,70	-2,04		3,89	3,02	-2,74	-5,11	
		↑	↓		↑	↓	↓	↓	
	p-Value	0,00E+00	8,52E-03		2,00E-06	8,00E-06	2,62E-03	1,55E-02	
		***	***		***	***	*	*	
Day 3	Regulation	6,56	-3,90		2,35				
		↑	↓		↑				
	p-Value	2,22E-04	4,33E-03		1,68E-02				
		***	**		*				
	Alloy	Mg-2Ag				Mg-2Ag + D609			
	Gene	CASR	PLCG2	MAPK1	PPP3CA	CASR	PLCG2	MAPK1	PPP3CA
Day 1	Regulation			-1,37		-1,65	-2,24		
				↓		↓	↓		
	p-Value			2,57E-02		9,40E-05	2,32E-02		
				*		***	*		
Day 2	Regulation				2,04	1,51			
					↑	↑			
	p-Value				2,61E-02	1,71E-02			
					*	*			
Day 3	Regulation	3,62					-1,58		-1,83
		↑					↓		↓
	p-Value	1,95E-03					2,29E-02		2,30E-02
		**					*		*
	Alloy	Mg-10Gd				Mg-10Gd + D609			
	Gene	CASR	PLCG2	MAPK1	PPP3CA	CASR	PLCG2	MAPK1	PPP3CA
Day 1	Regulation	1,93		2,08		-3,60			
		↑		↑		↓			
	p-Value	6,39E-03		9,34E-03		3,59E-04			
		**		**		***			
Day 2	Regulation	1,65			5,37				
		↑			↑				
	p-Value	1,43E-03			2,22E-02				
		**			*				
Day 3	Regulation		-2,54	-1,94					
			↓	↓					
	p-Value		5,24E-03	1,30E-02					
			**	*					

Gene expressions were analysed after 1 and 3 days treatment and presented in Table 9 Since the PLC inhibitor also effects pathways, which are necessary for the survival of the cell, analyses over a period of maximum 3 days were chosen. The effect of the PLC inhibitor was most visible in samples treated with Mg-10Gd. This was to be assumed as Gd is known to activate the CASR. Interestingly, the influence of the PLC inhibitor in combination with Mg-Pure and Mg-2Ag was almost undetectable until the 3rd day. This may be due to the fact that the Mg ions already have a weaker connection to the CASR and thus a further reduction can no longer occur or the response is triggered *via* other pathways. On the third day, an increased *CASR* expression was measured in the samples without PLC inhibitor, but this did not occur in connection with the PLC inhibitor.

The effect on HA formation was assessed using the experimental setup and staining of the OsteoImage kit (Figure 35). There is hardly any difference in signal intensity between the individual samples of Mg-Pure, Mg-6Ag, $MgCl_2$ and $AgNO_3$. However, there is a trend to a reduced HA formation in the samples treated with the PLC Inhibitor. Conversely, Mg-10Gd extract seemed to support (significant at day 3) the formation more than $GdCl_3$ exposition. Nevertheless, the mineralisation was not totally suppressed with Mg-10Gd extracts + D609 which may suggest other mineralisation pathways involved or a synergistic effect of Mg and Gd. As expected, PLC inhibitor D609 leads to a weaker signal and thus to a reduced HA formation. Taking the results together, the CSAR is probably a part of the positive influence of Mg-10Gd extracts on HA formation.

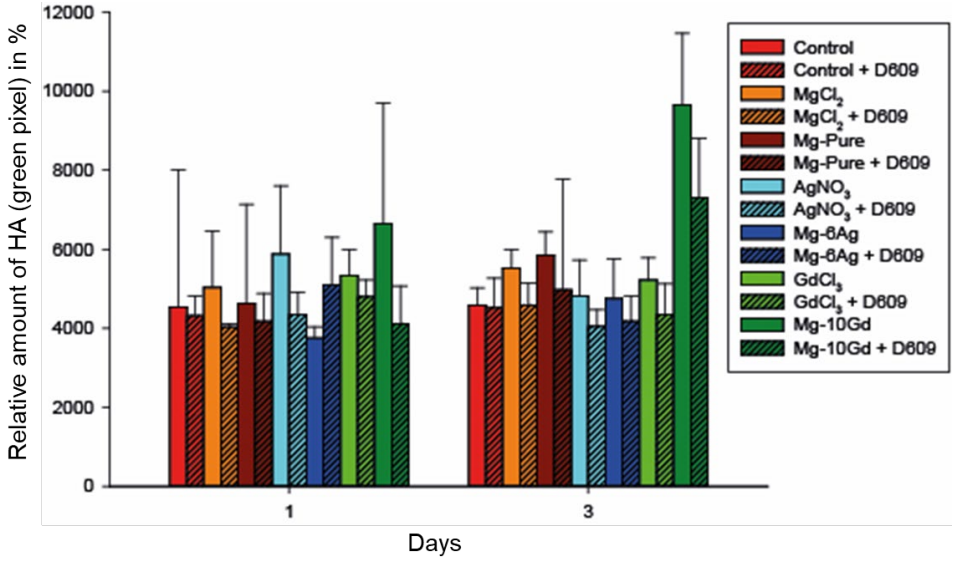

Figure 35: Evaluation of the HA formation represented by the FITC signal intensity of the Control, Mg-Pure and Mg-6Ag and Mg-10Gd as well as $MgCl_2$, $AgNO_3$ and $GdCl_3$ treated cell cultures with and without PLC inhibitor D609. (Day 1 and 3). Bars (n=6) represent mean ± standard deviation (SD). Stars indicate statistically significant difference (Holm-Sidak post-hoc test) between treatment and corresponding control (p =< 0.05).*

4.3 Response of OB and OC directly cultured on magnesium alloys

After the composition of the materials was analysed by SEM (Table 10), the coculture was cultivated and examined.

Table 10: Material composition for direct assay

	Mg in ppm	Ag in ppm	Gd in ppm	Fe in ppm	Ni in ppm	Cu in ppm	Si in ppm
Mg-Pure	999300	x	x	11	<2	x	x
Mg-2Ag	x	21200	x	19,1	9,1	17,2	38,1
Mg-10Gd	x	x	92000-96000	400	<37	19	18

4.3.1 Impact of direct material contact on proliferation

In order to determine how the cells, react during a direct contact with the alloys, the cells were cultured over a period of 28 days on the surface of different samples. The supernatant and DNA were collected after 3, 7, 14, 21 and 28 days as well as a Live/Dead staining were performed to determine the viability of the cells. In addition, the degradation rate of the materials was determined. Because of the direct contact of the cells with the material, the DNA content can depend on factors such as degradation speed and material incompatibility of the cells.

At the beginning, there seem to be more cells on Mg-10Gd than on Mg-Pure, because the DNA content was significantly higher on Mg-10Gd than on Mg-Pure. On day 7, however, the DNA content in the samples grown on Mg-10Gd was the lowest of all three materials. At the following measuring points, the DNA content of Mg-Pure and Mg-2Ag did not differ significantly (Figure 36).

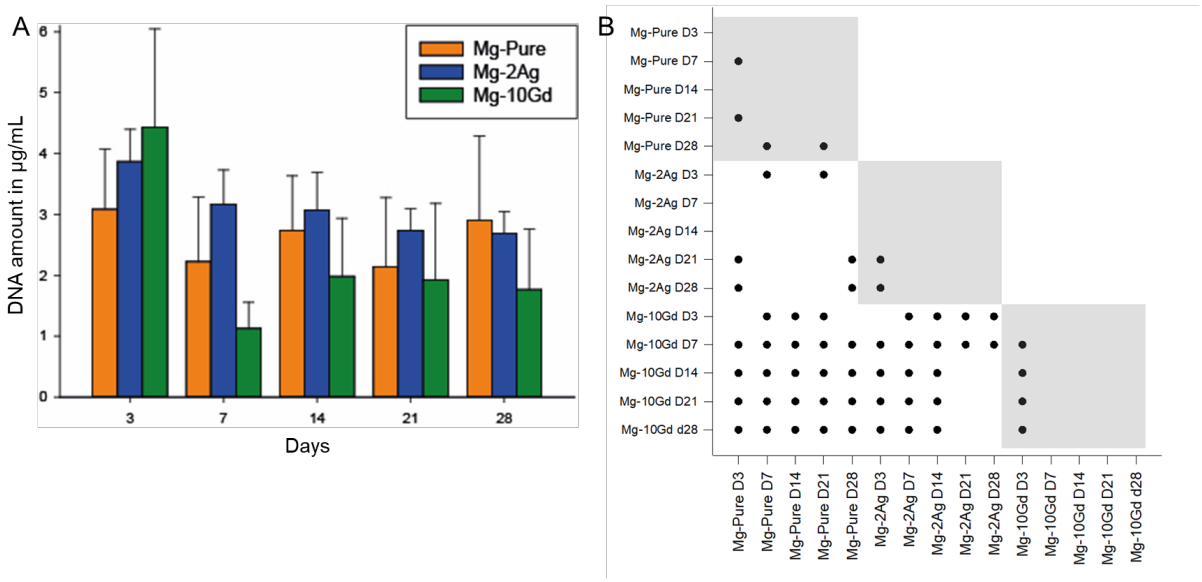

Figure 36: DNA content of cells comparison to the control in % during culture on Mg-Pure and Mg-10Gd samples. A: Comparison Mg-Pure, Mg-2Ag and Mg-10Gd Samples; B: Significances (Holm-Sidak post-hoc test). Bars (n=6) represent mean ± standard deviation (SD). Stars indicate statistically significant difference (Holm-Sidak post-hoc test) between treatment and corresponding control (Mg-Pure disc) (p =< 0.05). Grey blocks represent the difference within one condition or for one material over all time points.*

4.3.2 Influence of direct material contact on ALP activity

The ALP activity measured in the supernatant of direct cultures showed that the ALP activity of cells growing on Mg-Pure and Mg-10Gd increased significantly after just 7 days. The ALP activity of the cells growing on Mg-2Ag differed significantly on day 14 only from the measurement on day 3. In the samples grown on Mg-10Gd the ALP activity remained almost constant from day 7 until day 28. The ALP release of the cells growing on Mg-Pure also remained constant from day 7 until day 28. The variation of the ALP release of the cells growing on Mg-Pure was, however, wider than in the cells growing on Mg-10Gd (Figure 37).

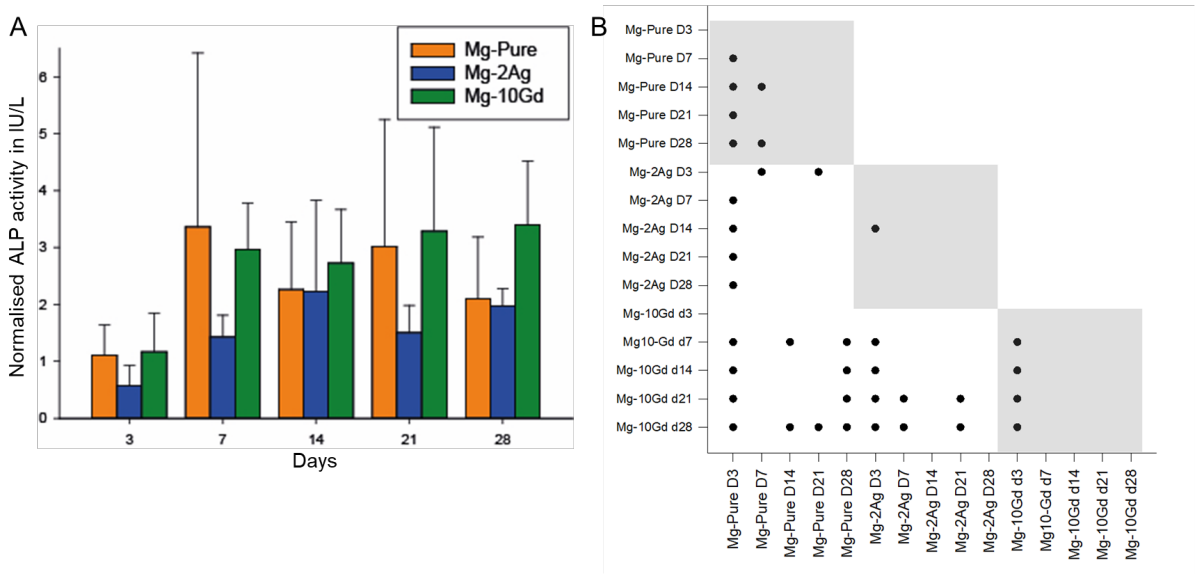

Figure 37: ALP activity of cells in comparison the control (Mg-Pure) in % A: Comparison Mg-Pure, Mg-2Ag and Mg-10Gd Samples; B: Significances (Holm-Sidak post-hoc test). Bars (n=6) represent mean ± standard deviation (SD). Stars indicate statistically significant difference (Holm-Sidak post-hoc test) between treatment and corresponding control (Mg-Pure disc)l (p =< 0.05). Grey blocks represent the difference within one condition or for one material over all time points.*

4.3.3 Impact of direct material contact on TRAP activity

To measure TRAP activity as an indicator of cell function of OC, the supernatants were checked for that activity. It turned out that the culturing of the cells on the Mg-2Ag samples seemed to have hardly any effect on the TRAP release. The TRAP release of the cells on the Mg-2Ag samples was lower than the TRAP release of the cells growing on Mg-Pure or Mg-10Gd over the entire duration of the experiment. The TRAP release of the cells growing on Mg-Pure and Mg-10Gd had a significantly increased on day 7 compared to the previous measurement point. Afterwards there were no significant changes (Figure 38).

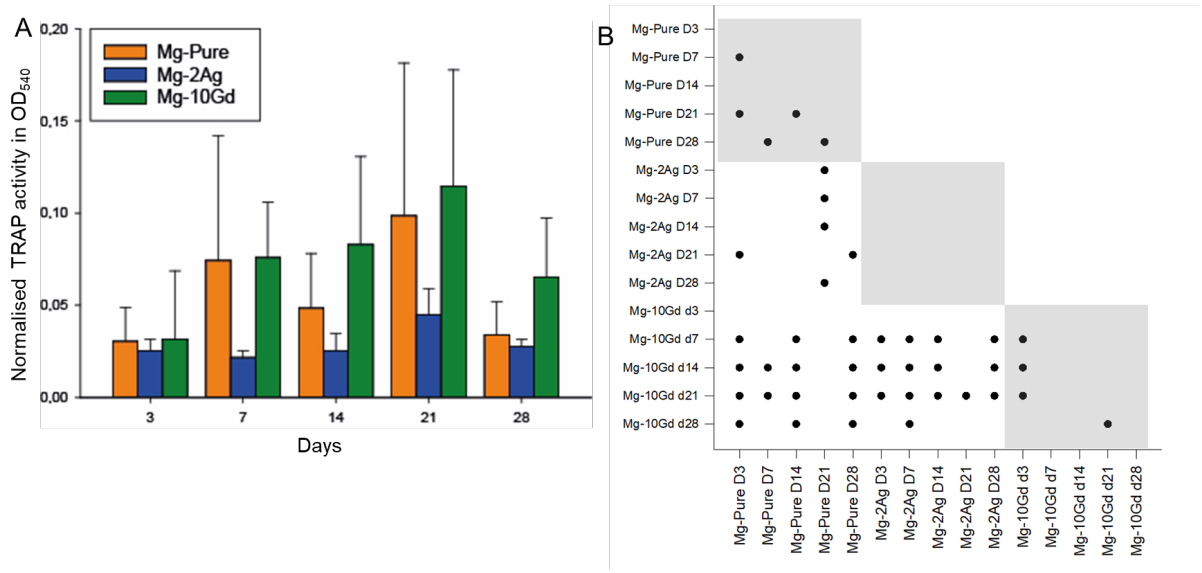

Figure 38: TRAP activity of cells comparison with control in % after treatment on Mg-Pure-and Mg-10Gd samples. A: Comparison Mg-Pure, Mg-2Ag and Mg-10Gd Samples; B: Significances (Holm-Sidak post-hoc test). Bars (n=6) represent mean ± standard deviation (SD). Stars indicate statistically significant difference (Holm-Sidak post-hoc test) between treatment and corresponding control (p =< 0.05). Grey blocks represent the difference within one condition or for one material over all time points.*

4.3.4 Influence of direct material contact on cell viability

The viability of OB and OC was detected using a Live/Dead staining assay. The micrographs demonstrate that the cells were able to grow on each of the material surfaces for up to 28 days. At the end of the experiment, cells of different sizes (small OB, big OC) were especially visible in the samples treated with Mg-2Ag (Figure 39; B & E).

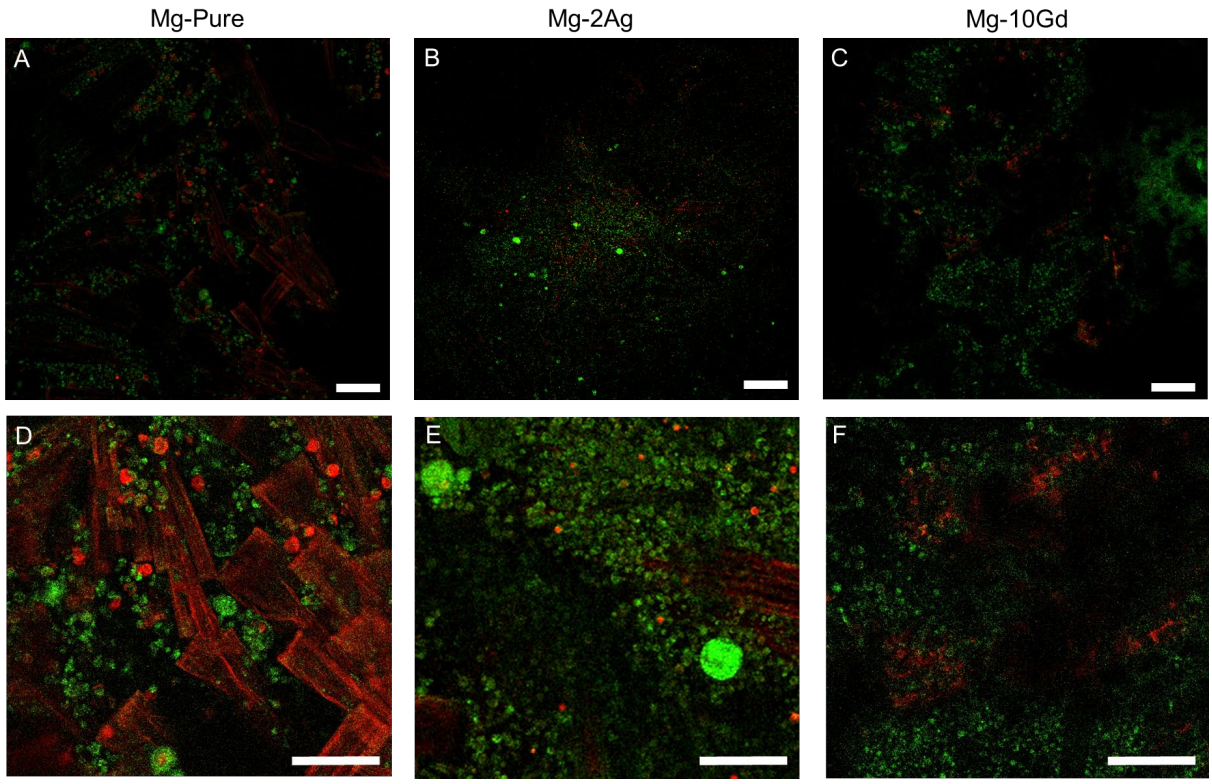

Figure 39: Live/Dead staining of the coculture grown for 28 days on Mg-Pure (A & D), Mg-2Ag (B & E) or Mg-10Gd (C & F) the samples. The coculture was incubated for 28 days in α-MEM medium with 10 % FBS and 1 % pen/strep. (green, alive, and red, dead cells; scale bar: 100 µm).

4.3.5 Immersion test of different magnesium alloys

In order to determine whether the cells had an influence on the degradation rate, the materials were cultured with and without cells for 28 days. According to the difference between the weight before and after treatment with chromic acid the weight of the degradation layer (Figure 40; B & E) was determined. The weight of the degradation layer shows how soluble the materials are. If the degradation layer is heavier, the solubility of the materials is lower and *vice versa*. The difference between the weight of the samples at the start of the experiment and the weight after chromic acid treatment was determined. The average degradation depth can be calculated from this weight loss (Figure 40; A & E). Mean degradation depth shows how much of the material has degraded in relation to the entire material surface. The higher the degradation depth are the faster the material is degraded. After 14 days, the weight of Mg-Pure and Mg-2Ag differed remarkably. The weight of the degradation layer of Mg-10Gd was much higher than the one of Mg-Pure. There was no significant impact of cells on the degradation. The initial degradation depth of the Mg-10Gd samples was higher than that of Mg-Pure. However, the degradation rate of Mg-10Gd was from day 3 lower than the

degradation rate of Mg-Pure. Within the first 3 days Mg-10Gd thus has the largest degradation depth followed by Mg-2Ag and finally Mg-Pure. After the first 3 days, however, the pattern turns, so that Mg-10Gd has the lowest degradation rate, followed by Mg-Pure and Mg-2Ag. In addition, the experiment has shown that within the 28 days the cell layer has no significant influence on the degradation rate (Figure 40; C & F). However, as the difference in the degradation rate between with ad without cells generally increases over time, it can be assumed that the influence of the cells could be significant later.

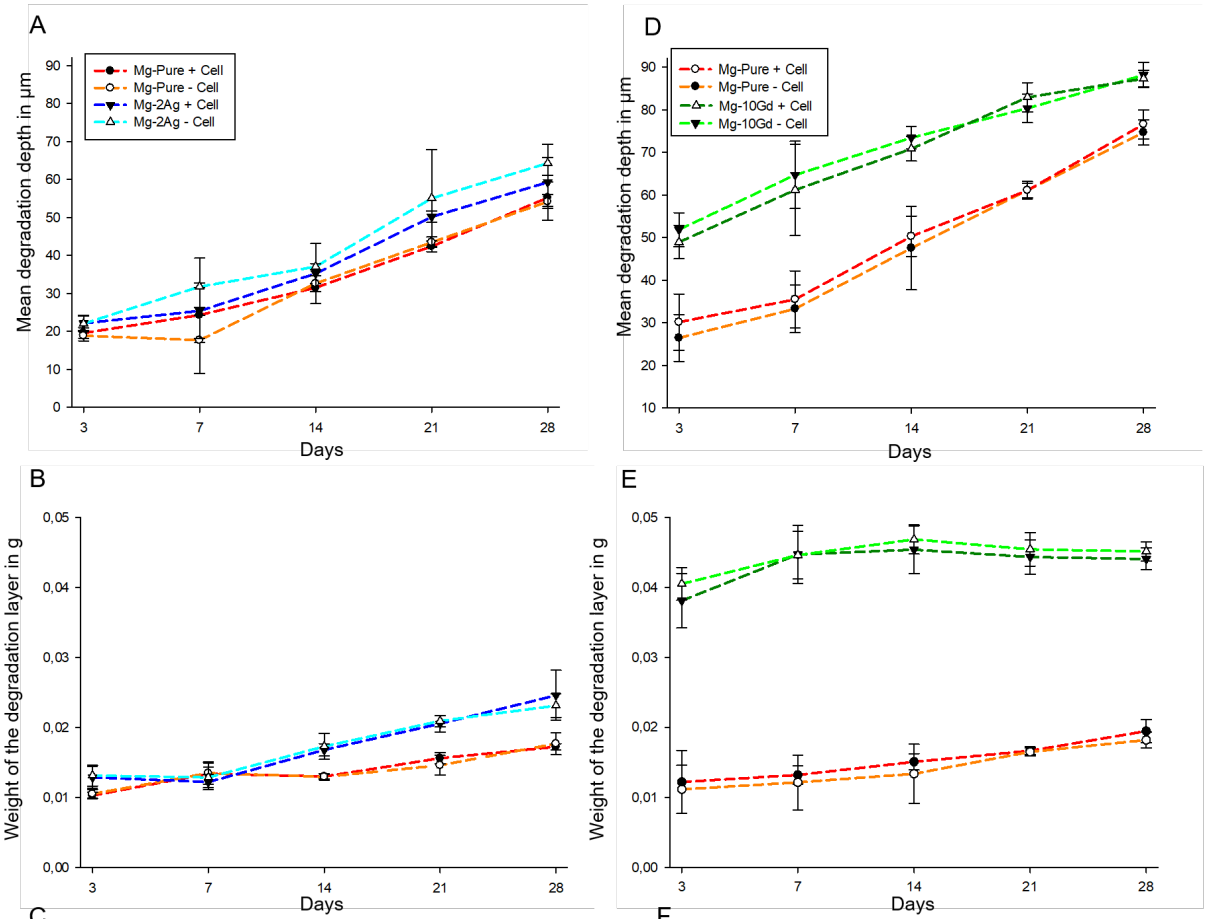

C

Degradation Rate in µm/day

Day	3	7	14	21	28
Mg-Pure + Cell	1.15 ± 0.08	1.15 ± 0.35	1.12 ± 0.04	1.21 ± 0.04	1.31 ± 0.14
Mg-Pure - Cell	1.34 ± 0.10	0.98 ± 0.48	1.30 ± 0.08	1.36 ± 0.04	1.39 ± 0.05
Mg-2Ag + Cell	1.19 ± 0.12	1.12 ± 0.32	1.19 ± 0.27	1.37 ± 0.04	1.36 ± 0.15
Mg-2Ag - Cell	1.08 ± 0.10	1.30 ± 0.31	1.18 ± 0.03	1.43 ± 0.33	1.41 ± 0.11

F

Degradation Rate in µm/day

Day	3	7	14	21	28
Mg-Pure + Cell	1.13 ± 0.25	1.16 ± 0.22	1.34 ± 0.13	1.37 ± 0.05	1.49 ± 0.07
Mg-Pure - Cell	1.14 ± 0.25	1.22 ± 0.21	1.39 ± 0.29	1.48 ± 0.04	1.55 ± 0.06
Mg-10Gd + Cell	0.89 ± 0.07	1.04 ± 0.18	1.07 ± 0.04	1.14 ± 0.05	1.09 ± 0.02
Mg-10Gd - Cell	1.01 ± 0.08	1.17 ± 0.14	1.18 ± 0.04	1.16 ± 0.05	1.16 ± 0.04

Figure 40: The difference (mass loss) was used to calculate the weight of the degradation layer and the mean degradation depth. A-C: Mg-Pure and Mg-2Ag; D-F: Mg-Pure and Mg-10Gd. A and D: Mean degradation depth; B and E: Weight of the degradation layer; C and F: Degradation rate (n=6) with standard deviation (SD).

5 Discussion

Frequently, to study bone tissue, either OB or OC are selected (using immortal cell lines or primary cells) or only one of the two cell types had a primary origin [194,195]. Only few studies could be found in which both cells had a primary origin. In one study the OB precursor were incubated for 14 days. Afterwards the OC precursors were seeded onto the formed OB cell layer [196]. In another study the precursors were incubated separately from each other and later combined into a coculture [197].

Here, coculture of PBMC and HUCPV cells has been established as a prerequisite for studying the influence of degradable magnesium alloys on the cells. In the experiments performed, the influence of degradation products on the communication between bone forming and bone resorbing cells and thus the influence of the materials on the balance of the cells and the influence on bone formation was investigated. HUCPV and PBMC fully differentiated into OB [198] and OC, respectively within 28 days. The demonstrated resorption activity of the OC showed that the self-differentiating coculture was successfully established. One major advantage of this coculture is the heterotypic contact of cells. This contact strongly influence and regulate the cells and is important for the bone homeostasis. Therefore, it can be used as model for cell communication. In addition, both cell types evolve from primary precursor cells (HUCPV and PBMC) to OB and OC. Thus, the influence of novel implant materials such as degradable biometals on their differentiation can also be shown.

5.1 Interfering effect of Gadolinium

For a suitable degradable metal-based material for bone implants, it is necessary to select a non-toxic, biocompatible alloy that does not degrade too fast in the body. As Mg alloys fulfil all these requirements, the degradable Mg alloys have recently been intensively investigated. The degradation rate of the Mg-10Gd alloy for example was studied in various *in vitro* immersion test settings. The degradation rate of Mg-10Gd was promising in all studies over 3 days [16], 10 days [199] and 1 to 4 weeks [173]. Over the culture period, Gd, whether as salt solution, as extract or as alloy, appeared to have a positive effect on the formation of HA. Since the staining has shown that HA only occurs in the direct neighbourhood of OB, it is most likely an OB driven process which is influenced by Gd. Indeed, as also observed in another study, an increased mineralization process was observed by OB [69]. The staining of the HA represents the activity of the OB, because HA is a calcium phosphate mineral, formed by OB in the early phase of bone growth [200]. The mechanisms behind the observed effect of Gd on the HA formation remain so far not fully understood. However, because it supports the formation of HA, as an

implant material it could reduce the time of bone healing. It is possible that Mg-10Gd or other Gd-alloys could also promote bone healing even in degenerative bone diseases.

Actually, Gd is known for blocking the voltage-dependent Ca channels at a certain concentration [201]. This effect has been demonstrated, for example, in the rat cell line G H4C1 between 0.5 and 5 µM Gd^{3+} [18] and in the human cell line tsA-201 between 1 and 0.1 µM Gd^{3+} [202]. Both studies showed a dose-dependent inhibitory effect on the voltage-dependent Ca channel. This inhibitory effect could be due to Gd (0.94 Å) having a comparable ionic radius to Ca (0.97 Å) one, but Gd has a higher positive charge. Thus, Gd could interact with the same binding sites than Ca and could alter Ca effect on enzyme activity or receptor binding [203,204].

The influence of Gd on *e.g.* OB was strongly time- and concentration-dependent. The Gd concentrations measured and applied in the indirect assays were much smaller (0.73 – 3.13 nM) than the concentrations necessary to block Ca channels (between 0.5 and 5 µM Gd^{3+}). In mouse OB, Gd initially has an inhibitory effect on the proliferation, differentiation and calcification of OB. Which turns positive at day 14 [153]. A study showed that Gd induced the highest *in vitro* viability at a concentration until 1 mM (approx. 120 % compare to untreated MG63) of MG63 cells compared to other rare earth elements. The viability decreased dramatically to 25 % at a concentration of 2 mM. Also other cell types like RAW264.7 and HUCPV were observed in this experiment, but the decrease of viability between 1 and 2 mM Gd was not observed with these cell types [19].

Even if Gd above a concentration of 0.5 µM blocks the voltage-dependent Ca channels, the indirect assay has shown that lower concentrations of Gd have a positive effect on OB and could therefore be used as an alloying element.

5.2 Cytotoxic effect of Silver

Ag is also an interesting alloying element for implant materials. Although MgAg (1.36 µm/day with cells at day 28; 1.41 µm/day without cells at day 28) usually degrades faster than MgGd (1.15 µm/day with cells at day 28; 1.10 µm/day without cells at day 28), Ag has antibacterial properties which could be very useful after surgery. However, Ag ions could exhibit a certain cytotoxic effect. A 50 % inhibition of the cell viability occurred at a concentration of 57 mM (OB) and 62 mM (OC) $AgNO_3$. However, a much higher concentration of Ag nanoparticles was required to inhibit the cell viability to the same level as $AgNO_3$ did [163]. Interestingly, in the primary human coculture of HUCPV and PBMC cells a very strong inhibition of the cells viability was already visible at quite low Ag concentrations ($AgNO_3$ = 3.42 nM, Mg-8Ag = 5.84 nM).

This effect may be related to the different species (differences between human and mouse) but also to the short incubation time in the mouse cell culture experiment (6 days). Within the first 7 days of the present experiments, the effects of $AgNO_3$ were also still moderate in the coculture. The strong inhibitory effect only reached a maximum after 14 to 21 days.

The negative effect of $AgNO_3$ is probably due to the Ag induced production of ROS, which supports mineralisation (*e.g.* below 0.3 mmol/L H_2O_2) [205] but only up to a certain level and then negatively affects cell viability [206,207].

The extracellular Ag ions enter the cell *via* various transporters. For example, the copper transporter 1 (CTR1) [156] and the divalent metal transporter (DMT1) [157] are responsible for maintaining the homeostasis of copper but can also transport Ag. These transporters are found in mesenchymal stem cells and could then influence the development of OB [208,209]. After Ag was carried by these transporters into the OB, Ag causes an increased ROS production in the mitochondria [158]. The released ROS do not only support the differentiation of mouse OB [21], but also promote the release of ALP [205,210]. Normally, ROS-mediated ALP production is triggered by phosphates, since P also leads to an increased ROS production and is provided by ALP for bone formation [211]. It is important at this point that the P provided by ALP form organophosphates (Figure 41) could be found in the vicinity of the matrix vesicles and be transported into these vesicles. Moreover, the P provided by ALP does not necessarily trigger a higher ALP expression [212]. Thus, MgAg alloys can also have a positive effect on bone formation through ALP.

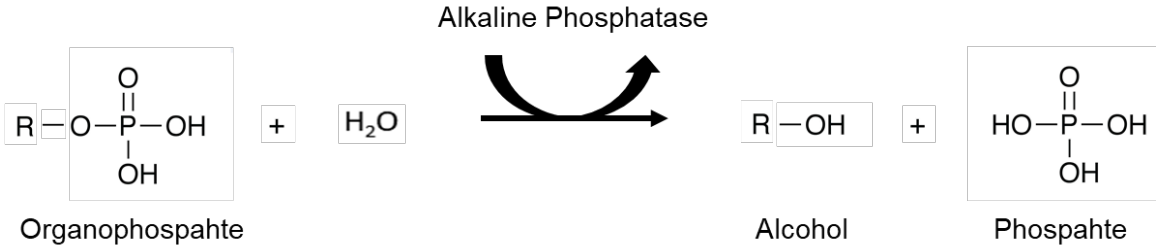

Figure 41: Cleavage of organophosphates by ALP.

Furthermore, the protein BMP2 induces the synthesis of ROS *via* the activation of NADPH oxidase 4 (NOX4). These ROS lead to the production of ALP *via* the PI3K pathway and SMAD5 pathway [213]. As Ag also leads to the production of ROS [214] it is likely that Ag also has a positive effect on bone formation *via* these pathways. Since the samples treated with Mg-8Ag showed quite high ALP activity, but a very low DNA content and viability, it can be assumed that the high Ag concentrations leads to a high ROS concentration, which finally has a negative effect on the cell viability [215].

Finally, higher OC resorption activity could be detected with Mg-Pure compared to MgAg treated samples. This is most likely due to the mentioned cytotoxic effect of Ag. The viability of the cells decreases with Mg-8Ag but with Mg-2Ag and Mg-4Ag more OC were identified [163]. Furthermore, it has already been shown in vivo that MgAg alloy inhibits the differentiation and function of osteoclasts [216,92].

5.3 Effect of materials on mineralisation

Remarkably, although the ALP activity was higher in all samples than in the control, only the samples treated with Gd showed a significant increase of HA formation (Ch. 4.2.1 Page 40; Ch. 4.2.2 Page 45; Ch. 4.2.3 Page 49; Ch. 4.2.5 Page 55). The addition of Mg and Ag seemed to support osteoblastogenesis by increasing ALP activity but inhibited or not influenced HA formation.

Like ALP, HA is more stable in a neutral or alkaline milieu. In an environment with lower pH, stability shifts in favour of other phosphate molecules [217]. HA ($Ca_5(PO_4)_3(OH)$) is stable in a pH range from ~5.5 to ~11. In a lower pH environment, other phosphate molecules such as octacalcium phosphate (pH ~ 5; $Ca_8(HPO_4)_2(PO_4) \times 5H_2O$) or monocalicum phosphate (pH < 3; $Ca(H_2PO_4)_2$) are formed. If the pH is higher, the phosphate molecule tricalcium phosphate (pH > 10; $Ca_4(PO_4)_2O$) is more likely to occur instead of HA.

In 1968 a publication determined the ratio of the mean ion radii of different ions for 75 natural and synthetic apatite species in order to be able to make predictions about the stability of the apatite structure with an almost unknown chemical composition [218]. The structure of the hydroxyapatite does not always have to be based on the same ions. An isomorphic replacement by other ions in the HA molecule is possible [219]. That this exchange is possible for different ions such as Na^+, Mg^{2+}, K^+, Sr^{2+}, Cu^{2+}, Zn^{2+}, Fe, Mn^{2+} and Al^{3+}, or anions like F^-, Cl^-, SO_4^{2-}, and CO_3^{2-} has been demonstrated in various studies [220,221]. Furthermore, the exchange potential of lanthanides (La^{3+}, Sm^{3+}, Gd^{3+}, Ho^{3+}, Yb^{3+} and Lu^{3+}) in the HA matrix was investigated [222]. It was shown that the binding constant for the exchange of lanthanoids into HA increases with decreasing ion size.

ALP is an essential factor for the calcification and the matrix vesicle formation [223]. Since Mg and Gd have a similar positive influence on ALP activity (Ag effect on ALP activity is lower), it is reasonable to assume that additional factors influenced the mineralisation. Gd may be embedded in the HA matrix instead of Ca in the second phase of the HA formation.

Since the calcification process is also Ca-dependent, it is possible that HA formation is supported by the higher positive charge of Gd [40]. The higher charge of Gd could lead to a stronger interaction with the enzyme BSP. Several studies have shown that BSP has a potent

influence on HA formation [224,225]. BSP seems to provide a flexible template for the rapid self-organisation of Ca and phosphate ions, thereby supporting the growth of HA crystals [226]. In the presence of 60 mM KCl (pH of solution 6.8), BSP can bind 83 Ca^{2+}/protein with a binding constant between 0.5 - 1.0 mM [227]. Furthermore, the binding properties of Ca^{2+} and Y^{3+} of BSP were investigated. It turned out that the Y^{3+} (0.1 mM YCl_3) bond to BSP was stronger than that of Ca^{2+} (40 mM $CaCl_2$) [228].

To identify the binding site of the ions, the cDNA of BSP from different mammals were studied. It was found that only 45% of the complete sequence matched, but conserved regions matched around 90%. These conserved regions consisted of two polyglutamic acid sequences, one arginine-glycine-aspartic acid sequence [229]. Aspartic acid and glutamic acid are the only amino acids that have a negative charge at a physiological pH. Replacing these conserved sequences led to a significant reduction in the formation of HA by BSP [225]. Since the activity of BSP seems to depend on the negatively charged amino acid sequences, and since BSP has been shown to interact with both Ca^{2+} and Y^{3+}, it is reasonable to assume that BSP also acts with other positive-charged ions such as Mg^{2+}, Ag^{+} and Gd^{3+} as it has a strong negative charge. The higher charge of Gd like yttrium could allow a strong interaction with BSP. This could also explain the increased deposition of Gd in the bone when Gd-based contrast agents are used [230] (Figure 42).

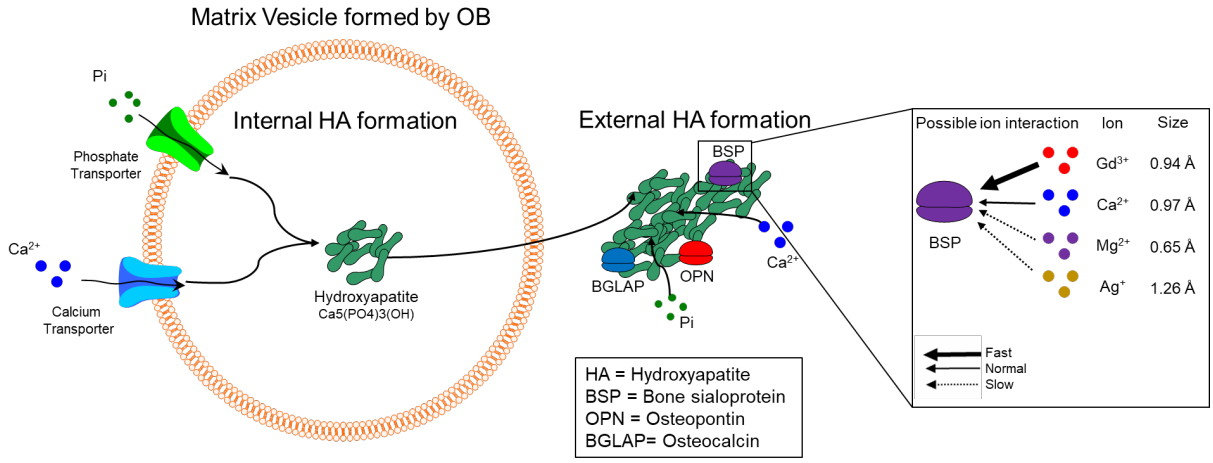

Figure 42: HA formation in- and outside of the matrix vesicle [40,203,204,223–225,229].

Another reason for the higher HA synthesis induced by Gd-containing cell culture medium solutions could be the positive charged Gd^{3+} forming a complex with the negatively charged phosphate molecules. Such complexes favour HA formation, additionally [231,40]. However, this process has only been shown in rats so far [232]. The phosphate is released from ATP by enzymes to form polyphosphate complexes and may interact with Gd.

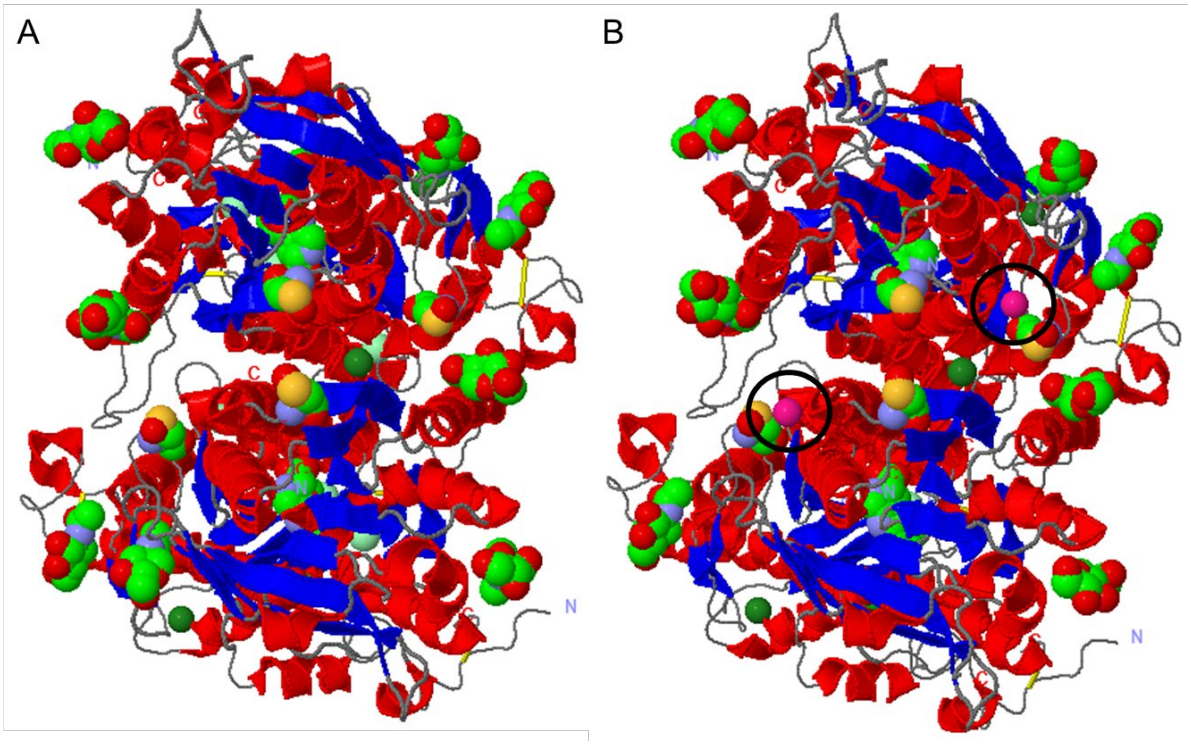

Figure 43: Crystal structure of the calcium sensing receptor protein from human (Jena Library) based on the work of Zhang et al. 2016 [233]. A is without ion binding. B is with Gd^{3+} binding (black circle).

The pronounced HA formation could also be a consequence of the activation of the CASR by Gd. The CASR is anchored in the cell membrane and has two lobes protruding into the extracellular space. This structure looks like a Venus flytrap and binds Ca or other ions with a double positive charge like Mg [234]. Several studies have shown that there are five calcium-binding sites on the surface of the two lobes, which consist of clusters of neutral and negatively charged amino acids [187,186,188]. Consequently, this receptor is specific for positive ions but not only for Ca. Alternatively, Gd has already been successfully used as an activator for this receptor [171]. Figure 43 shows the crystal structure of the CASR and the interaction of Gd with the receptor at tow locis. This demonstrates that Gd interacts with the CASR and can thus influence the activity of the CSAR. Furthermore the binding and activation of this receptor by Mg^{2+} have been proven [189,190]. The interaction is weaker compared to Ca, as shown by an induction of about half or two-third of the Ca signal intensity by Mg.

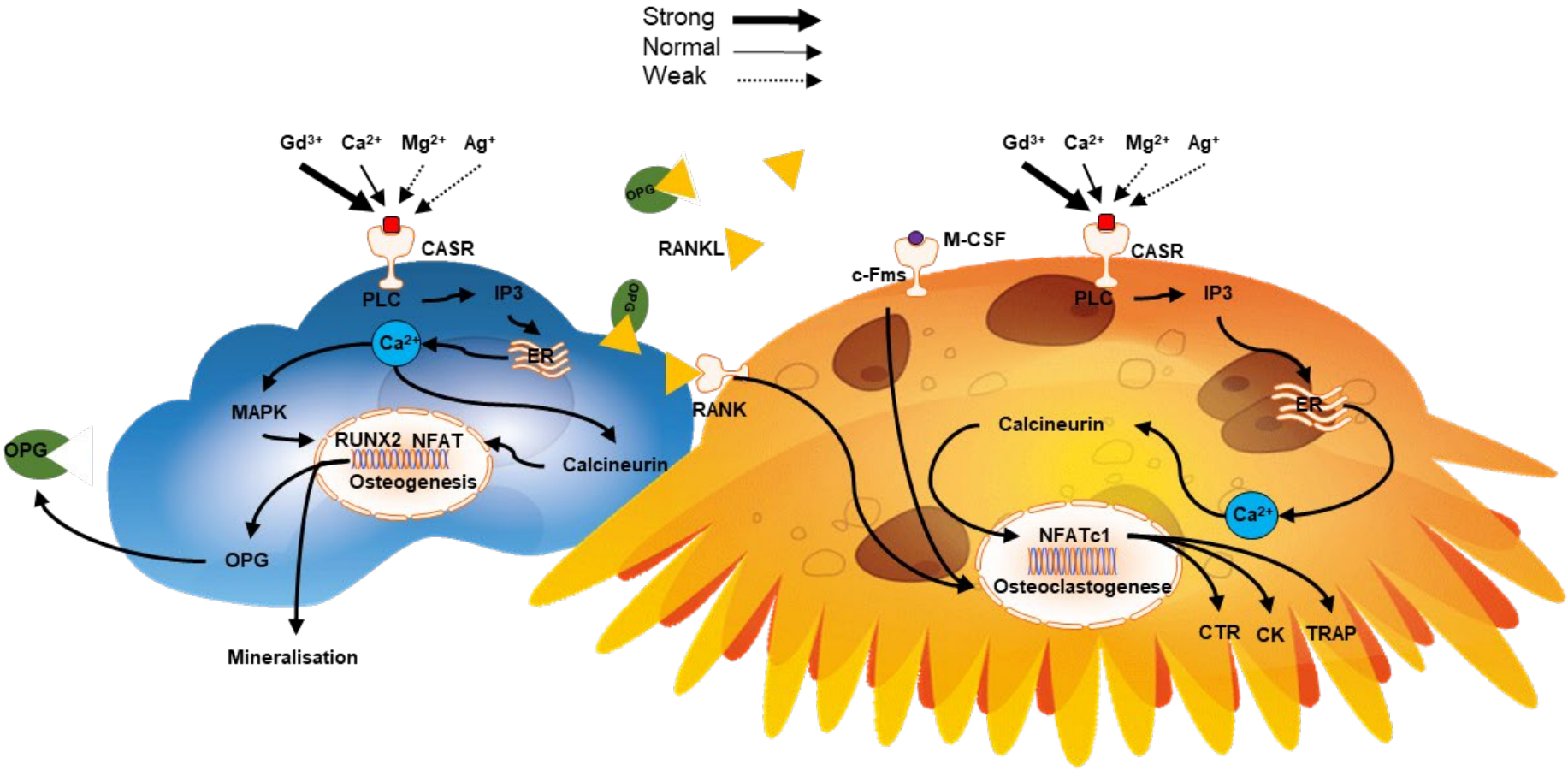

Figure 44: Examined pathways in the OB (blue) and OC (orange) influenced by the degradation products of Mg based alloys. *The arrows (with various thickness) show the possible interaction of the different ions with the CASR.*

Experiments on gene expression of CASR have shown that Mg and Gd have an activating effect on CASR (4.2.8 Page 65). Since CASR is triggered by a positive charge, this effect should be higher in cells cultured with Mg-10Gd extract. While Gd activates the CASR and Mg stimulates osteoblastogenesis *via* the TRPM7/PI3K pathway [235].

Furthermore, Ag^+ could also interact with the CASR, since the PLC inhibitor has a similar effect on the cocultures treated with Ag as on those treated with Mg. The effect of Ag on CASR could be due to the positive charge and equal ionic radius of Ag compared to Ca [203]. Thus, Ag may also reduce the formation of HA as Mg does (Mg smaller than Ca; Ag lower charge than Ca), *via* a weaker interaction with the CASR than Ca. The reduced HA formation could be demonstrated here in both treatments (Ag and Mg) and also the inhibitory effect of PLC-inhibitors on the CASR linked pathway was demonstrated *via* gene expression. However, the PLC inhibitor blocks every pathway in which the PLC is involved and not just the one at the beginning of the CASR cascade. The CASR mediated Ca release from the ER is supported by the calcium binding protein calmodulin (CaM), which is able to bind up to 4 Ca ions (Figure 44). One of the most common CaM binding partner is calcineurin. Calcineurin, dephosphorylates the nuclear factor of activated T cells (NFAT) present in the cytoplasm. This dephosphorylation translocate the NFAT into the cell nucleus and for example the expression of Wnt4 and Frizzled9 as well as decreased the expression of the Wnt inhibitors secreted frizzled-related protein 2 (sfrp2) and Dickkopf 2 (DKK2). This regulation induces the Wnt/Wingless pathway and has a positive influence on the OB differentiation [191].

Bone formation is not only influenced by CASR activation and the CASR is also involved in different cellular processes. Therefore, the resulting Ca cascade also activates the protein kinase C, which in turn leads to the expression of *RANKL* [192]. Consequently, the differentiation of OC is stimulated. This process is probably responsible for the higher TRAP activity in cell cocultures, which were exposed to the Mg-10Gd extract. Another possible pathway supporting OC differentiation is the Ca-dependent NFATC1 pathway. The CASR cascade activates the Ca-dependent proteins calmodulin and calcineurin. The activation of CaM leads *via* the calcium/calmodulin-dependent protein kinase II (CaMKII) to the activation of cFos and increases the expression of *NFATC1*. Calcineurin in combination with NFATC1 can activate genes relevant for osteoclastogenesis, such as TRAP, cathepsin K and OSCAR [236]. Another study also showed that the stimulatory effect of M-CSF is also Ca- and PLC dependent [237]. The complex pathways of these processes and the regulatory factors are illustrated in the extended Figure 45.

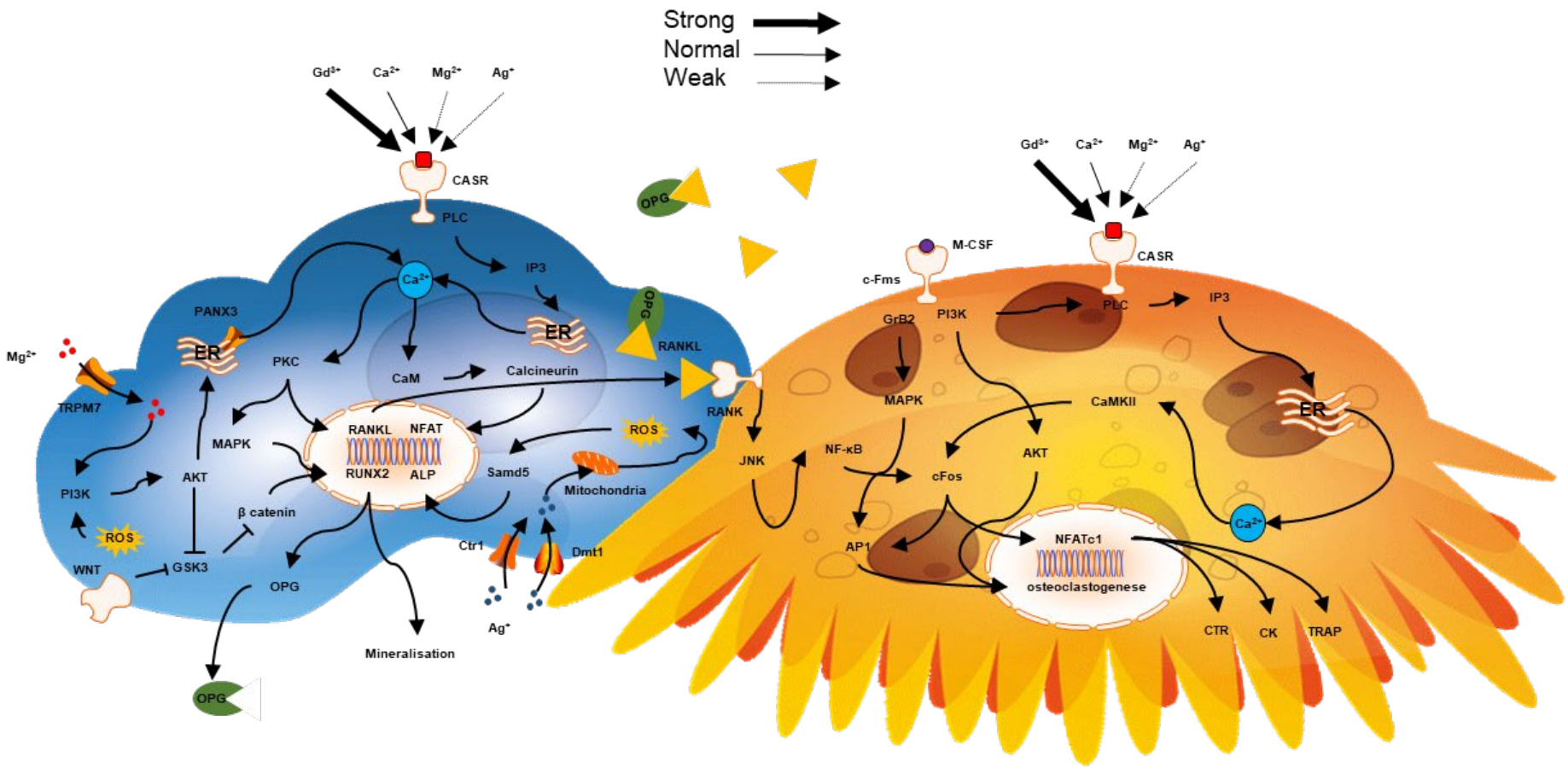

Figure 45: Possible pathways in OB (blue) and OC (orange) influenced by the degradation products of Mg based alloys. The arrows in the different strengths show the possible interaction of the different ions with the CASR. The arrows in the cells indicate the signalling pathways. Figure 44(measured pathways) is extended according to literature information [156–158,171,189–192,203,205,210,212,223,234–236,238–242].

Mg enters the cell *via* the TRPM7 channel and initiates a Ca cascade *via* PI3K and AKT (Protein kinase B) through Pannexin 3 [235,238]. Furthermore, AKT blocks glycogen synthase kinase-3 which otherwise ensures that β catenin remains in a phosphorylated stage. In a phosphorylated form, β catenin increases *RUNX2* expression and thus *ALP* expression [239,223]. The mobilised Ca^{2+} stimulate protein kinase C (PKC) and consequently influence the RUNX2 pathway in OB through MAPK [212]. The RUNX2 pathway regulates for example the *RANKL* and *OPG* expression [240]. Thus, it is also involved in the development of OC [192]. RUNX2 is considered as the master regulator of OB differentiation [243]. The qPCR analyses support this statement because the expression of the genes for OB development in the samples treated with $MgCl_2$ was upregulated in comparison to the extracts. On the other hand, $AgNO_3$ exhibited gene expressions that support the development of OB. However, these differences may also be due to the degradation products contained in the Mg extract or a combination of pH, osmolality and degradation products. The ALP activity measured in the $GdCl_3$ treated coculture was lower than in the samples treated with extracts and the expression of OC-related genes was higher, demonstrating the effect of pH or its synergistic effect in the extract.

The solutions of $MgCl_2$ and $GdCl_3$ seemed to have an inhibitory effect on the ALP activity. The analysis of qPCR showed that the genes for OC development were expressed higher in the samples treated with $MgCl_2$ and $GdCl_3$ than in the associated extracts. This effect did not occur when comparing $AgNO_3$ to Mg-6Ag. The measured ALP activity was higher for $AgNO_3$, but qPCR analyses showed that both treatments promoted OB development.

Compared to Mg-Pure, the samples treated with Mg-10Gd showed a trend to higher ALP activity (not significant). The positive effect of Gd on ALP activity was confirmed by the qPCR. Since Gd has a positive effect on the expression of *RUNX2*, it could also has a positive effect on the ALP expression *via* this pathway [244].

Although it is known that Ag stimulates ROS production and thus OC differentiation [241], the MgAg alloys appeared to have a negative effect on TRAP activity, which was confirmed by the qPCR results. The enzyme TRAP depends on the expression of *NFATC1* [242]. However, the *NFATC1* expression is often downregulated in all MgAg alloys treatments, but not with $AgNO_3$. Therefore, the alloys seemed to disturb the OC differentiation and thus the TRAP production as well as the associated resorption activity. An inhibited TRAP activity can also be seen in $MgCl_2$ and Mg-Pure extract treatments as already reported in a other study [245]. Therefore, it could be assumed that *NFATC1* was down regulated by the contained Mg and that the Ag had no additional effect. Table 11 gives a general overview of how the different salts and extracts affect the various aspects of the development and function of OB and OC.

Table 11: Summary of the impact of salts and extracts on the coculture (↑ elevated, ↓ attenuated, → balanced and empty for no results)

Process	**$MgCl_2$**	**Mg -Pure**	**$GdCl_3$**	**Mg5-Gd**	**Mg-10Gd**
Cell amount	↓	→	↓	→	→
Mitochondrial activity	→	↑	↑	↑	→
OC development gene level	→	→	↑		↑
OB development gene level	↑	→	→		↑
Mineralization ALP	↑	↑	→	→	↑
Mineralization HA	↓	↓	↑		↑
OC - TRAP	→	→	→	→	↑
Resorption activity		↑		↑	↑
Process	**$AgNO_3$**	**Mg-2Ag**	**Mg-4Ag**	**Mg-6Ag**	**Mg-8Ag**
Cell amount	↓	→	→	→	↓
Mitochondrial activity	↓	→	→	→	↓
OC development gene level	↑	↓	→	↑	
OB development gene level	↑	→	↓	↓	
Mineralization ALP	→	→	→	→	→
Mineralization HA	↓			↓	
OC - TRAP	→	→	→	↑	↓
Resorption activity		↓	↓	↓	↓

5.4 Differences between extracts and corresponding salt solutions

Although selecting the same ion concentrations, the studies showed differences between the extracts and the corresponding salt solutions, *e.g.* increased TRAP activity, or ALP activity in the presence of the solutions. These differences could be attributed to the difference in pH and osmolality between the media. It has already been shown that a rather acidic environment (pH 6.4 - 7.2) favours the development of OC and their activity. OC number and activity decrease at a higher pH (>7.5) [246]. OB on the other side prefer an alkaline pH [247]. In addition to the influence of pH, an osmolality increase in the cell culture medium can lead to a reduced protein synthesis [248]. It has been shown that an increase of 0.4 osmol/L is necessary to achieve an inhibition of protein synthesis 60 %. In a study with NaCl, an inhibition of protein synthesis was measured between 380 and 430 osmol/Kg [249]. Although the activity (WST assay) of the cells in the media with increased osmolality is also reduced in this study, the highest measured osmolality is 320 osmol/Kg and thus not yet in the range where an inhibition could be expected.

It should be mentioned that the added chloride ions by the $MgCl_2$ and $GdCl_3$ can be converted by monocytes [250] to hypochloric acid (HOCl) by the myeloperoxidase (MPO). HOCl has a higher reactivity than H_2O_2 [251,252]. Since HOCl belongs to the ROS, it also supports OC development. This could also explain the higher expression of *CTSK* and *NFATC1* in the presence of $MgCl_2$ compared to Mg-Pure treatment. This difference cannot be seen with $GdCl_3$ and Mg-10Gd because the amount of salt used of 3.14 nM (+0.0078 % Cl^- addition to medium) is much lower than the 10 mM $MgCl_2$ (+16.6 % Cl^- addition to medium). In addition to supporting osteoclastogenesis, HOCl formed by the PBMC could inhibit for example OB activity by inactivating various biomolecules like endothelial nitric oxide synthase (eNOS). HOCl chlorinates and thus deactivates the eNOS substrate L-arginine. This reduces OB activity, because eNOS have an essential role in OB activity regulation. [253,254]. This may also partly explain the reduced ALP activity and decreased gene expression in samples treated with $MgCl_2$. On the other side, MPO is supposed to hinder the differentiation of OC [255]. This would slow down the differentiation from PBMC to mature OC. This could explain why *NFATC1* from day 7 to day 21 is always lower for samples treated with $MgCl_2$ than for samples treated with Mg-Pure extract.

However, it is also possible that these differences are due to the degradation products contained in the Mg extract or a combination of the degradation products, pH and osmolality effects.

Mg from Mg based alloys dissolves in aqueous solution according to the following equations:

$$\text{Anodic reaction } Mg \rightarrow Mg^2 + 2e$$

$$\text{Cathodic reaction } 2H_2O + 2e \rightarrow H_2 + 2OH^-$$

The chloride ions (Cl^-) contained in the medium can react with $Mg(OH)_2$ and convert it into soluble $MgCl_2$. This can lead to an increase in OH^- ions, which in turn would increase the pH of the solution. This higher pH can also lead to a further solution of Mg by corroding of the $Mg(OH)_2$ protective layer [256]. If $PO4^-$ and Ca^{2+} are present in the solution, they can react with OH^- and form HA ($Ca_{10}(PO_4)_6(OH)_2$). However, these must be present in sufficient quantity to neutralize the inhibitory effect of Mg^{2+}, pyrophosphates and citrates on crystal formation [257–259] These degradation products have good biocompatibility and can promote osteoinductivity in pigs [172].

5.5 Impact of direct cell-material contact

The direct assay showed that the degradation of Mg-2Ag was very similar to that of Mg-Pure. Also other *in vivo* tests in rats have shown that the degradation rate of these two alloys is similar [173]. The implants (pins) were implanted in the femoral bones of each rat. Mg-Pure had a slightly higher degradation rate (0.4 mm/year) at the beginning (one week after surgery), but decreased to less than 0.2 mm/year in the 4th week. Mg-2Ag pin degraded in a rate of 0.2 mm/year at the beginning, then degradation rose to 0.3 mm/year in the 4th week. After 12 weeks both alloys had a degradation rate inferior to 0.2 mm/year. In the experiments it was observable that Mg-2Ag had a slightly higher influence on ALP activity than Mg-Pure, this could be attributed to higher ROS production.

The degradation rate of an element and its deposition in tissues depends on its intake way and its chemical form. For example, the Gd half-life of gadopentate-dimeglumin ($C_{28}H_{54}GdN_5O_{20}$) in the lungs of rats supplied as aerosol was 2.16 hours [260]. In another experiment, the degradation rate of $GdCl_3$ in rat lung was investigated. In contrast to gadopentate-dimeglumin, this compound was deposited in insoluble form in the lung and is metabolized very slowly with a half-life of 136 days [261].

The experiments to investigate the half-life of Gd in tissues have so far only been performed with single Gd treatment. The degradation experiments whereas show the influence of a continuous release of Gd to the body. Thus, no concrete statements can be made about the half-life of Gd from degradable Gd alloys in the body. However, in tissues which absorb less Gd (brain and muscle), a saturation curve seems to be visible [262].

Also the accumulation of Gd in the various tissues were studied [262]. The Sprague–Dawley® rats were implanted with Mg-10Gd implants (pins) and the individual organs were examined for their Mg and Gd concentration after 4, 12, 24 and 36 weeks. While Mg did not cause a significant change in concentration of the studied organs, there was an increase in Gd concentration in the brain, muscle, heart and kidney organs until week 24. Until week 36 the concentration fell again or did not increase significantly. In the tissues lung, liver and spleen the Gd also accumulated to 36w. After 36 weeks the brain showed the lowest accumulation of 1.1 ± 0.3 µg/kg wet mass. The highest concentration of Gd was measured in the spleen with 2000 ± 800 µg/kg moist mass.

It has been shown that Gd can be harmful to people with kidney disease [263]. This is probably attributable to the high accumulation of Gd in this organ. Gd chelates are used as a contrast agent for magnetic resonance imaging in a concentration of 0.03 – 0.10 mmol/L [264]. The contrast agents consist of complex Gd-containing molecules and, like Gd-ions, cannot easily

pass through the cell membrane. Even if Gd is present in the contrast media as complex, they degrade in an aqueous solution under UV radiation. As a result, only 3 % of the initial concentration of the contrast agent Gd-BOPTA remains, *e.g.* after 300 min [265].

The MAGNEZIX® CS 3.2 Mg screw from Syntellix (Hannover, Germany) weights about 150 mg [266]. An Mg-10Gd screw of similar weight would result in a 0.09 mM (150 mg Mg-10Gd = 135 mg magnesium (5,56 mM), 15 mg gadolinium (0,09 mM)) concentration in case of complete solubilisation and homogenous distribution. For Gd-based contrast agents a no-effect level are approved for a serum concentration of 0.1 mM. Table 12 shows exemplary the amount of Gd containing contrast agent needed for an MRI image of a 70 kg weighing Person and the corresponding amount of Mg-10Gd screws which would contain the same amount.

Table 12: Comparison of Gd amount in contrast agent and screw

Contrast agent	g/mol	Percentage of Gd	Gd amount in mmol for 70kg bodyweight person	Amount Gd of Mg-10Gd Screw in mM	Amount of screws for a 70kg Person
Gd BOPTA	667.72	23.55	1.10	0.09	11.54

Consequently, up to 11 screws would have to be used, which would also have to be completely degraded at the same moment to achieve the same concentration in the body like one MRI examination of the 70 kg person. However, since the screws are not immediately degraded, the Gd contained in the screw is released over a longer period of time, thus distributing the Gd load over a longer period of time. The ICP-MS analysis of the initial extract showed a Gd content of 3.4 mg/L, which corresponds to a concentration of 0.02 mmol/L which is already 5 times lower at the low volume than is used for contrast medium images.

As already mentioned, Gd showed positive properties on cell viability up to a certain concentration. At higher concentrations, however, it could block the voltage-dependent calcium channels and leads to cell death. In order to describe a first list of symptoms a survey on the self-described toxicity of patients in connection with Gadolinium-based contrast agent administration were performed. The following symptoms were most frequently described: Head/bone/joint pain, head/neck symptoms and hearing loss. As these are self-described symptoms, this description may be influenced by the subjective perception of the patients [267].

In addition to the mentioned study, other side effects of gadodiamide administration such as hypercalicemia at concentrations of 0.2 mmol/kg or higher (especially in people with renal insufficiency) have been observed [268]. However, administration of gadobenate dimeglumin

($C_{28}H_{54}GdN_5O_{20}$) to the brain of young rats in doses of 0.6, 1.25, 2.5 mmol/kg and 15 mmol/kg did not lead to adverse clinical effects [269].

To determine whether Gd favours the development of Parkinson's disease, a population-based study were conducted. This study included 246 557 patients who underwent at least one MRI examination during the study. Of these, 99,739 patients received at least one dose of gadolinium and 2446 patients received 4 or more. The study revealed that 1.17 % of gadolinium-exposed patients evolved a Parkinson's disease. However, Parkinson's was also diagnosed in 1.16 % of non-exposed patients. Thus, no significant association between Parkinson's disease and gadolinium exposure was found [270].

Thus, it has been proven that Gd is deposited in body tissues but so far, no serious side effects have been attributed to this deposition. In addition, it could be shown that the contained Gd, at least *in vitro*, has a positive effect on the formation of HA and thus seems to support bone formation.

5.6 Further work

This study has shown that Mg-alloys have positive effects *in vitro* especially on ALP activity or on the mineralisation in cocultures of OB and OC. It turned out one of the involved signalling pathways is related to the CASR receptor. Especially the use of Gd showed modulations of the mineralisation process. To observe a concentration-dependent influence of Gd, the experiments could be repeated with other Gd alloys. Furthermore, the influence of Gd on BSP should also be determined.

In order to investigate the influenced molecular pathways in a more comprehensive way, the influence of materials on TRPM7/PI3K and CaMKII pathways should be examined. This would allow to elucidate the synergistic effect of Mg and Gd on CASR and BSP.

Due to the ubiquitous occurrence and impact of ROS the influence on OB and OC. ROS production should be monitored while the cells are treated with the different alloys.

6 Conclusion

This study could show that the developed coculture is a useful tool to investigate a complex system. With this tool it could be shown that traces of gadolinium have a beneficial effect on hydroxyapatite formation and thus on new bone formation. Although magnesium has a positive effect on genes relevant for bone formation, no positive influence on the formation of hydroxyapatite could be observed. Also silver can have a positive effect on genes involved in bone formation, but the cytotoxic effect of silver has also been shown. For this reason, it would be interesting to investigate a combined alloy of magnesium, gadolinium and silver to exploit the combination of the positive properties of these materials and possibly counteract the negative effect of silver on cells. Should the combination of these materials work, the resulting implant would not only reduce postoperative infections, it would also support bone formation as well.

7 References

References

[1] O.S. Schindler, S.R. Cannon, T.W.R. Briggs, G.W. Blunn, Composite ceramic bone graft substitute in the treatment of locally aggressive benign bone tumours, Journal of orthopaedic surgery (Hong Kong) 16 (2008) 66–74 DOI:10.1177/230949900801600116.

[2] M. Hamadouche, A. Meunier, D.C. Greenspan, C. Blanchat, J.P. Zhong, G.P. La Torre, L. Sedel, Long-term in vivo bioactivity and degradability of bulk sol-gel bioactive glasses, J. Biomed. Mater. Res. 54 (2001) 560–566 DOI:10.1002/1097-4636(20010315)54:4<560:AID-JBM130>3.0.CO;2-J.

[3] C.K. Seal, K. Vince, M.A. Hodgson, Biodegradable surgical implants based on magnesium alloys – A review of current research, IOP Conf. Ser.: Mater. Sci. Eng. 4 (2009) 12011 DOI:10.1088/1757-899X/4/1/012011.

[4] I. Gotman, Characteristics of metals used in implants, Journal of endourology 11 (1997) 383–389 DOI:10.1089/end.1997.11.383.

[5] N. Sumitomo, K. Noritake, T. Hattori, K. Morikawa, S. Niwa, K. Sato, M. Niinomi, Experiment study on fracture fixation with low rigidity titanium alloy: Plate fixation of tibia fracture model in rabbit, Journal of materials science. Materials in medicine 19 (2008) 1581–1586 DOI:10.1007/s10856-008-3372-y.

[6] W.Z.W. Teo, P.C. Schalock, Metal Hypersensitivity Reactions to Orthopedic Implants, Dermatology and therapy 7 (2017) 53–64 DOI:10.1007/s13555-016-0162-1.

[7] L.S. Nair, C.T. Laurencin, Biodegradable polymers as biomaterials, Progress in Polymer Science 32 (2007) 762–798 DOI:10.1016/j.progpolymsci.2007.05.017.

[8] K.W.K. Yeung, K.H.M. Wong, Biodegradable metallic materials for orthopaedic implantations: A review, Technology and health care official journal of the European Society for Engineering and Medicine (2012) 345–362 DOI:10.3233/THC-2012-0685.

[9] M. Moravej, D. Mantovani, Biodegradable metals for cardiovascular stent application: interests and new opportunities, International journal of molecular sciences 12 (2011) 4250–4270 DOI:10.3390/ijms12074250.

[10] J.-M. Seitz, R. Eifler, F.-W. Bach, H.J. Maier, Magnesium degradation products: effects on tissue and human metabolism, J Biomed Mater Res A 102 (2014) 3744–3753 DOI:10.1002/jbm.a.35023.

[11] G. van Ooijen, J.S. O'Neill, Intracellular magnesium and the rhythms of life, Cell cycle (Georgetown, Tex.) 15 (2016) 2997–2998 DOI:10.1080/15384101.2016.1214030.

[12] S. Galli, M. Stocchero, M. Andersson, J. Karlsson, W. He, T. Lilin, A. Wennerberg, R. Jimbo, The effect of magnesium on early osseointegration in osteoporotic bone: A

histological and gene expression investigation, Osteoporosis international a journal established as result of cooperation between the European Foundation for Osteoporosis and the National Osteoporosis Foundation of the USA 28 (2017) 2195–2205 DOI:10.1007/s00198-017-4004-5.

[13] L. Wu, B.J.C. Luthringer, F. Feyerabend, A.F. Schilling, R. Willumeit, Effects of extracellular magnesium on the differentiation and function of human osteoclasts, Acta biomaterialia 10 (2014) 2843–2854 DOI:10.1016/j.actbio.2014.02.010.

[14] L.Y. He, X.M. Zhang, B. Liu, Y. Tian, W.H. Ma, Effect of magnesium ion on human osteoblast activity, Brazilian journal of medical and biological research = Revista brasileira de pesquisas medicas e biologicas 49 (2016) e5257 DOI:10.1590/1414-431X20165257.

[15] O. Charyeva, O. Dakischew, U. Sommer, C. Heiss, R. Schnettler, K.S. Lips, Biocompatibility of magnesium implants in primary human reaming debris-derived cells stem cells in vitro, Journal of orthopaedics and traumatology official journal of the Italian Society of Orthopaedics and Traumatology 17 (2016) 63–73 DOI:10.1007/s10195-015-0364-9.

[16] F. Cecchinato, N.A. Agha, A.H. Martinez-Sanchez, B.J.C. Luthringer, F. Feyerabend, R. Jimbo, R. Willumeit-Römer, A. Wennerberg, Influence of Magnesium Alloy Degradation on Undifferentiated Human Cells, PloS one 10 (2015) e0142117 DOI:10.1371/journal.pone.0142117.

[17] M. Rogosnitzky, S. Branch, Gadolinium-based contrast agent toxicity: A review of known and proposed mechanisms, Biometals an international journal on the role of metal ions in biology, biochemistry, and medicine 29 (2016) 365–376 DOI:10.1007/s10534-016-9931-7.

[18] B.A. Biagi, J.J. Enyeart, Gadolinium blocks low- and high-threshold calcium currents in pituitary cells, The American journal of physiology 259 (1990) C515-20 DOI:10.1152/ajpcell.1990.259.3.C515.

[19] F. Feyerabend, J. Fischer, J. Holtz, F. Witte, R. Willumeit, H. Drücker, C. Vogt, N. Hort, Evaluation of short-term effects of rare earth and other elements used in magnesium alloys on primary cells and cell lines, Acta biomaterialia 6 (2010) 1834–1842 DOI:10.1016/j.actbio.2009.09.024.

[20] H.M. Frost, Skeletal structural adaptations to mechanical usage (SATMU): 2. Redefining Wolff's law: the remodeling problem, The Anatomical record 226 (1990) 414–422 DOI:10.1002/ar.1092260403.

[21] X. Feng, Chemical and Biochemical Basis of Cell-Bone Matrix Interaction in Health and Disease, Current chemical biology 3 (2009) 189–196 DOI:10.2174/187231309788166398.

[22] S.-F. Zhao, Q.-H. Jiang, S. Peel, X.-X. Wang, F.-M. He, Effects of magnesium-substituted nanohydroxyapatite coating on implant osseointegration, Clinical oral implants research 24 Suppl A100 (2013) 34–41 DOI:10.1111/j.1600-0501.2011.02362.x.

[23] Seibel M.J., Robins S.P., and Bilezikian J.P., Markers of Bone Metabolism, in: G.M. Moldenhauer (Ed.), Principles and practice of endocrinology and metabolism, Wolters Kluwer Health, Philadelphia, PA, 2002, pp. 1543–1571.

[24] H. Hsu, D.L. Lacey, C.R. Dunstan, I. Solovyev, A. Colombero, E. Timms, H.L. Tan, G. Elliott, M.J. Kelley, I. Sarosi, L. Wang, X.Z. Xia, R. Elliott, L. Chiu, T. Black, S. Scully, C. Capparelli, S. Morony, G. Shimamoto, M.B. Bass, W.J. Boyle, Tumor necrosis factor receptor family member RANK mediates osteoclast differentiation and activation induced by osteoprotegerin ligand, Proceedings of the National Academy of Sciences of the United States of America 96 (1999) 3540–3545.

[25] M.C. Chapuy, M.E. Arlot, F. Duboeuf, J. Brun, B. Crouzet, S. Arnaud, P.D. Delmas, P.J. Meunier, Vitamin D3 and calcium to prevent hip fractures in the elderly women, The New England journal of medicine 327 (1992) 1637–1642 DOI:10.1056/NEJM199212033272305.

[26] K.E.S. Poole, J. Reeve, Parathyroid hormone - a bone anabolic and catabolic agent, Current opinion in pharmacology 5 (2005) 612–617 DOI:10.1016/j.coph.2005.07.004.

[27] J. Wang, J. Zhou, C.M. Cheng, J.J. Kopchick, C.A. Bondy, Evidence supporting dual, IGF-I-independent and IGF-I-dependent, roles for GH in promoting longitudinal bone growth, The Journal of endocrinology 180 (2004) 247–255 DOI:10.1677/joe.0.1800247.

[28] R.S. Weinstein, R.L. Jilka, A.M. Parfitt, S.C. Manolagas, Inhibition of osteoblastogenesis and promotion of apoptosis of osteoblasts and osteocytes by glucocorticoids. Potential mechanisms of their deleterious effects on bone, The Journal of clinical investigation 102 (1998) 274–282 DOI:10.1172/JCI2799.

[29] N. Udagawa, N. Takahashi, T. Akatsu, H. Tanaka, T. Sasaki, T. Nishihara, T. Koga, T.J. Martin, T. Suda, Origin of osteoclasts: mature monocytes and macrophages are capable of differentiating into osteoclasts under a suitable microenvironment prepared by bone marrow-derived stromal cells, Proceedings of the National Academy of Sciences of the United States of America 87 (1990) 7260–7264.

[30] L.C. Hofbauer, D.L. Lacey, C.R. Dunstan, T.C. Spelsberg, B.L. Riggs, S. Khosla, Interleukin-1beta and tumor necrosis factor-alpha, but not interleukin-6, stimulate

osteoprotegerin ligand gene expression in human osteoblastic cells, Bone 25 (1999) 255–259.

[31] J. Aubin, Lian J.B., Stein G.S., Bone formation: maturation and functional activities of osteoblast lineage cells., in: M.J. Favus (Ed.), Primer on the metabolic bone diseases and disorders of mineral metabolism: An official publication of the American Society for Bone and Mineral Research, 6th ed., American Society for Bone and Mineral Research, Washington, 2006, pp. 20–29.

[32] N.H. Hart, S. Nimphius, T. Rantalainen, A. Ireland, A. Siafarikas, R.U. Newton, Mechanical basis of bone strength: influence of bone material, bone structure and muscle action, Journal of Musculoskeletal & Neuronal Interactions 17 (2017) 114–139.

[33] M. Centrella, T.L. McCarthy, E. Canalis, Transforming growth factor-beta and remodeling of bone, The Journal of bone and joint surgery. American volume 73 (1991) 1418–1428.

[34] S.E. Harris, M.A. Harris, P. Mahy, J. Wozney, J.Q. Feng, G.R. Mundy, Expression of bone morphogenetic protein messenger RNAs by normal rat and human prostate and prostate cancer cells, The Prostate 24 (1994) 204–211.

[35] S. Vukicevic, V. Latin, P. Chen, R. Batorsky, A.H. Reddi, T.K. Sampath, Localization of osteogenic protein-1 (bone morphogenetic protein-7) during human embryonic development: high affinity binding to basement membranes, Biochemical and biophysical research communications 198 (1994) 693–700 DOI:10.1006/bbrc.1994.1100.

[36] S. Vukicevic, V.M. Paralkar, N.S. Cunningham, J.S. Gutkind, A.H. Reddi, Autoradiographic localization of osteogenin binding sites in cartilage and bone during rat embryonic development, Developmental biology 140 (1990) 209–214.

[37] D.J. Hadjidakis, I.I. Androulakis, Bone remodeling, Annals of the New York Academy of Sciences 1092 (2006) 385–396 DOI:10.1196/annals.1365.035.

[38] K. Nakashima, X. Zhou, G. Kunkel, Z. Zhang, J.M. Deng, R.R. Behringer, B. de Crombrugghe, The novel zinc finger-containing transcription factor osterix is required for osteoblast differentiation and bone formation, Cell 108 (2002) 17–29 DOI:10.1016/s0092-8674(01)00622-5.

[39] R. Garimella, X. Bi, H.C. Anderson, N.P. Camacho, Nature of phosphate substrate as a major determinant of mineral type formed in matrix vesicle-mediated in vitro mineralization: An FTIR imaging study, Bone 38 (2006) 811–817 DOI:10.1016/j.bone.2005.11.027.

[40] H.C. Anderson, Molecular biology of matrix vesicles, Clinical orthopaedics and related research (1995) 266–280.

[41] W. Zhao, M.H. Byrne, B.F. Boyce, S.M. Krane, Bone resorption induced by parathyroid hormone is strikingly diminished in collagenase-resistant mutant mice, The Journal of clinical investigation 103 (1999) 517–524 DOI:10.1172/JCI5481.

[42] S.L. Teitelbaum, Bone resorption by osteoclasts, Science (New York, N.Y.) 289 (2000) 1504–1508.

[43] J. Rubin, E.M. Greenfield, Osteoclast: Origin and Differentiation, in: F. Bronner, M.C. Farach-Carson, J. Rubin (Eds.), Bone Resorption, Springer-Verlag London Limited, London, 2005, pp. 1–23.

[44] H.K. Väänänen, H. Zhao, M. Mulari, J.M. Halleen, The cell biology of osteoclast function, Journal of cell science 113 (Pt 3) (2000) 377–381.

[45] G.D. Roodman, Cell biology of the osteoclast, Experimental Hematology 27 (1999) 1229–1241 DOI:10.1016/S0301-472X(99)00061-2.

[46] D.L. Lacey, E. Timms, H.L. Tan, M.J. Kelley, C.R. Dunstan, T. Burgess, R. Elliott, A. Colombero, G. Elliott, S. Scully, H. Hsu, J. Sullivan, N. Hawkins, E. Davy, C. Capparelli, A. Eli, Y.X. Qian, S. Kaufman, I. Sarosi, V. Shalhoub, G. Senaldi, J. Guo, J. Delaney, W.J. Boyle, Osteoprotegerin ligand is a cytokine that regulates osteoclast differentiation and activation, Cell 93 (1998) 165–176.

[47] E. Jimi, I. Nakamura, T. Ikebe, S. Akiyama, N. Takahashi, T. Suda, Activation of NF-kappaB is involved in the survival of osteoclasts promoted by interleukin-1, The Journal of biological chemistry 273 (1998) 8799–8805 DOI:10.1074/jbc.273.15.8799.

[48] A.P. Armstrong, M.E. Tometsko, M. Glaccum, C.L. Sutherland, D. Cosman, W.C. Dougall, A RANK/TRAF6-dependent signal transduction pathway is essential for osteoclast cytoskeletal organization and resorptive function, The Journal of biological chemistry 277 (2002) 44347–44356 DOI:10.1074/jbc.M202009200.

[49] E. Jimi, I. Nakamura, L.T. Duong, T. Ikebe, N. Takahashi, G.A. Rodan, T. Suda, Interleukin 1 induces multinucleation and bone-resorbing activity of osteoclasts in the absence of osteoblasts/stromal cells, Experimental cell research 247 (1999) 84–93 DOI:10.1006/excr.1998.4320.

[50] W.L. Ries, M.C. Seeds, L.L. Key, Interleukin-2 stimulates osteoclastic activity: increased acid production and radioactive calcium release, Journal of periodontal research 24 (1989) 242–246 DOI:10.1111/j.1600-0765.1989.tb01788.x.

[51] E. Lubberts, L.A.B. Joosten, M. Chabaud, L. van den Bersselaar, B. Oppers, C.J.J. Coenen-de Roo, C.D. Richards, P. Miossec, W.B. van den Berg, IL-4 gene therapy for collagen arthritis suppresses synovial IL-17 and osteoprotegerin ligand and prevents bone erosion, The Journal of clinical investigation 105 (2000) 1697–1710.

[52] D.L. Lacey, J.M. Erdmann, S.L. Teitelbaum, H.L. Tan, J. Ohara, A. Shioi, Interleukin 4, interferon-gamma, and prostaglandin E impact the osteoclastic cell-forming potential of murine bone marrow macrophages, Endocrinology 136 (1995) 2367–2376 DOI:10.1210/endo.136.6.7750457.

[53] A.C. Bendixen, N.K. Shevde, K.M. Dienger, T.M. Willson, C.D. Funk, J.W. Pike, IL-4 inhibits osteoclast formation through a direct action on osteoclast precursors via peroxisome proliferator-activated receptor γ1, Proceedings of the National Academy of Sciences of the United States of America 98 (2001) 2443–2448 DOI:10.1073/pnas.041493198.

[54] W. Wiktor-Jedrzejczak, A. Bartocci, A.W. Ferrante, A. Ahmed-Ansari, K.W. Sell, J.W. Pollard, E.R. Stanley, Total absence of colony-stimulating factor 1 in the macrophage-deficient osteopetrotic (op/op) mouse, Proceedings of the National Academy of Sciences of the United States of America 87 (1990) 4828–4832.

[55] Y.Y. Kong, H. Yoshida, I. Sarosi, H.L. Tan, E. Timms, C. Capparelli, S. Morony, A.J. Oliveira-dos-Santos, G. Van, A. Itie, W. Khoo, A. Wakeham, C.R. Dunstan, D.L. Lacey, T.W. Mak, W.J. Boyle, J.M. Penninger, OPGL is a key regulator of osteoclastogenesis, lymphocyte development and lymph-node organogenesis, Nature 397 (1999) 315–323 DOI:10.1038/16852.

[56] L.C. Hofbauer, M. Schoppet, Clinical implications of the osteoprotegerin/RANKL/RANK system for bone and vascular diseases, JAMA 292 (2004) 490–495 DOI:10.1001/jama.292.4.490.

[57] W.S. Simonet, D.L. Lacey, C.R. Dunstan, M. Kelley, M.S. Chang, R. Lüthy, H.Q. Nguyen, S. Wooden, L. Bennett, T. Boone, G. Shimamoto, M. DeRose, R. Elliott, A. Colombero, H.L. Tan, G. Trail, J. Sullivan, E. Davy, N. Bucay, L. Renshaw-Gegg, T.M. Hughes, D. Hill, W. Pattison, P. Campbell, S. Sander, G. Van, J. Tarpley, P. Derby, R. Lee, W.J. Boyle, Osteoprotegerin: a novel secreted protein involved in the regulation of bone density, Cell 89 (1997) 309–319.

[58] E.M. Sordillo, R.N. Pearse, RANK-Fc: a therapeutic antagonist for RANK-L in myeloma, Cancer 97 (2003) 802–812 DOI:10.1002/cncr.11134.

[59] T. Negishi-Koga, H. Takayanagi, Bone cell communication factors and Semaphorins, BoneKEy Reports 1 (2012) 183 DOI:10.1038/bonekey.2012.183.

[60] K. Redlich, J.S. Smolen, Inflammatory bone loss: pathogenesis and therapeutic intervention, Nature reviews Drug discovery 11 (2012) 234–250 DOI:10.1038/nrd3669.

[61] T.A. Einhorn, R.J. Majeska, E.B. Rush, P.M. Levine, M.C. Horowitz, The expression of cytokine activity by fracture callus, Journal of Bone and Mineral Research 10 (1995) 1272–1281.

[62] L.J. Raggatt, N.C. Partridge, Cellular and molecular mechanisms of bone remodeling, The Journal of biological chemistry 285 (2010) 25103–25108 DOI:10.1074/jbc.R109.041087.

[63] P. Honegger, Overview of cell and tissue culture techniques, Current protocols in pharmacology Chapter 12 (2001) Unit12.1 DOI:10.1002/0471141755.ph1201s04.

[64] Jakoby, W.B. and Pastan, I.H., Methods Enzymology. Cell Culture, Academic, New York, 1979 ISBN: 0121819582.

[65] H.I. Cheong, J. Johnson, M. Cormier, K. Hosseini, In vitro cytotoxicity of eight beta-blockers in human corneal epithelial and retinal pigment epithelial cell lines: Comparison with epidermal keratinocytes and dermal fibroblasts, Toxicology in vitro an international journal published in association with BIBRA 22 (2008) 1070–1076 DOI:10.1016/j.tiv.2008.01.013.

[66] E. Soheili M., M. Goldberg, L. Stanislawski, In vitro effects of ascorbate and Trolox on the biocompatibility of dental restorative materials, Biomaterials 24 (2003) 3–9 DOI:10.1016/S0142-9612(02)00221-1.

[67] J. Fischer, D. Pröfrock, N. Hort, R. Willumeit, F. Feyerabend, Improved cytotoxicity testing of magnesium materials, Materials Science and Engineering: B 176 (2011) 830–834 DOI:10.1016/j.mseb.2011.04.008.

[68] X. Gu, Y. Zheng, Y. Cheng, S. Zhong, T. Xi, In vitro corrosion and biocompatibility of binary magnesium alloys, Biomaterials 30 (2009) 484–498 DOI:10.1016/j.biomaterials.2008.10.021.

[69] N. Ahmad Agha, R. Willumeit-Römer, D. Laipple, B. Luthringer, F. Feyerabend, The Degradation Interface of Magnesium Based Alloys in Direct Contact with Human Primary Osteoblast Cells, PloS one 11 (2016) e0157874 DOI:10.1371/journal.pone.0157874.

[70] M.S. Sader, R.Z. Legeros, G.A. Soares, Human osteoblasts adhesion and proliferation on magnesium-substituted tricalcium phosphate dense tablets, Journal of materials science. Materials in medicine 20 (2009) 521–527 DOI:10.1007/s10856-008-3610-3.

[71] Y.L. Cai, J.J. Zhang, S. Zhang, S.S. Venkatraman, X.T. Zeng, H.J. Du, D. Mondal, Osteoblastic cell response on fluoridated hydroxyapatite coatings: The effect of magnesium incorporation, Biomedical materials (Bristol, England) 5 (2010) 54114 DOI:10.1088/1748-6041/5/5/054114.

[72] Y. Yamasaki, Y. Yoshida, M. Okazaki, A. Shimazu, T. Uchida, T. Kubo, Y. Akagawa, Y. Hamada, J. Takahashi, N. Matsuura, Synthesis of functionally graded MgCO3 apatite accelerating osteoblast adhesion, J. Biomed. Mater. Res. 62 (2002) 99–105 DOI:10.1002/jbm.10220.

7 References

[73] H. Zreiqat, C.R. Howlett, A. Zannettino, P. Evans, G. Schulze-Tanzil, C. Knabe, M. Shakibaei, Mechanisms of magnesium-stimulated adhesion of osteoblastic cells to commonly used orthopaedic implants, J. Biomed. Mater. Res. 62 (2002) 175–184 DOI:10.1002/jbm.10270.

[74] A. Burmester, R. Willumeit-Römer, F. Feyerabend, Behavior of bone cells in contact with magnesium implant material, Journal of biomedical materials research. Part B, Applied biomaterials 105 (2017) 165–179 DOI:10.1002/jbm.b.33542.

[75] H.-S. Wang, S.-C. Hung, S.-T. Peng, C.-C. Huang, H.-M. Wei, Y.-J. Guo, Y.-S. Fu, M.-C. Lai, C.-C. Chen, Mesenchymal stem cells in the Wharton's jelly of the human umbilical cord, Stem cells (Dayton, Ohio) 22 (2004) 1330–1337 DOI:10.1634/stemcells.2004-0013.

[76] Z. Li, C. Liu, Z. Xie, P. Song, R.C.H. Zhao, L. Guo, Z. Liu, Y. Wu, Epigenetic dysregulation in mesenchymal stem cell aging and spontaneous differentiation, PloS one 6 (2011) e20526 DOI:10.1371/journal.pone.0020526.

[77] N. Zebardast, D. Lickorish, J.E. Davies, Human umbilical cord perivascular cells (HUCPVC): A mesenchymal cell source for dermal wound healing, Organogenesis 6 (2010) 197–203 DOI:10.4161/org.6.4.12393.

[78] J.B. Park, J.D. Bronzino, Biomaterials: Principles and applications, CRC Press, Boca Raton, 2002 ISBN: 0849314917.

[79] R. Sarugaser, L. Hanoun, A. Keating, W.L. Stanford, J.E. Davies, Human mesenchymal stem cells self-renew and differentiate according to a deterministic hierarchy, PloS one 4 (2009) e6498 DOI:10.1371/journal.pone.0006498.

[80] S. Kajiyama, Y. Ujiie, S. Nishikawa, K. Inoue, S. Shirakawa, N. Hanada, R. Liddell, J.E. Davies, K. Gomi, Bone formation by human umbilical cord perivascular cells, J Biomed Mater Res A 103 (2015) 2807–2814 DOI:10.1002/jbm.a.35396.

[81] P. Liu, B.O. Oyajobi, R.G. Russell, A. Scutt, Regulation of osteogenic differentiation of human bone marrow stromal cells: interaction between transforming growth factor-beta and 1,25(OH)(2) vitamin D(3) In vitro, Calcified tissue international 65 (1999) 173–180 DOI:10.1007/s002239900678.

[82] J.S. Adams, M. Hewison, Update in vitamin D, The Journal of clinical endocrinology and metabolism 95 (2010) 471–478 DOI:10.1210/jc.2009-1773.

[83] S. Geng, S. Zhou, Z. Bi, J. Glowacki, Vitamin D metabolism in human bone marrow stromal (mesenchymal stem) cells, Metabolism: clinical and experimental 62 (2013) 768–777 DOI:10.1016/j.metabol.2013.01.003.

[84] A. Parfitt, The physiologic and clinical significance of bone histomorphometric data. Bone Histomorphometry: Techniques and Interpretation 1983 143–223.

[85] H. Yasuda, N. Shima, N. Nakagawa, K. Yamaguchi, M. Kinosaki, S. Mochizuki, A. Tomoyasu, K. Yano, M. Goto, A. Murakami, E. Tsuda, T. Morinaga, K. Higashio, N. Udagawa, N. Takahashi, T. Suda, Osteoclast differentiation factor is a ligand for osteoprotegerin/osteoclastogenesis-inhibitory factor and is identical to TRANCE/RANKL, Proceedings of the National Academy of Sciences of the United States of America 95 (1998) 3597–3602.

[86] G.C. Nicholson, M. Malakellis, F.M. Collier, P.U. Cameron, W.R. Holloway, T.J. Gough, C. Gregorio-King, M.A. Kirkland, D.E. Myers, Induction of osteoclasts from CD14-positive human peripheral blood mononuclear cells by receptor activator of nuclear factor kappaB ligand (RANKL), Clinical science (London, England 1979) 99 (2000) 133–140.

[87] J. Costa-Rodrigues, A. Fernandes, M.H. Fernandes, Spontaneous and induced osteoclastogenic behaviour of human peripheral blood mononuclear cells and their CD14(+) and CD14(-) cell fractions, Cell proliferation 44 (2011) 410–419 DOI:10.1111/j.1365-2184.2011.00768.x.

[88] M. Susa, N.-H. Luong-Nguyen, D. Cappellen, N. Zamurovic, R. Gamse, Human primary osteoclasts: In vitro generation and applications as pharmacological and clinical assay, Journal of translational medicine 2 (2004) 6 DOI:10.1186/1479-5876-2-6.

[89] A. Hammerl, C.E. Diaz Cano, E.M. De-Juan-Pardo, M. van Griensven, P.S.P. Poh, A Growth Factor-Free Co-Culture System of Osteoblasts and Peripheral Blood Mononuclear Cells for the Evaluation of the Osteogenesis Potential of Melt-Electrowritten Polycaprolactone Scaffolds, International journal of molecular sciences 20 (2019) 1068 DOI:10.3390/ijms20051068.

[90] A. Klinder, A. Seyfarth, D. Hansmann, R. Bader, A. Jonitz-Heincke, Inflammatory Response of Human Peripheral Blood Mononuclear Cells and Osteoblasts Incubated With Metallic and Ceramic Submicron Particles, Frontiers in immunology 9 (2018) 831 DOI:10.3389/fimmu.2018.00831.

[91] D. Maradze, D. Musson, Y. Zheng, J. Cornish, M. Lewis, Y. Liu, High Magnesium Corrosion Rate has an Effect on Osteoclast and Mesenchymal Stem Cell Role During Bone Remodelling, Scientific reports 8 (2018) 10003 DOI:10.1038/s41598-018-28476-w.

[92] L. Wu, F. Feyerabend, A.F. Schilling, R. Willumeit-Römer, B.J.C. Luthringer, Effects of extracellular magnesium extract on the proliferation and differentiation of human osteoblasts and osteoclasts in coculture, Acta biomaterialia 27 (2015) 294–304 DOI:10.1016/j.actbio.2015.08.042.

[93] A.F. Schilling, S. Filke, S. Brink, H. Korbmacher, M. Amling, J.M. Rueger, Osteoclasts and Biomaterials, Eur J Trauma 32 (2006) 107–113 DOI:10.1007/s00068-006-6043-1.

[94] F. Tortelli, N. Pujic, Y. Liu, N. Laroche, L. Vico, R. Cancedda, Osteoblast and osteoclast differentiation in an in vitro three-dimensional model of bone, Tissue engineering. Part A 15 (2009) 2373–2383 DOI:10.1089/ten.tea.2008.0501.

[95] G.L. Jones, A. Motta, M.J. Marshall, A.J. El Haj, S.H. Cartmell, Osteoblast, Biomaterials 30 (2009) 5376–5384 DOI:10.1016/j.biomaterials.2009.07.028.

[96] V. Bloemen, T.J. Vries, T. Schoenmaker, V. Everts, Intercellular adhesion molecule-1 clusters during osteoclastogenesis, Biochemical and biophysical research communications 385 (2009) 640–645 DOI:10.1016/j.bbrc.2009.05.145.

[97] S. Greiner, A. Kadow-Romacker, G. Schmidmaier, B. Wildemann, Cocultures of osteoblasts and osteoclasts are influenced by local application of zoledronic acid incorporated in a poly(D,L-lactide) implant coating, J Biomed Mater Res A 91 (2009) 288–295 DOI:10.1002/jbm.a.32245.

[98] G. Mbalaviele, N. Jaiswal, A. Meng, L. Cheng, C. van den Bos, M. Thiede, Human mesenchymal stem cells promote human osteoclast differentiation from CD34+ bone marrow hematopoietic progenitors, Endocrinology 140 (1999) 3736–3743 DOI:10.1210/endo.140.8.6880.

[99] A. Bernhardt, S. Thieme, H. Domaschke, A. Springer, A. Rösen-Wolff, M. Gelinsky, Crosstalk of osteoblast and osteoclast precursors on mineralized collagen--towards an in vitro model for bone remodeling, J Biomed Mater Res A 95 (2010) 848–856 DOI:10.1002/jbm.a.32856.

[100] G.O. Hofmann, Biodegradable implants in traumatology: A review on the state-of-the-art, Archives of orthopaedic and trauma surgery 114 (1995) 123–132.

[101] K.E. Rehm, H.J. Helling, C. Gatzka, Neue Entwicklungen beim Einsatz resorbierbarer Implantate, Der Orthopade 26 (1997) 489–497.

[102] M. Geetha, A.K. Singh, R. Asokamani, A.K. Gogia, Ti based biomaterials, the ultimate choice for orthopaedic implants – A review, Progress in Materials Science 54 (2009) 397–425 DOI:10.1016/j.pmatsci.2008.06.004.

[103] E.A. Fritz, T.T. Glant, C. Vermes, J.J. Jacobs, K.A. Roebuck, Titanium particles induce the immediate early stress responsive chemokines IL-8 and MCP-1 in osteoblasts, Journal of orthopaedic research official publication of the Orthopaedic Research Society 20 (2002) 490–498 DOI:10.1016/S0736-0266(01)00154-1.

[104] S.-S. Lee, A.R. Sharma, B.-S. Choi, J.-S. Jung, J.-D. Chang, S. Park, E.A. Salvati, E.P. Purdue, D.-K. Song, J.-S. Nam, The effect of TNFα secreted from macrophages activated by titanium particles on osteogenic activity regulated by WNT/BMP signaling in osteoprogenitor cells, Biomaterials 33 (2012) 4251–4263 DOI:10.1016/j.biomaterials.2012.03.005.

[105] X. Mao, X. Pan, X. Peng, T. Cheng, X. Zhang, Inhibition of titanium particle-induced inflammation by the proteasome inhibitor bortezomib in murine macrophage-like RAW 264.7 cells, Inflammation 35 (2012) 1411–1418 DOI:10.1007/s10753-012-9454-5.

[106] J. Pajarinen, V.-P. Kouri, E. Jämsen, T.-F. Li, J. Mandelin, Y.T. Konttinen, The response of macrophages to titanium particles is determined by macrophage polarization, Acta biomaterialia 9 (2013) 9229–9240 DOI:10.1016/j.actbio.2013.06.027.

[107] Y. Jiang, T. Jia, W. Gong, P.H. Wooley, S.-Y. Yang, Titanium particle-challenged osteoblasts promote osteoclastogenesis and osteolysis in a murine model of periprosthestic osteolysis, Acta biomaterialia 9 (2013) 7564–7572 DOI:10.1016/j.actbio.2013.03.010.

[108] M. Sundfeldt, L.V. Carlsson, C.B. Johansson, P. Thomsen, C. Gretzer, Aseptic loosening, not only a question of wear: A review of different theories, Acta orthopaedica 77 (2006) 177–197 DOI:10.1080/17453670610045902.

[109] D.A. Puleo, W.W. Huh, Acute toxicity of metal ions in cultures of osteogenic cells derived from bone marrow stromal cells, Journal of applied biomaterials an official journal of the Society for Biomaterials 6 (1995) 109–116 DOI:10.1002/jab.770060205.

[110] C. Lhotka, T. Szekeres, I. Steffan, K. Zhuber, K. Zweymüller, Four-year study of cobalt and chromium blood levels in patients managed with two different metal-on-metal total hip replacements, Journal of orthopaedic research official publication of the Orthopaedic Research Society 21 (2003) 189–195 DOI:10.1016/S0736-0266(02)00152-3.

[111] J.Y. Wang, B.H. Wicklund, R.B. Gustilo, D.T. Tsukayama, Titanium, chromium and cobalt ions modulate the release of bone-associated cytokines by human monocytes/macrophages in vitro, Biomaterials 17 (1996) 2233–2240.

[112] M. Heiden, E. Walker, L. Stanciu, Magnesium, Iron and Zinc Alloys, the Trifecta of Bioresorbable Orthopaedic and Vascular Implantation - A Review, J Biotechnol Biomater 05 (2015) 1000178 DOI:10.4172/2155-952X.1000178.

[113] R. Guo, M. Yamashita, Q. Zhang, Q. Zhou, C. Di, D.G. Reynolds, H.A. Awad, L. Yanoso, L. Zhao, E.M. Schwarz, Ubiquitin ligase Smurf1 mediates tumor necrosis factor-induced systemic bone loss by promoting proteasomal degradation of bone morphogenetic signaling proteins, Journal of Biological Chemistry 283 (2008) 23084–23092 DOI:10.1074/jbc.M709848200.

[114] Z. Sheikh, S. Najeeb, Z. Khurshid, V. Verma, H. Rashid, M. Glogauer, Biodegradable Materials for Bone Repair and Tissue Engineering Applications, Materials (Basel, Switzerland) 8 (2015) 5744–5794 DOI:10.3390/ma8095273.

7 References

[115] R.B. Osman, M.V. Swain, A Critical Review of Dental Implant Materials with an Emphasis on Titanium versus Zirconia, Materials (Basel, Switzerland) 8 (2015) 932–958 DOI:10.3390/ma8030932.

[116] L.L. Hench, Bioceramics and the origin of life, J. Biomed. Mater. Res. 23 (1989) 685–703 DOI:10.1002/jbm.820230703.

[117] K.F. Farraro, K.E. Kim, S.L.-Y. Woo, J.R. Flowers, M.B. McCullough, Revolutionizing orthopaedic biomaterials: The potential of biodegradable and bioresorbable magnesium-based materials for functional tissue engineering, Journal of biomechanics 47 (2013) 1979–1986 DOI:10.1016/j.jbiomech.2013.12.003.

[118] T. Kokubo, Bioceramics and their clinical applications, Woodhead Pub. and Maney Pub. on behalf of Institute of Materials Minerals & Mining, Cambridge, England, Boca Raton, 2008 ISBN: 9781420072075.

[119] B.J.C. Luthringer, F. Feyerabend, R. Willumeit-Römer, Magnesium-based implants: A mini-review, Magnesium research 27 (2014) 142–154 DOI:10.1684/mrh.2015.0375.

[120] J. Durlach, P. Bac, M. Bara, A. Guiet-Bara, Physiopathology of symptomatic and latent forms of central nervous hyperexcitability due to magnesium deficiency: a current general scheme, Magnesium research 13 (2000) 293–302.

[121] Lambotte A., L'utilisation du magnesium comme materiel perdu dans l'osteosynthèse., Bull Mém Soc Nat Chir (1932) 1325–1334.

[122] A. Purnama, H. Hermawan, J. Couet, D. Mantovani, Assessing the biocompatibility of degradable metallic materials: state-of-the-art and focus on the potential of genetic regulation, Acta biomaterialia 6 (2010) 1800–1807 DOI:10.1016/j.actbio.2010.02.027.

[123] D. Höche, C. Blawert, S.V. Lamaka, N. Scharnagl, C. Mendis, M.L. Zheludkevich, The effect of iron re-deposition on the corrosion of impurity-containing magnesium, Physical chemistry chemical physics PCCP 18 (2016) 1279–1291 DOI:10.1039/c5cp05577f.

[124] N.E. Saris, E. Mervaala, H. Karppanen, J.A. Khawaja, A. Lewenstam, Magnesium. An update on physiological, clinical and analytical aspects, Clinica chimica acta; international journal of clinical chemistry 294 (2000) 1–26.

[125] E. Zhang, L. Xu, G. Yu, F. Pan, K. Yang, In vivo evaluation of biodegradable magnesium alloy bone implant in the first 6 months implantation, Journal of biomedical materials research. Part A 90 (2009) 882–893 DOI:10.1002/jbm.a.32132.

[126] F. Witte, The history of biodegradable magnesium implants: a review, Acta biomaterialia 6 (2010) 1680–1692 DOI:10.1016/j.actbio.2010.02.028.

[127] J. Verbrugge, Le matériel métallique résorbable en chirurgie osseuse., Presse Med (1934) 460–465.

[128] Maier O., Über die Verwendbarkeit von Leichtmetallen in der Chirurgie (metallisches Magnesium als Reizmittel zur Knochenneubildung)., Deut Z Chir (1940) 552–556.

[129] G. Stroganov, E. Savitsky, N. Tikhova, V.F. Terekhova, M.V. Volkov, K.M. Sivash, et al., Magnesium-base alloy for use in bone surgery, US patent.

[130] J.-W. Lee, H.-S. Han, K.-J. Han, J. Park, H. Jeon, M.-R. Ok, H.-K. Seok, J.-P. Ahn, K.E. Lee, D.-H. Lee, S.-J. Yang, S.-Y. Cho, P.-R. Cha, H. Kwon, T.-H. Nam, J.H. Lo H., H.-J. Rho, K.-S. Lee, Y.-C. Kim, D. Mantovani, Long-term clinical study and multiscale analysis of in vivo biodegradation mechanism of Mg alloy, Proceedings of the National Academy of Sciences of the United States of America 113 (2016) 716–721 DOI:10.1073/pnas.1518238113.

[131] Y. Sun, H. Wu, W. Wang, R. Zan, H. Peng, S. Zhang, X. Zhang, Translational status of biomedical Mg devices in China, Bioactive Materials 4 (2019) 358–365 DOI:10.1016/j.bioactmat.2019.11.001.

[132] C. Guo, J. Li, C. She, X. Shao, B. Teng, J. Feng, J.Q. Feng, P.-G. Ren, Bioeffects of micron-size magnesium particles on inflammatory cells and bone turnover in vivo and in vitro, Journal of biomedical materials research. Part B, Applied biomaterials 104 (2016) 923–931 DOI:10.1002/jbm.b.33411.

[133] H. Ebel, T. Günther, Magnesium metabolism: A review, Journal of clinical chemistry and clinical biochemistry. Zeitschrift fur klinische Chemie und klinische Biochemie 18 (1980) 257–270.

[134] M.J. Laires, C.P. Monteiro, M. Bicho, Role of cellular magnesium in health and human disease, Frontiers in bioscience a journal and virtual library 9 (2004) 262–276 DOI:10.2741/1223.

[135] W.B. Weglicki, Hypomagnesemia and inflammation: clinical and basic aspects, Annual review of nutrition 32 (2012) 55–71 DOI:10.1146/annurev-nutr-071811-150656.

[136] S. Long, A.M. Romani, Role of Cellular Magnesium in Human Diseases, Austin journal of nutrition and food sciences 2 (2014) 1051.

[137] J.H.F. Baaij, J.G.J. Hoenderop, R.J.M. Bindels, Regulation of magnesium balance: Lessons learned from human genetic disease, Clinical kidney journal 5 (2012) i15-i24 DOI:10.1093/ndtplus/sfr164.

[138] A.C. Alfrey, N.L. Miller, R. Trow, Effect of age and magnesium depletion on bone magnesium pools in rats, The Journal of clinical investigation 54 (1974) 1074–1081 DOI:10.1172/JCI107851.

[139] M.T.F. Wolf, Inherited and acquired disorders of magnesium homeostasis, Current opinion in pediatrics 29 (2017) 187–198 DOI:10.1097/MOP.0000000000000450.

7 References

[140] A.J. Ulmer, W. Scholz, M. Ernst, E. Brandt, H.D. Flad, Isolation and subfractionation of human peripheral blood mononuclear cells (PBMC) by density gradient centrifugation on Percoll, Immunobiology 166 (1984) 238–250 DOI:10.1016/S0171-2985(84)80042-X.

[141] L.T. Iseri, J.H. French, Magnesium: nature's physiologic calcium blocker, American heart journal 108 (1984) 188–193.

[142] L.A. Sonna, C.A. Hirshman, T.L. Croxton, Role of calcium channel blockade in relaxation of tracheal smooth muscle by extracellular Mg2+, The American journal of physiology 271 (1996) 7.

[143] S. Banai, L. Haggroth, S.E. Epstein, W. Casscells, Influence of extracellular magnesium on capillary endothelial cell proliferation and migration, Circ Res 67 (1990) 645–650 DOI:10.1161/01.RES.67.3.645.

[144] W.B. Weglicki, T.M. Phillips, A.M. Freedman, M.M. Cassidy, B.F. Dickens, Magnesium-deficiency elevates circulating levels of inflammatory cytokines and endothelin, Mol. Cell. Biochem. 110 (1992) 169–173.

[145] D. Blache, S. Devaux, O. Joubert, N. Loreau, M. Schneider, P. Durand, M. Prost, V. Gaume, M. Adrian, P. Laurant, A. Berthelot, Long-term moderate magnesium-deficient diet shows relationships between blood pressure, inflammation and oxidant stress defense in aging rats, Free Radical Biology and Medicine 41 (2006) 277–284 DOI:10.1016/j.freeadbiomed.2006.04.008.

[146] R.K. Rude, H.E. Gruber, Magnesium deficiency and osteoporosis: animal and human observations, Journal of Nutritional Biochemistry 15 (2004) 710–716 DOI:10.1016/j.jnutbio.2004.08.001.

[147] C. Malpuech-Brugere, Z. Nowacki, E. Gueux, J. Kuryszko, E. Rock, Y. Rayssiguier, A. Mazur, Accelerated thymus involution in magnesium-deficient rats is related to enhanced apoptosis and sensitivity to oxidative stress, British Journal of Nutrition 81 (1999) 405–411.

[148] G.K. Schwalfenberg, S.J. Genuis, The Importance of Magnesium in Clinical Healthcare, Scientifica 2017 (2017) 4179326 DOI:10.1155/2017/4179326.

[149] H.B.T. Tam, O. Dowling, X.Y. Xue, D. Lewis, B. Rochelson, C.N. Metz, H.B. Tam Tam, O. Dowling, X. Xue, D. Lewis, B. Rochelson, C.N. Metz, Magnesium sulfate ameliorates maternal and fetal inflammation in a rat model of maternal infection, American Journal of Obstetrics and Gynecology 204 (2011) 364.e1-8 DOI:10.1016/j.ajog.2010.11.006.

[150] H. Suzuki-Kakisaka, J. Sugimoto, M. Tetarbe, A.M. Romani, C.M.R. Kitchen, H.B. Bernstein, Magnesium Sulfate Increases Intracellular Magnesium Reducing Inflammatory Cytokine Release in Neonates, American Journal of Reproductive Immunology 70 (2013) 213–220 DOI:10.1111/aji.12118.

[151] B. Mizrahi, L. Shapira, A.J. Domb, Y. Houri-Haddad, Citrus oil and MgCl2 as antibacterial and anti-inflammatory agents, Journal of periodontology 77 (2006) 963–968 DOI:10.1902/jop.2006.050278.

[152] M. Nishikawa, N. Shimada, M. Kanzaki, T. Ikegami, T. Fukuoka, M. Fukushima, K. Asano, The characteristics of patients with hypermagnesemia who underwent emergency hemodialysis, Acute medicine & surgery 5 (2018) 222–229 DOI:10.1002/ams2.334.

[153] J. Zhang, Y. LI, Q. Zhang, X. Hao, S. Wang, Effects of gadolinium on proliferation, differentiation and calcification of primary mouse osteoblasts in vitro, Journal of Rare Earths 30 (2012) 831–834 DOI:10.1016/S1002-0721(12)60139-2.

[154] A.B.G. Lansdown, A pharmacological and toxicological profile of silver as an antimicrobial agent in medical devices, Advances in pharmacological sciences 2010 (2010) 910686 DOI:10.1155/2010/910686.

[155] N. Lubick, Nanosilver toxicity: Ions, nanoparticles or both?, Environ. Sci. Technol. 42 (2008) 8617 DOI:10.1021/es8026314.

[156] R.J. Clifford, E.B. Maryon, J.H. Kaplan, Dynamic internalization and recycling of a metal ion transporter: Cu homeostasis and CTR1, the human Cu^{+} uptake system, Journal of cell science 129 (2016) 1711–1721 DOI:10.1242/jcs.173351.

[157] N.A. Wolff, M.D. Garrick, L. Zhao, L.M. Garrick, A.J. Ghio, F. Thévenod, A role for divalent metal transporter (DMT1) in mitochondrial uptake of iron and manganese, Scientific reports 8 (2018) 211 DOI:10.1038/s41598-017-18584-4.

[158] A. Onodera, F. Nishiumi, K. Kakiguchi, A. Tanaka, N. Tanabe, A. Honma, K. Yayama, Y. Yoshioka, K. Nakahira, S. Yonemura, I. Yanagihara, Y. Tsutsumi, Y. Kawai, Short-term changes in intracellular ROS localisation after the silver nanoparticles exposure depending on particle size, Toxicology reports 2 (2015) 574–579 DOI:10.1016/j.toxrep.2015.03.004.

[159] N.R. Jena, DNA damage by reactive species: Mechanisms, mutation and repair, Journal of biosciences 37 (2012) 503–517 DOI:10.1007/s12038-012-9218-2.

[160] S. Srinivasan, A. Koenigstein, J. Joseph, L. Sun, B. Kalyanaraman, M. Zaidi, N.G. Avadhani, Role of mitochondrial reactive oxygen species in osteoclast differentiation, Annals of the New York Academy of Sciences 1192 (2010) 245–252 DOI:10.1111/j.1749-6632.2009.05377.x.

[161] C. Greulich, S. Kittler, M. Epple, G. Muhr, M. Köller, Studies on the biocompatibility and the interaction of silver nanoparticles with human mesenchymal stem cells (hMSCs), Langenbeck's archives of surgery 394 (2009) 495–502 DOI:10.1007/s00423-009-0472-1.

[162] C. Greulich, D. Braun, A. Peetsch, J. Diendorf, B. Siebers, M. Epple, M. Köller, The toxic effect of silver ions and silver nanoparticles towards bacteria and human cells occurs in the same concentration range, RSC Adv. 2 (2012) 6981 DOI:10.1039/c2ra20684f.

[163] C.E. Albers, W. Hofstetter, K.A. Siebenrock, R. Landmann, F.M. Klenke, In vitro cytotoxicity of silver nanoparticles on osteoblasts and osteoclasts at antibacterial concentrations, Nanotoxicology 7 (2013) 30–36 DOI:10.3109/17435390.2011.626538.

[164] A. Panácek, M. Kolár, R. Vecerová, R. Prucek, J. Soukupová, V. Krystof, P. Hamal, R. Zboril, L. Kvítek, Antifungal activity of silver nanoparticles against Candida spp, Biomaterials 30 (2009) 6333–6340 DOI:10.1016/j.biomaterials.2009.07.065.

[165] M. Ueno, H. Miyamoto, M. Tsukamoto, S. Eto, I. Noda, T. Shobuike, T. Kobatake, M. Sonohata, M. Mawatari, Silver-Containing Hydroxyapatite Coating Reduces Biofilm Formation by Methicillin-Resistant Staphylococcus aureus In Vitro and In Vivo, BioMed research international 2016 (2016) 8070597 DOI:10.1155/2016/8070597.

[166] K. Yu, Y. Dai, Z. Luo, H. Long, M. Zeng, Z. Li, J. Zhu, L. Cheng, Y. Zhang, H. Liu, Y. Zhu, In vitro and in vivo evaluation of novel biodegradable Mg-Ag-Y alloys for use as resorbable bone fixation implant, J Biomed Mater Res A 106 (2018) 2059–2069 DOI:10.1002/jbm.a.36397.

[167] M.C. Heinrich, M.K. Kuhlmann, S. Kohlbacher, M. Scheer, A. Grgic, M.B. Heckmann, M. Uder, Cytotoxicity of iodinated and gadolinium-based contrast agents in renal tubular cells at angiographic concentrations: In vitro study, Radiology 242 (2007) 425–434 DOI:10.1148/radiol.2422060245.

[168] S. Bartolami, S. Gaboyard, J. Quentin, C. Travo, M. Cavalier, J. Barhanin, C. Chabbert, Critical roles of transitional cells and Na/K-ATPase in the formation of vestibular endolymph, The Journal of neuroscience the official journal of the Society for Neuroscience 31 (2011) 16541–16549 DOI:10.1523/JNEUROSCI.2430-11.2011.

[169] A.M. Tang, J.S. Ananta, H. Zhao, B.T. Cisneros, E.Y. Lam, S.T. Wong, L.J. Wilson, K.K. Wong, Cellular uptake and imaging studies of gadolinium-loaded single-walled carbon nanotubes as MRI contrast agents, Contrast media & molecular imaging 6 (2011) 93–99 DOI:10.1002/cmmi.410.

[170] L.-J. Fu, J.-X. Li, X.-G. Yang, K. Wang, Gadolinium-promoted cell cycle progression with enhanced S-phase entry via activation of both ERK and PI3K signaling pathways in NIH 3T3 cells, Journal of biological inorganic chemistry JBIC a publication of the Society of Biological Inorganic Chemistry 14 (2009) 219–227 DOI:10.1007/s00775-008-0442-z.

[171] S.-L. Feng, M.-R. Sun, T.-T. Li, X. Yin, C.-Q. Xu, Y.-H. Sun, Activation of calcium-sensing receptor increases TRPC3 expression in rat cardiomyocytes, Biochemical and

biophysical research communications 406 (2011) 278–284 DOI:10.1016/j.bbrc.2011.02.033.

[172] F. Witte, V. Kaese, H. Haferkamp, E. Switzer, A. Meyer-Lindenberg, C.J. Wirth, H. Windhagen, In vivo corrosion of four magnesium alloys and the associated bone response, Biomaterials 26 (2005) 3557–3563 DOI:10.1016/j.biomaterials.2004.09.049.

[173] A. Myrissa, N.A. Agha, Y. Lu, E. Martinelli, J. Eichler, G. Szakács, C. Kleinhans, R. Willumeit-Römer, U. Schäfer, A.-M. Weinberg, In vitro and in vivo comparison of binary Mg alloys and pure Mg, Materials science & engineering. C, Materials for biological applications 61 (2016) 865–874 DOI:10.1016/j.msec.2015.12.064.

[174] D. Tie, F. Feyerabend, W.-D. Müller, R. Schade, K. Liefeith, K.U. Kainer, R. Willumeit, Antibacterial biodegradable Mg-Ag alloys, eCM 25 (2013) 284–298 DOI:10.22203/eCM.v025a20.

[175] Z. Liu, R. Schade, B. Luthringer, N. Hort, H. Rothe, S. Müller, K. Liefeith, R. Willumeit-Römer, F. Feyerabend, Influence of the Microstructure and Silver Content on Degradation, Cytocompatibility, and Antibacterial Properties of Magnesium-Silver Alloys In Vitro, Oxidative medicine and cellular longevity 2017 (2017) 8091265 DOI:10.1155/2017/8091265.

[176] M.M. Gawlik, M. Steiner, B. Wiese, J. González, F. Feyerabend, M. Dahms, T. Ebel, R. Willumeit-Römer, The Effects of HAc Etching on the Degradation Behavior of Mg-5Gd. Journal of Medical Materials and Technologies, Vol 1 No 2 (2017): Proceedings of Euro BioMAT (2017) 22–25 DOI:10.24354/medmat.v1i2.17.

[177] 10993-5:2009 I. Biological evaluation of medical devices. Part 5. Tests for in vitro cytotoxicity 2009.

[178] 10993-12:2012 I. Biological evaluation of medical devices. Part 12. Sample preparation and reference materials 2012.

[179] R. Sarugaser, D. Lickorish, D. Baksh, M.M. Hosseini, J.E. Davies, Human umbilical cord perivascular (HUCPV) cells: A source of mesenchymal progenitors, Stem cells (Dayton, Ohio) 23 (2005) 220–229 DOI:10.1634/stemcells.2004-0166.

[180] G.E. Truett, P. Heeger, R.L. Mynatt, A.A. Truett, J.A. Walker, M.L. Warman, Preparation of PCR-quality mouse genomic DNA with hot sodium hydroxide and tris (HotSHOT), BioTechniques 29 (2000) 52, 54.

[181] H.C. Bimboim, J. Doly, A rapid alkaline extraction procedure for screening recombinant plasmid DNA, Nucl Acids Res 7 (1979) 1513–1523 DOI:10.1093/nar/7.6.1513.

[182] L.S. Yasui, K. Chen, K. Wang, T.P. Jones, J. Caldwell, D. Guse, A.I. Kassis, Using Hoechst 33342 to target radioactivity to the cell nucleus, Radiation research 167 (2007) 167–175 DOI:10.1667/RR0584.1.

[183] C.L. Long, W.L. Berry, Y. Zhao, X.-H. Sun, M.B. Humphrey, E proteins regulate osteoclast maturation and survival, Journal of bone and mineral research the official journal of the American Society for Bone and Mineral Research 27 (2012) 2476–2489 DOI:10.1002/jbmr.1707.

[184] Y.-H. Chiu, K.A. Mensah, E.M. Schwarz, Y. Ju, M. Takahata, C. Feng, L.A. McMahon, D.G. Hicks, B. Panepento, P.C. Keng, C.T. Ritchlin, Regulation of human osteoclast development by dendritic cell-specific transmembrane protein (DC-STAMP), Journal of bone and mineral research the official journal of the American Society for Bone and Mineral Research 27 (2012) 79–92 DOI:10.1002/jbmr.531.

[185] C. Mülhardt, Der Experimentator: Molekularbiologie/ Genomics, 6th ed., Spektrum Akad. Verl; Springer, Heidelberg, Heidelberg, 2009 ISBN: 978-3-8274-2036-7.

[186] Y. Huang, Y. Zhou, W. Yang, R. Butters, H.-W. Lee, S. Li, A. Castiblanco, E.M. Brown, J.J. Yang, Identification and dissection of Ca(2+)-binding sites in the extracellular domain of Ca(2+)-sensing receptor, The Journal of biological chemistry 282 (2007) 19000–19010 DOI:10.1074/jbc.M701096200.

[187] Y. Huang, Y. Zhou, A. Castiblanco, W. Yang, E.M. Brown, J.J. Yang, Multiple Ca(2+)-binding sites in the extracellular domain of the Ca(2+)-sensing receptor corresponding to cooperative Ca(2+) response, Biochemistry 48 (2009) 388–398 DOI:10.1021/bi8014604.

[188] C. Silve, C. Petrel, C. Leroy, H. Bruel, E. Mallet, D. Rognan, M. Ruat, Delineating a Ca2+ binding pocket within the venus flytrap module of the human calcium-sensing receptor, The Journal of biological chemistry 280 (2005) 37917–37923 DOI:10.1074/jbc.M506263200.

[189] H. Bräuner-Osborne, A.A. Jensen, P.O. Sheppard, P. O'Hara, P. Krogsgaard-Larsen, The agonist-binding domain of the calcium-sensing receptor is located at the amino-terminal domain, The Journal of biological chemistry 274 (1999) 18382–18386.

[190] M. Ruat, A.M. Snowman, L.D. Hester, S.H. Snyder, Cloned and expressed rat Ca2+-sensing receptor, The Journal of biological chemistry 271 (1996) 5972–5975.

[191] M.M. Winslow, M. Pan, M. Starbuck, E.M. Gallo, L. Deng, G. Karsenty, G.R. Crabtree, Calcineurin/NFAT signaling in osteoblasts regulates bone mass, Developmental cell 10 (2006) 771–782 DOI:10.1016/j.devcel.2006.04.006.

[192] M. Takami, N. Takahashi, N. Udagawa, C. Miyaura, K. Suda, J.T. Woo, T.J. Martin, K. Nagai, T. Suda, Intracellular calcium and protein kinase C mediate expression of receptor activator of nuclear factor-kappaB ligand and osteoprotegerin in osteoblasts, Endocrinology 141 (2000) 4711–4719 DOI:10.1210/endo.141.12.7852.

[193] R.M. Adibhatla, J.F. Hatcher, A. Gusain, Tricyclodecan-9-yl-xanthogenate (D609) mechanism of actions: A mini-review of literature, Neurochemical research 37 (2012) 671–679 DOI:10.1007/s11064-011-0659-z.

[194] J.J. Jolly, K.-Y. Chin, M.F.N. Farhana, E. Alias, K.H. Chua, W.N.W. Hasan, S. Ima-Nirwana, Optimization of the Static Human Osteoblast/Osteoclast Co-culture System, Iranian Journal of Medical Sciences 43 (2018) 208–213.

[195] V. Kartsogiannis, K.W. Ng, Cell lines and primary cell cultures in the study of bone cell biology, Molecular and cellular endocrinology 228 (2004) 79–102 DOI:10.1016/j.mce.2003.06.002.

[196] C. Heinemann, S. Heinemann, H. Worch, T. Hanke, Development of an osteoblast/osteoclast co-culture derived by human bone marrow stromal cells and human monocytes for biomaterials testing, European cells & materials 21 (2011) 80–93 DOI:10.22203/ecm.v021a07.

[197] F. Schmid, C. Kleinhans, F. Schmid, P. Kluger, Osteoclast Formation within a Human Co-Culture System on Bone Material as an In Vitro Model for Bone Remodeling Processes, JFMK 3 (2018) 17 DOI:10.3390/jfmk3010017.

[198] W.P. Tsang, Y. Shu, P.L. Kwok, F. Zhang, K.K.H. Lee, M.K. Tang, G. Li, K.M. Chan, W.-Y. Chan, C. Wan, CD146+ human umbilical cord perivascular cells maintain stemness under hypoxia and as a cell source for skeletal regeneration, PloS one 8 (2013) e76153 DOI:10.1371/journal.pone.0076153.

[199] O. Charyeva, In Vitro Resorption of Magnesium Materials and its Effect on Surface and Surrounding Environment, MOJT 1 (2015) 23–28 DOI:10.15406/mojt.2015.01.00004.

[200] L.C. Palmer, C.J. Newcomb, S.R. Kaltz, E.D. Spoerke, S.I. Stupp, Biomimetic systems for hydroxyapatite mineralization inspired by bone and enamel, Chemical reviews 108 (2008) 4754–4783 DOI:10.1021/cr8004422.

[201] G.W. Bourne, J.M. Trifaró, The gadolinium ion: A potent blocker of calcium channels and catecholamine release from cultured chromaffin cells, Neuroscience 7 (1982) 1615–1622 DOI:10.1016/0306-4522(82)90019-7.

[202] O. Babich, J. Reeves, R. Shirokov, Block of CaV1.2 channels by Gd3+ reveals preopening transitions in the selectivity filter, The Journal of general physiology 129 (2007) 461–475 DOI:10.1085/jgp.200709733.

[203] B. Cordero, V. Gómez, A.E. Platero-Prats, M. Revés, J. Echeverría, E. Cremades, F. Barragán, S. Alvarez, Covalent radii revisited, Dalton transactions (Cambridge, England 2003) (2008) 2832–2838 DOI:10.1039/b801115j.

[204] A.D. Sherry, P. Caravan, R.E. Lenkinski, Primer on gadolinium chemistry, Journal of magnetic resonance imaging JMRI 30 (2009) 1240–1248 DOI:10.1002/jmri.21966.

[205] D.H. Lee, B.-S. Lim, Y.-K. Lee, H.-C. Yang, Effects of hydrogen peroxide (H2O2) on alkaline phosphatase activity and matrix mineralization of odontoblast and osteoblast cell lines, Cell biology and toxicology 22 (2006) 39–46 DOI:10.1007/s10565-006-0018-z.

[206] H.-J. Park, J.Y. Kim, J. Kim, J.-H. Lee, J.-S. Hahn, M.B. Gu, J. Yoon, Silver-ion-mediated reactive oxygen species generation affecting bactericidal activity, Water research 43 (2009) 1027–1032 DOI:10.1016/j.watres.2008.12.002.

[207] S.W. Ryter, H.P. Kim, A. Hoetzel, J.W. Park, K. Nakahira, X. Wang, A.M.K. Choi, Mechanisms of cell death in oxidative stress, Antioxidants & redox signaling 9 (2007) 49–89 DOI:10.1089/ars.2007.9.49.

[208] S. Li, M. Wang, X. Chen, S.-F. Li, J. Li-Ling, H.-Q. Xie, Inhibition of osteogenic differentiation of mesenchymal stem cells by copper supplementation, Cell proliferation 47 (2014) 81–90 DOI:10.1111/cpr.12083.

[209] F. Liu, W.-L. Zhang, H.-Z. Meng, Z.-Y. Cai, M.-W. Yang, Regulation of DMT1 on autophagy and apoptosis in osteoblast, International journal of medical sciences 14 (2017) 275–283 DOI:10.7150/ijms.17860.

[210] L. Wang, X. Zhang, Y. Guo, X. Chen, R. Li, L. Liu, C. Shi, C. Guo, Y. Zhang, Involvement of BMPs/Smad signaling pathway in mechanical response in osteoblasts, Cellular physiology and biochemistry international journal of experimental cellular physiology, biochemistry, and pharmacology 26 (2010) 1093–1102 DOI:10.1159/000323987.

[211] T. Okamoto, M. Taguchi, T. Osaki, S. Fukumoto, T. Fujita, Phosphate enhances reactive oxygen species production and suppresses osteoblastic differentiation, Journal of bone and mineral metabolism 32 (2014) 393–399 DOI:10.1007/s00774-013-0516-z.

[212] J.L. Millán, The Role of Phosphatases in the Initiation of Skeletal Mineralization, Calcified tissue international 93 (2012) 299–306 DOI:10.1007/s00223-012-9672-8.

[213] C.C. Mandal, S. Ganapathy, Y. Gorin, K. Mahadev, K. Block, H.E. Abboud, S.E. Harris, G. Ghosh-Choudhury, N. Ghosh-Choudhury, Reactive oxygen species derived from Nox4 mediate BMP2 gene transcription and osteoblast differentiation, The Biochemical journal 433 (2011) 393–402 DOI:10.1042/BJ20100357.

[214] M.M. Cortese-Krott, M. Münchow, E. Pirev, F. Hessner, A. Bozkurt, P. Uciechowski, N. Pallua, K.-D. Kröncke, C.V. Suschek, Silver ions induce oxidative stress and intracellular zinc release in human skin fibroblasts, Free radical biology & medicine 47 (2009) 1570–1577 DOI:10.1016/j.freeradbiomed.2009.08.023.

[215] E. Zielinska, C. Tukaj, M.W. Radomski, I. Inkielewicz-Stepniak, Molecular Mechanism of Silver Nanoparticles-Induced Human Osteoblast Cell Death: Protective Effect of Inducible Nitric Oxide Synthase Inhibitor, PloS one 11 (2016) e0164137 DOI:10.1371/journal.pone.0164137.

[216] K. Jähn, H. Saito, H. Taipaleenmäki, A. Gasser, N. Hort, F. Feyerabend, H. Schlüter, J.M. Rueger, W. Lehmann, R. Willumeit-Römer, E. Hesse, Intramedullary Mg2Ag nails augment callus formation during fracture healing in mice, Acta biomaterialia 36 (2016) 350–360 DOI:10.1016/j.actbio.2016.03.041.

[217] D.E.C. Corbridge, Phosphorus: An outline of its chemistry, biochemistry, and technology, 3rd ed., Elsevier Science Publishers, Amsterdam, New York, 1985 ISBN: 9780444417503.

[218] A.G. Cockbain, The Crystal Chemistry of Apatites, Mineralogical Magazine 1968 281:54.

[219] J. Birkenstock, Synthese und Kristallchemie von Na-Ca -Apatiten, Mainz, 1995.

[220] C.H. Jang, Y.B. Cho, C.H. Choi, Y.S. Jang, W.-K. Jung, J.K. Lee, Comparision of osteoconductivity of biologic and artificial synthetic hydroxyapatite in experimental mastoid obliteration, Acta oto-laryngologica 134 (2014) 255–259 DOI:10.3109/00016489.2013.859397.

[221] J.A. Rincón-López, J.A. Hermann-Muñoz, A.L. Giraldo-Betancur, A. Vizcaya-Ruiz, J.M. Alvarado-Orozco, J. Muñoz-Saldaña, Synthesis, Characterization and In Vitro Study of Synthetic and Bovine-Derived Hydroxyapatite Ceramics: A Comparison, Materials (Basel, Switzerland) 11 (2018) E333 DOI:10.3390/ma11030333.

[222] J.F. Cawthray, A.L. Creagh, C.A. Haynes, C. Orvig, Ion exchange in hydroxyapatite with lanthanides, Inorganic chemistry 54 (2015) 1440–1445 DOI:10.1021/ic502425e.

[223] E.E. Golub, K. Boesze-Battaglia, The role of alkaline phosphatase in mineralization, Current Opinion in Orthopaedics 18 (2007) 444–448 DOI:10.1097/BCO.0b013e3282630851.

[224] G.K. Hunter, H.A. Goldberg, Nucleation of hydroxyapatite by bone sialoprotein, Proceedings of the National Academy of Sciences of the United States of America 90 (1993) 8562–8565 DOI:10.1073/pnas.90.18.8562.

[225] C.E. Tye, K.R. Rattray, K.J. Warner, J.A.R. Gordon, J. Sodek, G.K. Hunter, H.A. Goldberg, Delineation of the hydroxyapatite-nucleating domains of bone sialoprotein, Journal of Biological Chemistry 278 (2003) 7949–7955 DOI:10.1074/jbc.M211915200.

[226] K. Vincent, M.C. Durrant, A structural and functional model for human bone sialoprotein, Journal of molecular graphics & modelling 39 (2013) 108–117 DOI:10.1016/j.jmgm.2012.10.007.

[227] Y. Chen, B.S. Bal, J.P. Gorski, Calcium and collagen binding properties of osteopontin, bone sialoprotein, and bone acidic glycoprotein-75 from bone, Journal of Biological Chemistry 267 (1992) 24871–24878.

7 References

[228] P.A. Williams, A.R. Peacocke, The binding of calcium and yttrium ions to a glycoprotein from bovine cortical bone, The Biochemical journal 105 (1967) 1177–1185 DOI:10.1042/bj1051177.

[229] B. Ganss, R.H. Kim, J. Sodek, Bone sialoprotein, Critical reviews in oral biology and medicine an official publication of the American Association of Oral Biologists 10 (1999) 79–98 DOI:10.1177/10454411990100010401.

[230] N. Murata, L.F. Gonzalez-Cuyar, K. Murata, C. Fligner, R. Dills, D. Hippe, K.R. Maravilla, Macrocyclic and Other Non-Group 1 Gadolinium Contrast Agents Deposit Low Levels of Gadolinium in Brain and Bone Tissue: Preliminary Results From 9 Patients With Normal Renal Function, Investigative radiology 51 (2016) 447–453 DOI:10.1097/RLI.0000000000000252.

[231] X. Wang, J. Huang, K. Wang, M. Neufurth, H.C. Schröder, S. Wang, W.E.G. Müller, The morphogenetically active polymer, inorganic polyphosphate complexed with GdCl3, as an inducer of hydroxyapatite formation in vitro, Biochemical pharmacology 102 (2016) 97–106 DOI:10.1016/j.bcp.2015.12.011.

[232] B. Lorenz, J. Münkner, M.P. Oliveira, A. Kuusksalu, J.M. Leitão, W.E.G. Müller, H.C. Schröder, Changes in metabolism of inorganic polyphosphate in rat tissues and human cells during development and apoptosis, Biochimica et Biophysica Acta (BBA) - General Subjects 1335 (1997) 51–60 DOI:10.1016/S0304-4165(96)00121-3.

[233] C. Zhang, T. Zhang, J. Zou, C.L. Miller, R. Gorkhali, J.-Y. Yang, A. Schilmiller, S. Wang, K. Huang, E.M. Brown, K.W. Moremen, J. Hu, J.J. Yang, Structural basis for regulation of human calcium-sensing receptor by magnesium ions and an unexpected tryptophan derivative co-agonist, Science advances 2 (2016) e1600241 DOI:10.1126/sciadv.1600241.

[234] T.I. Alfadda, A.M.A. Saleh, P. Houillier, J.P. Geibel, Calcium-sensing receptor 20 years later, American journal of physiology. Cell physiology 307 (2014) C221-31 DOI:10.1152/ajpcell.00139.2014.

[235] X. Zhang, H. Zu, D. Zhao, K. Yang, S. Tian, X. Yu, F. Lu, B. Liu, B. Wang, W. Wang, S. Huang, Y. Wang, Z. Wang, Z. Zhang, Ion channel functional protein kinase TRPM7 regulates Mg ions to promote the osteoinduction of human osteoblast via PI3K pathway: In vitro simulation of the bone-repairing effect of Mg-based alloy implant, Acta biomaterialia 63 (2017) 369–382 DOI:10.1016/j.actbio.2017.08.051.

[236] B.-C. Jeong, J.H. Kim, K. Kim, I. Kim, S. Seong, N. Kim, ATF3 modulates calcium signaling in osteoclast differentiation and activity by associating with c-Fos and NFATc1 proteins, Bone 95 (2017) 33–40 DOI:10.1016/j.bone.2016.11.005.

[237] C.M.V. Barbosa, C. Bincoletto, C.C. Barros, A.T. Ferreira, E.J. Paredes-Gamero, PLCγ2 and PKC are important to myeloid lineage commitment triggered by M-SCF and G-CSF, Journal of cellular biochemistry 115 (2014) 42–51 DOI:10.1002/jcb.24653.

[238] M. Ishikawa, T. Nakamura, A. Doyle, S. Fukumoto, Y. Yamada, Pannexin 3 functions as an ER Ca(2+) channel, hemichannel, and gap junction to promote osteoblast differentiation, The Journal of cell biology 193 (2011) 1257–1274 DOI:10.1083/jcb.201101050.

[239] I.M. McGonnell, A.E. Grigoriadis, E.W.-F. Lam, J.S. Price, A. Sunters, A specific role for phosphoinositide 3-kinase and AKT in osteoblasts?, Frontiers in endocrinology 3 (2012) 88 DOI:10.3389/fendo.2012.00088.

[240] C. Maes, H.M. Kronenberg, Bone Development and Remodeling, in: A. Grossman, D.M. Kretser, G.C. Weir, J.L. Jameson, J.T. Potts, L.J. DeGroot, L. Giudice, S. Melmed (Eds.), Endocrinology: Adult & pediatric, Elsevier/Saunders, Philadelphia, PA, 2016, 1038-1062.e8.

[241] L. Kong, B. Wang, X. Yang, H. Guo, K. Zhang, Z. Zhu, J. Liu, D. Hao, Picrasidine I from Picrasma Quassioides Suppresses Osteoclastogenesis via Inhibition of RANKL Induced Signaling Pathways and Attenuation of ROS Production, Cellular physiology and biochemistry international journal of experimental cellular physiology, biochemistry, and pharmacology 43 (2017) 1425–1435 DOI:10.1159/000481874.

[242] J.H. Kim, N. Kim, Regulation of NFATc1 in Osteoclast Differentiation, Journal of bone metabolism 21 (2014) 233–241 DOI:10.11005/jbm.2014.21.4.233.

[243] T. Komori, Regulation of osteoblast differentiation by Runx2, Advances in experimental medicine and biology 658 (2010) 43–49 DOI:10.1007/978-1-4419-1050-9_5.

[244] T. Fujita, Y. Azuma, R. Fukuyama, Y. Hattori, C. Yoshida, M. Koida, K. Ogita, T. Komori, Runx2 induces osteoblast and chondrocyte differentiation and enhances their migration by coupling with PI3K-Akt signaling, The Journal of cell biology 166 (2004) 85–95 DOI:10.1083/jcb.200401138.

[245] Z. Zhai, X. Qu, H. Li, K. Yang, P. Wan, L. Tan, Z. Ouyang, X. Liu, B. Tian, F. Xiao, W. Wang, C. Jiang, T. Tang, Q. Fan, A. Qin, K. Dai, The effect of metallic magnesium degradation products on osteoclast-induced osteolysis and attenuation of NF-κB and NFATc1 signaling, Biomaterials 35 (2014) 6299–6310 DOI:10.1016/j.biomaterials.2014.04.044.

[246] M. Muzylak, T.R. Arnett, J.S. Price, M.A. Horton, The in vitro effect of pH on osteoclasts and bone resorption in the cat: Implications for the pathogenesis of FORL, Journal of cellular physiology 213 (2007) 144–150 DOI:10.1002/jcp.21103.

7 References

[247] A.-M. Galow, A. Rebl, D. Koczan, S.M. Bonk, W. Baumann, J. Gimsa, Increased osteoblast viability at alkaline pH in vitro provides a new perspective on bone regeneration, Biochemistry and biophysics reports 10 (2017) 17–25 DOI:10.1016/j.bbrep.2017.02.001.

[248] P.G. Petronini, M. Tramacere, J.E. Kay, A.F. Borghetti, Adaptive response of cultured fibroblasts to hyperosmolarity, Experimental cell research 165 (1986) 180–190 DOI:10.1016/0014-4827(86)90542-2.

[249] L. Wu, B.J.C. Luthringer, F. Feyerabend, Z. Zhang, H.G. Machens, M. Maeda, H. Taipaleenmäki, E. Hesse, R. Willumeit-Römer, A.F. Schilling, Increased levels of sodium chloride directly increase osteoclastic differentiation and resorption in mice and men, Osteoporosis international a journal established as result of cooperation between the European Foundation for Osteoporosis and the National Osteoporosis Foundation of the USA 28 (2017) 3215–3228 DOI:10.1007/s00198-017-4163-4.

[250] S.J. Klebanoff, Myeloperoxidase: friend and foe, Journal of leukocyte biology 77 (2005) 598–625 DOI:10.1189/jlb.1204697.

[251] V. Izzi, L. Masuelli, I. Tresoldi, P. Sacchetti, A. Modesti, F. Galvano, R. Bei, The effects of dietary flavonoids on the regulation of redox inflammatory networks, Frontiers in bioscience (Landmark edition) 17 (2012) 2396–2418 DOI:10.2741/4061.

[252] U. Förstermann, N. Xia, H. Li, Roles of Vascular Oxidative Stress and Nitric Oxide in the Pathogenesis of Atherosclerosis, Circulation research 120 (2017) 713–735 DOI:10.1161/CIRCRESAHA.116.309326.

[253] T.N. Crotti, R.P. O'Sullivan, Z. Shen, M.R. Flannery, R.J. Fajardo, F.P. Ross, S.R. Goldring, K.P. McHugh, Bone matrix regulates osteoclast differentiation and annexin A8 gene expression, Journal of cellular physiology 226 (2011) 3413–3421 DOI:10.1002/jcp.22699.

[254] R.J. van'T Hof, S.H. Ralston, Nitric oxide and bone, Immunology 103 (2001) 255–261 DOI:10.1046/j.1365-2567.2001.01261.x.

[255] V. Panagopoulos, V. Liapis, I. Zinonos, S. Hay, D.A. Leach, W. Ingman, M.O. DeNichilo, G.J. Atkins, D.M. Findlay, A.C.W. Zannettino, A. Evdokiou, Peroxidase enzymes inhibit osteoclast differentiation and bone resorption, Molecular and cellular endocrinology 440 (2017) 8–15 DOI:10.1016/j.mce.2016.11.007.

[256] D. Persaud-Sharma, A. McGoron, Biodegradable Magnesium Alloys: A Review of Material Development and Applications, Journal of biomimetics, biomaterials, and tissue engineering 12 (2012) 25–39 DOI:10.4028/www.scientific.net/JBBTE.12.25.

[257] H. Orimo, The mechanism of mineralization and the role of alkaline phosphatase in health and disease, Journal of Nippon Medical School = Nippon Ika Daigaku zasshi 77 (2010) 4–12 DOI:10.1272/jnms.77.4.

[258] H. Ding, H. Pan, X. Xu, R. Tang, Toward a Detailed Understanding of Magnesium Ions on Hydroxyapatite Crystallization Inhibition, Crystal Growth & Design 14 (2014) 763–769 DOI:10.1021/cg401619s.

[259] C. Berg, H.G. Tiselius, The effects of citrate on hydroxyapatite induced calcium oxalate crystallization and on the formation of calcium phosphate crystals, Urological research 17 (1989) 167–172 DOI:10.1007/bf00256245.

[260] Y. Berthezène, A. Mühler, P. Lang, D.M. Shames, O. Clément, W. Rosenau, R. Kuwatsuru, R.C. Brasch, Safety aspects and pharmacokinetics of inhaled aerosolized gadolinium, Journal of magnetic resonance imaging JMRI 3 (1993) 125–130 DOI:10.1002/jmri.1880030121.

[261] S. Yoneda, N. Emi, Y. Fujita, M. Ohmichi, S. Hirano, K.T. Suzuki, Effects of gadolinium chloride on the rat lung following intratracheal instillation, Fundamental and applied toxicology official journal of the Society of Toxicology 28 (1995) 65–70 DOI:10.1006/faat.1995.1147.

[262] A. Myrissa, S. Braeuer, E. Martinelli, R. Willumeit-Römer, W. Goessler, A.-M. Weinberg, Gadolinium accumulation in organs of Sprague-Dawley® rats after implantation of a biodegradable magnesium-gadolinium alloy, Acta biomaterialia 48 (2017) 521–529 DOI:10.1016/j.actbio.2016.11.024.

[263] M.A. Perazella, Gadolinium-contrast toxicity in patients with kidney disease: Nephrotoxicity and nephrogenic systemic fibrosis, Current drug safety 3 (2008) 67–75 DOI:10.2174/157488608783333989.

[264] A.A. Malayeri, K.M. Brooks, L.H. Bryant, R. Evers, P. Kumar, D.S. Reich, D.A. Bluemke, National Institutes of Health Perspective on Reports of Gadolinium Deposition in the Brain, Journal of the American College of Radiology JACR 13 (2016) 237–241 DOI:10.1016/j.jacr.2015.11.009.

[265] M. Birka, J. Roscher, M. Holtkamp, M. Sperling, U. Karst, Investigating the stability of gadolinium based contrast agents towards UV radiation, Water research 91 (2016) 244–250 DOI:10.1016/j.watres.2016.01.012.

[266] C. Plaass, S. Ettinger, L. Sonnow, S. Koenneker, Y. Noll, A. Weizbauer, J. Reifenrath, L. Claassen, K. Daniilidis, C. Stukenborg-Colsman, H. Windhagen, Early results using a biodegradable magnesium screw for modified chevron osteotomies, Journal of orthopaedic research official publication of the Orthopaedic Research Society 34 (2016) 2207–2214 DOI:10.1002/jor.23241.

7 References

[267] L.M.B. Burke, M. Ramalho, M. AlObaidy, E. Chang, M. Jay, R.C. Semelka, Self-reported gadolinium toxicity: A survey of patients with chronic symptoms, Magnetic resonance imaging 34 (2016) 1078–1080 DOI:10.1016/j.mri.2016.05.005.

[268] M.R. Prince, H. Zhang, Z. Zou, R.B. Staron, P.W. Brill, Incidence of immediate gadolinium contrast media reactions, AJR. American journal of roentgenology 196 (2011) W138-43 DOI:10.2214/AJR.10.4885.

[269] S. Bussi, L. Penard, R. Bonafè, C. Botteron, R. Celeste, A. Coppo, R. Queliti, M.A. Kirchin, F. Tedoldi, F. Maisano, Non-clinical assessment of safety and gadolinium deposition after cumulative administration of gadobenate dimeglumine (MultiHance®) to neonatal and juvenile rats, Regulatory toxicology and pharmacology RTP 92 (2018) 268–277 DOI:10.1016/j.yrtph.2017.12.016.

[270] B. Welk, E. McArthur, S.A. Morrow, P. MacDonald, J. Hayward, A. Leung, A. Lum, Association Between Gadolinium Contrast Exposure and the Risk of Parkinsonism, JAMA 316 (2016) 96–98 DOI:10.1001/jama.2016.8096.

8 Supplementary Material

Supplementary Table 1: Summary qPCR results of the coculture for CSAR signal cascade, transcription factors, communication and cell marker. p-value. Stars (*) indicate degree of significance (= p =< 0.05; ** = p =< 0.001; *** = p =< 0.0001).*

Group	CASR signal cascade															
Alloy	$MgCl_2$				Mg				$AgNO_3$				Mg-2Ag			
Gene	*CASR*	*PLCG2*	*MAPK1*	*PPP3CA*	*CASR*	*PLCG2*	*MAPK1*	*PPP3CA*	*CASR*	*PLCG2*	*MAPK1*	*PPP3CA*	*CASR*	*PLCG2*	*MAPK1*	*PPP3CA*
Regulation	-1,52					-1.91							-3,97			-2.44
	⇩					⇩							⇩			⇩
p-Value	1,09E-02					3,33E-02							2,57E-02			4,60E-05
	*					*							*			***
Regulation			1,29		10.52		3.5			1.75			-2,09	-1,80		2.93
			⇧		⇧		⇧			⇧			⇩	⇩		⇧
p-Value			2,64E-02		2,65E-04		1,00E-06			9,26E-03			2,10E-02	4,48E-02		1,39E-03
			*		***		***			**			*	**		**
Regulation			1,77	-3,1	-9.98	-4,13				1,59				-1,82	-1,64	-2,12
			⇧	⇩	⇩	⇩				⇧				⇩	⇩	⇩
p-Value			2,29E-02	3,50E-02	4,65E-03	3,74E-04				3,60E-02				1,26E-03	3,35E-02	3,43E-02
			*	*	**	***				*				**	*	*
Regulation		3,86	2,93			-8.75					1,54		1,69	-2.15	-1,79	
		⇧	⇧			⇩					⇧		⇧	⇩	⇩	
p-Value		1,60E-03	2,00E-06			1,35E-03					2,05E-02		4,87E-02	2,25E-03	3,09E-02	
		**	***			**					*		*	**	*	
Regulation	-1,72		-2,66							-1,57	-2,58					
	⇩		⇩							⇩	⇩					
p-Value	3,70E-02		8,51E-03							3,04E-02	1,34E-04					
	*		**							*	***					

Group	CASR signal cascade															
Alloy	Mg-4Ag				Mg-6Ag				$GdCl_3$				Mg-10Gd			
Gene	*CASR*	*PLCG2*	*MAPK1*	*PPP3CA*	*CASR*	*PLCG2*	*MAPK1*	*PPP3CA*	*CASR*	*PLCG2*	*MAPK1*	*PPP3CA*	*CASR*	*PLCG2*	*MAPK1*	*PPP3CA*
Regulation			-1,85	-1,45	2,40								6.39			
			⇩	⇩	⇧								⇧			
p-Value			1,79E-02	1,14E-02	2,29E-02								1,50E-05			
			✳	✳	✳								✳✳✳			
Regulation	-5.10				6,62	2,83	2,36		-1.38	1.32	1,30		5.74	2,39		5,51
	⇩				⇧	⇧	⇧		⇩	⇧	⇧		⇧	⇧		⇧
p-Value	1,80E-03				5,63E-03	5,82E-03	9,23E-03		4,98E-03	3,78E-03	4,66E-02		4,40E-05	1,12E-02		3,73E-02
	✳✳				✳✳	✳✳	✳✳		✳✳✳	✳✳	✳		✳✳✳	✳		✳
Regulation		-1,65					2,05		-2,27						4,59	3,70
		⇩					⇧		⇩						⇧	⇧
p-Value		6,50E-03					3,60E-02		2,05E-02						1,51E-02	3,60E-02
		✳✳					✳		✳						✳	✳
Regulation		-2.99				-3,13				1,68						
		⇩				⇩				⇧						
p-Value		3,10E-04				1,53E-02				7,33E-03						
		✳✳✳				✳				✳✳						
Regulation		-1,48								1,23	-1,56			-3,03		
		⇩								⇧	⇩			⇩		
p-Value		1,67E-02								4,57E-02	3,31E-02			1,26E-02		
		✳✳								✳	✳			✳		

Group	Transcription factors															
Alloy	$MgCl_2$		Mg		$AgNO_3$		Mg-2Ag		Mg-4Ag		Mg-6Ag		$GdCl_3$		Mg-10Gd	
Gene	*RUNX2*	*NFATC1*	*RUNX2*	*NFATC1*	*RUNX2*	*NFATC1*	*RUNX2*	*NFATC1*	*RUNX2*	*NFATC1*	*RUNX2*	*NFATC1*	*RUNX2*	*NFATC1*	*RUNX2*	*NFATC1*
Regulation					-3.13			-2.54	-1,73	-1,49						
					⇩			⇩	⇩	⇩						
p-Value					7,00E-05			3,74E-04	1,76E-02	4,36E-02						
					✳✳✳			✳✳✳	✳	✳						
Regulation			2,21	3.13					-2,16		4,06	2,48			2,28	2.84
			⇧	⇧					⇩		⇧	⇧			⇧	⇧
p-Value			2,10E-02	1,97E-04					3,55E-02		1,61E-03	6,15E-04			2,49E-02	2,79E-03
			✳	✳✳✳					✳✳		✳✳	✳✳✳			✳	✳✳✳
Regulation		-1,49		-4.77	2,04			-2.54		-3.99		-3,62	-2,05	-1,48	4.52	
		⇩		⇩	⇧			⇩		⇩		⇩	⇩	⇩	⇧	
p-Value		3,53E-02		4,70E-05	4,72E-02			3,02E-03		1,01E-03		2,19E-03	2,67E-02	3,67E-02	9,85E-03	
		✳		✳✳✳	✳			✳✳		✳✳		✳✳	✳	✳	✳✳	
Regulation				-2,37								-3,70	1,95	-2,05		
				⇩								⇩	⇧	⇩		
p-Value				3,43E-02								1,83E-03	1,75E-02	2,05E-03		
				✳								✳✳	✳	✳✳		
Regulation	-2,72	-1,51		-5.44	-1,93			-3.51		-2.12	-2,05	-5,16	-5,17			
	⇩	⇩		⇩	⇩			⇩		⇩	⇩	⇩	⇩			
p-Value	1,54E-02	4,33E-02		0,00E+00	1,74E-03			6,31E-04		8,65E-03	4,18E-02	1,10E-05	5,00E-06			
	✳	✳		✳✳✳	✳✳			✳✳✳		✳✳	✳	✳✳✳	✳✳✳			

8 Supplementary Material

Group	Communication															
Alloy	$MgCl_2$				Mg				$AgNO_3$				Mg-2Ag			
Gene	*RANKL*	*M-CSF*	*OPG*	*SEMA4D*	*RANKL*	*M-CSF*	*OPG*	*SEMA4D*	*RANKL*	*M-CSF*	*OPG*	*SEMA4D*	*RANKL*	*M-CSF*	*OPG*	*SEMA4D*
Regulation	-1,89							-1.56					-4.57	-2.73		-6.26
	⇩							⇩					⇩	⇩		⇩
p-Value	1,49E-04							1,85E-02					1,10E-04	1,27E-03		4,84E-04
	***							*					***	***		***
Regulation				1,45	6.16		-6.59	5.14		3,48		6,82				-2,48
				⇧	⇧		⇩	⇧		⇧		⇧				⇩
p-Value				4,94E-02	1,59E-03		3,60E-05	6,63E-03		1,38E-02		6,57E-03				1,03E-02
				*	**		***	**		*		**				*
Regulation					2,99		-3.31	-3.24	1,73							-1,86
					⇧		⇩	⇩	⇧							⇩
p-Value					3,18E-02		8,70E-05	7,16E-04	2,99E-02							2,15E-02
					*		***	***	*							*
Regulation					-2,04	-2.67	-2,68									-2,25
					⇩	⇩	⇩									⇩
p-Value					1,14E-02	8,30E-04	2,58E-03									1,91E-02
					*	***	**									*
Regulation		-1,44				-1.58	-10.73	-4.09	-1,98					1.85		
		⇩				⇩	⇩	⇩	⇩					⇧		
p-Value		9,58E-03				1,30E-03	5,40E-05	3,73E-03	1,74E-03					4,75E-03		
		**				**	***	**	**					**		

Group	Communication															
Alloy	Mg-4Ag				Mg-6Ag				$GdCl_3$				Mg-10Gd			
Gene	*RANKL*	*M-CSF*	*OPG*	*SEMA4D*	*RANKL*	*M-CSF*	*OPG*	*SEMA4D*	*RANKL*	*M-CSF*	*OPG*	*SEMA4D*	*RANKL*	*M-CSF*	*OPG*	*SEMA4D*
Regulation	-2.13	-5.15		-2,22	2,58								3.63			
	⇩	⇩		⇩	⇧								⇧			
p-Value	4,88E-03	2,20E-05		1,70E-02	2,30E-02								3,38E-03			
	**	***		*	*								**			
Regulation	-2,18			-1.68	3,47			4,21		3.19	-3,39	5,48	5.02		-4.8	3.49
	⇩			⇩	⇧			⇧		⇧	⇩	⇧	⇧		⇩	⇧
p-Value	4,47E-02			7,69E-03	5,85E-04			1,90E-05		8,66E-03	1,91E-04	8,53E-03	1,86E-03		1,52E-04	9,57E-04
	*			**	***			***		**	***	**	**		***	***
Regulation						-1,35	-3,73		-1,81			-1,56	5.32	1.78	-2.13	
						⇩	⇩		⇩			⇩	⇧	⇧	⇩	
p-Value						3,00E-02	5,00E-06		1,49E-04			4,01E-02	2,56E-03	3,96E-03	9,60E-03	
						**	***		***			*	**	**	***	
Regulation								-1,42							-3.02	4.80
								⇩							⇧	⇧
p-Value								4,07E-02							1,97E-03	1,96E-03
								**							**	**
Regulation	-4.28		-1,91				-2,96	-4,66		-1,85			2,04	1,63	-4.78	2.76
	⇩		⇩				⇩	⇩		⇩			⇧	⇧	⇩	⇧
p-Value	5,51E-04		1,61E-02				2,13E-03	8,09E-04		3,14E-03			1,22E-02	3,68E-03	3,53E-04	4,47E-03
	***		*				**	***		**			*	**	***	**

8 Supplementary Material

Group	Cell maker (Day 28)														
Alloy	$MgCl_2$			Mg			$AgNO_3$			Mg-2Ag			Mg-4Ag		
Gene	*ALP*	*BGLAP*	*CTSK*	*ALP*	*BGLAP*	*CTSK*	*ALP*	*BGLAP*	*CTSK*	*ALP*	*BGLAP*	*CTSK*	*ALP*	*BGLAP*	*CTSK*
Regulation		-1,63	-2,51	2.3	-1,47	-13.48			-2,41	5.33	1,24	4,22	1.70	-1,21	4,78
		⇩	⇩	⇧	⇩	⇩			⇩	⇧	⇧	⇧	⇧	⇩	⇧
p-Value		3,12E-03	3,07E-03	0,00E+00	9,25E-04	9,26E-04			2,59E-03	0,00E+00	2,83E-02	8,00E-06	1,67E-04	1,55E-02	1,00E-06
		**	**	**	***	***			**	***	*	***	***	*	***

Group	Cell maker (Day 28)								
Alloy	Mg-6Ag			$GdCl_3$			Mg-10Gd		
Gene	*ALP*	*BGLAP*	*CTSK*	*ALP*	*BGLAP*	*CTSK*	*ALP*	*BGLAP*	*CTSK*
Regulation	2,79					-2,63	3.25	2,02	5.02
	⇧					⇩	⇧	⇧	⇧
p-Value	0,00E+00					2,24E-03	0,00E+00	1,16E-02	1,76E-04
	***					*	**	*	***

9 Risk and Safty Statement

The following is a list of poteintiel hazardous chemicals with their respective hazards and safety instructions. The classification is carried out according to the Globally Harmonized System of Classification and Labelling of Chemicals (GHS).

9.1 Used poteintiel hazardous Chemicals

Compound	Chemical Abstracts Service No.	Hazard statements	GHS hazard	Precautionary statements
4',6-diamidino-2-phenylindole (DAPI)	28718-90-3	H315; H317; H335	GHS07	P264; P280; P362 + P364; P261; P272; P302 + P352; P332 + P313; P333 + P313; P309 + P311; P304 + P340
Acetone	67-64-1	H225; H319; H336; EUH 066	GHS02 GHS07	P210; P261; P280.3; P305 + P351 + P338; P403 + P233
Bisbenzimide	23491-45-4	H302; H315; H335; H341	GHS07 GHS08	P280; P301 + P312 + P330
Buffer RLT (RNeasy Mini Kit)	guanidinium thiocyanate 593-84-0	H302; H314; H412	GHS05 GHS07	P264; P280; P305 + P351 + P338 + P310
Buffer RW1 (RNeasy Mini Kit)	guanidinium thiocyanate 593-84-0 ethanol 64-17-5	H226; H318	GHS02 GHS07	P210; P280; P305 + P351 + P338 + P310
Compound	**Chemical Abstracts Service No.**	**Hazard statements**	**GHS hazard**	**Precautionary statements**
Chromic Acid	7738-94-5	H271; H290; H301; H312; H314; H317; H318; H330; H334; H340; H350; H361; H372; H410	GHS03 GHS05 GHS06 GHS07 GHS08	P201; P202; P210; P220; P221; P234; P260; P264; P270; P271; P272; P273; P280; P283; P284; P301 + P310 + P330; P301 + P330 + P331; P303 + P361 + P353; P304 + P340 + P310; P305 + P351 + P338 + P310; P306 + P360; P308 + P313; P333 + P313; P363; P370 + P378; P371 + P380 + P375; P390; P391; P403 + P233; P405; P406; P501
Dimethyl Sulfoxide	67-68-5	H227	GHS07	P210; P280

Ethanol	64-17-5	H225; H315 + H320; H335; H335	GHS02 GHS07	P210; P261; P305 + P351 + P338
Ethylenediamine-tetraacetic acid (EDTA)	6381-92-6	H332; H373	GHS07	P314
Gadolinium chloride	10138-52-0	H315; H319	GHS07	P305 + P351 + P338
Glutaraldehyde	111-30-8	H302; H314; H317; H330; H334; H335	GHS05 GHS06 GHS08	P260; P280; P302+P352; P303 + P361 + P353; P304+P340; P305 + P351 + P338; P310; P342 + P311; P403 + P233
HCl	7647-01-0	H290; H314	GHS05	P260; P280; P303 + P361 + P353; P305 + P351 + P338; P390; P501
Magnesium chloride	7786-30-3	H319	GHS07	P305 + P351 + P338
Methanol	67-56-1	H225; H301 + H311 + H331; H370	GHS02 GHS06 GHS08	P210; P233; P240; P241; P242; P243; P260; P264; P270; P271
n-Hexane	110-54-3	H225; H304; H315; H336; H361; H373; H411	GHS02 GHS07 GHS08 GHS09	P210; P241; P260; P273; P281; P301 + P310; P331; P370 + P378; P403 + P233; P403 + P235; P501
O-(octahydro-4,7-methano-1H-inden-5-yl) (D609)	83373-60-8	H302	GHS07	P264; P301+312; P330
Compound	**Chemical Abstracts Service No.**	**Hazard statements**	**GHS hazard**	**Precautionary statements**
Penicillin (Pen)/ Streptomycin (Strep)	Pen 69-57-8 Strep 3810-74-0	H315; H317; H320; H335	GHS07	P302 + P352; P333 + P313; P305 + P351 + P338; P337 + P313; P304 + P340; P312; P261; P271; P280; P264
Silver nitrate	7761-88-8	H290; H315; H319	GHS05	P280; P302 + P352; P305+ P351 + P338
Sodium Hydroxide	1310-73-2	H314; H402	GHS05	P260; P264; P273; P280; P301 + P330 + P331; P303 + P361 + P353; P304 + P340; P305 + P351 + P338; P310

Sodium Hypochlorite	7681-52-9	H314; H335; H410	GHS05 GHS07 GHS09	P260; P264; P271; P280; P273; P301 + P330 + P331; P303 + P361 + P353; P321; P363; P304 + P340; P312; P305 + P351 + P338; P310; P403 + P233; P405; P501
Sybr Green	Glycerol 56-81-5 Dimethyl sulfoxide 67-68-5	H318	GHS05	P280; P305 + P351 + P338; P310
Tetrazolium Salt (WST-1)	298-96-4	H315 H319 H335	GHS07	P261; P305 + P351 + P338
Toluidin Blue	92-31-9	H332; H315	GHS07	P261; P280; P304 + P340; P312; P321; P362
Tris	1185-53-1	H315; H319; H335	GHS07	P261; P280; P302 +P352; P305 + P351 + P338; P312; P403 + P233; P501
Vitamin D3	67-97-0	H301; H311; H330; H372	GHS06 GHS08	P260; P264; P280; P284; P301 + P310; P310; P302 + P352; P304 + P340; P314; P320; P330; P361 + P364

9.2 Hazard statements

H Codes	H Phrases
H225	Highly flammable liquid and vapour.
H226	Flammable liquid and vapour.
H271	May cause fire or explosion; strong oxidizer.
H290	May be corrosive to metals.
H301	Toxic if swallowed.
H302	Harmful if swallowed.
H304	May be fatal if swallowed and enters airways.
H311	Toxic in contact with skin.
H312	Harmful in contact with skin.
H314	Causes severe skin burns and eye damage.
H315	Causes skin irritation.
H317	May cause an allergic skin reaction.
H318	Causes serious eye damage.
H319	Causes serious eye irritation.
H330	Fatal if inhaled.
H331	Toxic if inhaled.
H332	Harmful if inhaled.
H334	May cause allergy or asthma symptoms or breathing difficulties if inhaled.
H335	May cause respiratory irritation.
H336	May cause drowsiness or dizziness.
H340	May cause genetic defects.
H341	Suspected of causing genetic defects.
H350	May cause cancer.
H361	Suspected of damaging fertility or the unborn child.
H370	Causes damage to organs.
H372	Causes damage to organs [...] through prolonged or repeated exposure [...]
H373	May cause damage to organs [...] through prolonged or repeated exposure [...].
H301 + H311 + H331	Toxic if swallowed, in contact with skin or if inhaled.
H315 + H320	Causes skin and eye irritation.
H410	Very toxic to aquatic life with long lasting effects.
H411	Toxic to aquatic life with long lasting effects.
H412	Harmful to aquatic life with long lasting effects.
EUH Code	**EUH Phrases**
EUH066	Repeated exposure may cause skin dryness or cracking.

9.3 GHS precautionary statements

P Codes	P Phrases
P201	Obtain special instructions before use.
P202	Do not handle until all safety precautions have been read and understood.
P210	Keep away from heat, hot surfaces, sparks, open flames and other ignition sources. No smoking.
P233	Keep container tightly closed.
P234	Keep only in original packaging.
P235	Keep cool.
P240	Ground and bond container and receiving equipment.
P241	Use explosion-proof [electrical/ventilating/lighting/…] equipment.
P242	Use non-sparking tools.
P243	Take action to prevent static discharges.
P260	Do not breathe dust/fume/gas/mist/vapours/spray.
P261	Avoid breathing dust/fume/gas/mist/vapours/spray.
P264	Wash … thoroughly after handling.
P270	Do no eat, drink or smoke when using this product.
P271	Use only outdoors or in a well-ventilated area.
P272	Contaminated work clothing should not be allowed out of the workplace.
P273	Avoid release to the environment.
P280	Wear protective gloves/protective clothing/eye protection/face protection.
P283	Wear fire resistant or flame retardant clothing.
P284	[In case of inadequate ventilation] wear respiratory protection.
P301	IF SWALLOWED:
P302	IF ON SKIN:
P303	IF ON SKIN (or hair):
P304	IF INHALED:
P305	IF IN EYES:
P306	IF ON CLOTHING:
P308	IF exposed or concerned:
P310	Immediately call a POISON CENTER/doctor/…
P311	Call a POISON CENTER/doctor/….
P312	Call a POISON CENTER/doctor/… if you feel unwell.
P313	Get medical advice/attention.
P314	Get medical advice/attention if you feel unwell.
P320	Specific treatment is urgent (see … on this label).
P321	Specific treatment (see … on this label).

P330	Rinse mouth.
P331	Do NOT induce vomiting.
P332	If skin irritation occurs:
P333	If skin irritation or rash occurs:
P337	If eye irritation persists:
P338	Remove contact lenses, if present and easy to do. Continue rinsing.
P340	Remove person to fresh air and keep comfortable for breathing.
P342	If experiencing respiratory symptoms:
P351	Rinse cautiously with water for several minutes.
P352	Wash with plenty of water/…
P353	Rinse skin with water [or shower].
P360	Rinse immediately contaminated clothing and skin with plenty of water before removing clothes.
P361	Take off immediately all contaminated clothing.
P362	Take off contaminated clothing.
P363	Wash contaminated clothing before reuse.
P364	And wash it before reuse.
P370	In case of fire:
P371	In case of major fire and large quantities:
P375	Fight fire remotely due to the risk of explosion.
P378	Use … to extinguish.
P380	Evacuate area.
P390	Absorb spillage to prevent material damage.
P391	Collect spillage.
P301+P310	IF SWALLOWED: Immediately call a POISON CENTER/doctor/….
P301+P312	IF SWALLOWED: Call a POISON CENTER/doctor/… if you feel unwell.
P301+P330+P331	IF SWALLOWED: Rinse mouth. Do NOT induce vomiting.
P302+P352	IF ON SKIN: Wash with plenty of water/…
P303+P361+P353	IF ON SKIN (or hair): Take off immediately all contaminated clothing. Rinse skin with water [or shower].
P304+P340	IF INHALED: Remove person to fresh air and keep comfortable for breathing.
P305+P351+P338	IF IN EYES: Rinse cautiously with water for several minutes. Remove contact lenses, if present and easy to do. Continue rinsing.
P306+P360	IF ON CLOTHING: rinse immediately contaminated clothing and skin with plenty of water before removing clothes.
P308+P313	IF exposed or concerned: Get medical advice/attention.
P332+P313	If skin irritation occurs: Get medical advice/attention.

P333+P313	If skin irritation or rash occurs: Get medical advice/attention.
P337+P313	If eye irritation persists: Get medical advice/attention.
P342+P311	If experiencing respiratory symptoms: Call a POISON CENTER/doctor/…
P361+P364	Take off immediately all contaminated clothing and wash it before reuse.
P362+P364	Take off contaminated clothing and wash it before reuse.
P370+P378	In case of fire: Use … to extinguish.
P371+P380+P375	In case of major fire and large quantities: Evacuate area. Fight fire remotely due to the risk of explosion.
P403	Store in a well-ventilated place.
P405	Store locked up.
P406	Store in a corrosion resistant/… container with a resistant inner liner.
P403+P233	Store in a well-ventilated place. Keep container tightly closed.
P403+P235	Store in a well-ventilated place. Keep cool.
P501	Dispose of contents/container to …

10 Acknowledgement

I would like to thank everyone who made this work possible and made it as pleasant as can be. Special thanks go to Prof. Regine Willumeit-Römer, who not only made the work possible, but also made me rethink my theories and approaches by challenging them intiligently. Dr. Beregere Luthringer-Feyerabend I would like to thank in particular here as well. During the time of my graduation she always supported me passionately and was always at my side with words and advice. I also owe Dr. Heike Helmholz a lot. She helped me with specific questions and emphases to evolve my partly unripe and unstructured theories to give the structure and plausibility. All have given me their continuous encouragement, support and advice during this work. I am very thankful to all of them for their efforts to train me in the scientific field.

I appreciate the opportunity to perform the experiments between February 2015 and April 2018 in the laboratory of the Department of Metallic Biomaterials of the Helmholtz Centre in Geesthacht. I am thankfull to the Asklepios Clinic Altona for providing the umbilical cord samples and to all donors for their altruistic cooperation. I would also like to thank Maria Geffken and Thomas Dominka from the Institute of Transfusion Medicine at the University Hospital Eppendorf for donating the blood for my research. My thanks also go to my colleagues at the Magnesium Innovation Center. Not only were they the ones who produced the materials for my experiments. These colleagues were also always there to help and advise me.

Many thanks to Angela Meyer-Rachner, Anke Schuster and Gabriele Salomon for the time you have invested in me. Be it at the beginning when I had to be trained or later for all the uncompromising technical support if my experimental setup led to problems. In particular, I would like to emphasize Angela Meyer-Rachner at this point, who has made many a difficult day with exuberant conversations easier.

At this point I would also like to thank my friends who helped me to overcome the sometimes difficult time. Especially Carlo, André, Sai, Lennart, Vallerie, Yasmin F. and Yasmin J. were always there for me during this time. I can't thank you enough for that. Without your support this thesis would not have been possible.

Finally I would like to try to express my thanks to my parents. It was you who supported me from the beginning with all the goals I set for myself. All my values, be it diligence, curiosity and always to see the good in things and people, you have conveyed to me. When I fell, you were always there to catch me or to help me back on my feet. With this you have made me the person I am today. I am overjoyed to be able to call myself your son. Thank you for all you have done for me. I love you.

11 Declaration upon oath

I hereby affirm on oath that I have written this dissertation myself and that I have not used any aids other than those indicated. The submitted written version corresponds to the one on the electronic storage medium. I assure you that this dissertation was not submitted in a previous promotion procedure.

Location, Date

Hamburg 26.05.2020 Siginture: _____